The impact of β5i-deficiency on structure and function of 20S proteasomes in *Listeria monocytogene*s infection

DISSERTATION

zur Erlangung des akademischen Grades

doctor rerum naturalium

(Dr. rer. nat.)

eingereicht an der

Mathematisch-Naturwissenschaftlichen Fakultät I

der Humboldt-Universität zu Berlin

von

Diplom-Biologe Thorsten Joeris

geboren am 15.Januar 1977 in Mönchengladbach

Präsident der Humboldt-Universität zu Berlin

Prof. Dr. Dr. h.c. Christoph Markschies

Dekan der Mathematisch-Naturwissenschaftlichen Fakultät I

Prof. Dr. Christian Limberg

Gutachter: 1. Prof. Dr. Richard Lucius

2. Prof. Dr. Peter-Michael Kloetzel

3. P.D. Dr. Ulrich Johannes Steinhoff

eingereicht am: 04.12.2007

Tag der mündlichen Prüfung: 27.06.2008

„Schätzelein, weisse Bescheid!“

Horst Schlämmer

ZUSAMMENFASSUNG 4

ABSTRACT 5

1 INTRODUCTION 6

1.1 The proteasome system 6
1.1.1 The ubiquitin-proteasome pathway 6
1.1.2 Proteasome structure 7
1.1.3 Proteasome assembly 9
1.1.4 Regulation of proteasome composition 12

1.2 The function of proteasomes in the immune response 14
1.2.1 The MHC class I pathway of antigen presentation 14
1.2.2 The influence of proteasome composition on epitope processing 16
1.2.3 Function of $CD8^+$ T cells 18
1.2.4 The impact of proteasome subunit composition on $CD8^+$ T-cell responses 19
1.2.5 The infection model of *Listeria monocytogenes* 20
1.2.6 Putative influences of the proteasome subunit composition on innate immune defence mechanisms 22

1.3 Aims of this study 23

2 MATERIAL AND METHODS 24

2.1 Methods 24
2.1.1 Mice 24
2.1.2 Cell culture 25
2.1.3 Biochemical methods 26
2.1.4 Molecular biological methods 30
2.1.5 Flow cytometry 33

2.2 Materials 35
2.2.1 Antibodies 35
2.2.2 Primer-sequences 36

3 RESULTS 37

3.1 Analysis of 20S proteasome assembly in *Listeria monocytogenes* infected *lmp7*$^{-/-}$ mice 37
3.1.1 The abundance of catalytic β-subunits in Listeria-infected WT and *lmp7*$^{-/-}$ mice 37
3.1.2 Analysis of proteasome assembly in WT and *lmp7*$^{-/-}$ mice 40
3.1.3 mRNA expression of the catalytic β-subunits in WT and *lmp7*$^{-/-}$ mice 44
3.1.4 Quantification of 20S proteasomes in Listeria infected WT and *lmp7*$^{-/-}$ mice 45
3.1.5 Analysis of POMP turnover in *lmp7*$^{-/-}$ mice 48
3.1.6 Overexpression of β5 in *lmp7*$^{-/-}$ MEFs 52
3.1.7 Overexpression of β5 in WT MEFs 53

3.2 Functional impact of β5i-deficiency on the immune response against *Listeria monocytogenes* 56
3.2.1 Determination of MHC class I surface expression on professional APCs of *lmp7*$^{-/-}$ mice 56
3.2.2 Analysis of $LLO_{296\text{-}304}$ epitope generation by 20S proteasomes isolated from *lmp7*$^{-/-}$ mice 59
3.2.3 Quantification of $LLO_{296\text{-}304}$ specific $CD8^+$ T cells in WT and *lmp7*$^{-/-}$ mice 61
3.2.4 Analysis of bacterial control in Listeria infected WT and *lmp7*$^{-/-}$ mice 63
3.2.5 Proinflammatory cytokine secretion by Listeria-infected *lmp7*$^{-/-}$ macrophages *in vitro* 64

4 DISCUSSION 66

4.1 The structural impact of β5i-deficiency on 20S proteasome assembly 66
4.1.1 Formation of m20S in *lmp7*$^{-/-}$ mice 66
4.1.2 β5 is a limiting factor for proteasome maturation in *lmp7*$^{-/-}$ mice 69
4.1.3 POMP regulates the integration efficiency of β5 and β5i 70
4.1.4 Regulation of the proteasome content 71
4.1.5 Model of competitive integration of catalytic β-subunits in 20S proteasome assembly 73

4.2 The effects of β5i-deficiency on the immune response against Listeria 76
4.2.1 Reduced MHC class I antigen presentation in *lmp7*$^{-/-}$ mice is not limiting for CD8^{+} T cell priming 76
4.2.2 Impaired recognition of non-lymphoid target cells in *lmp7*$^{-/-}$ mice 79
4.2.3 Possible influences of β5i-deficiency on innate immune defence mechanisms in Listeria infection 82

REFERENCES 84

ABBREVIATIONS 94

PUBLICATIONS 96

DANKSAGUNG 97

ERKLÄRUNG 98

Schlagworte

konstitutives Proteasom, Immunoproteasom, Proteasomassemblierung, POMP, β5i, β5, *lmp7*$^{-/-}$ Mäuse, Infektion, *Listeria monocytogenes*, Antigen-Prozessierung, MHC Klasse I Antigen Präsentation, CD8^{+} T-Zellen

Keywords

constitutive proteasome, immunoproteasome, proteasome assembly, POMP, β5i, β5, *lmp7*$^{-/-}$ mice, infection, *Listeria monocytogenes*, antigen processing, MHC class I antigen presentation, CD8^{+} T cells

Zusammenfassung

Der ubiquitin-abhängige Proteinabbau durch das Proteasom ist die Hauptquelle von Peptiden für die MHC Klasse I Antigen-Präsentation. In Vertebraten kann das Proteasomsystem durch die Expression unterschiedlicher Subtypen des 20S Proteasoms moduliert werden. Die häufigsten Subtypen sind konstitutive Proteasomen (c20S) mit den katalytischen Untereinheiten β1, β2 und β5 und Immunoproteasomen (i20S) mit den Immunountereinheiten β1i, β2i und β5i. Die Expression von i20S kann eine Verbesserung der MHC Klasse I Antigen-Präsentation bewirken, indem die Bildung von Peptiden mit hoher Affinität zu MHC I Molekülen verstärkt wird.

Laut dem aktuellen Stand der Forschung wird die Bildung von i20S durch kooperative Assemblierung reguliert, die auf der präferentiellen Interaktion zwischen den Immunountereinheiten beruht. In dieser Arbeit wurde die Assemblierung von 20S Proteasomen in β5i defizienten Mäusen (*lmp7*$^{-/-}$ Mäuse) im Laufe einer Infektion mit *Listeria monocytogenes* analysiert. In diesem Modell konnte keine präferentielle Interaktion zwischen konstitutiven bzw. Immunountereinheiten festgestellt werden. Stattdessen zeigen die Ergebnisse, daß die Integration von konstitutiven oder Immuno-Untereinheiten während der Proteasomassemblierung durch Kompetition reguliert wird. Desweiteren wurde während der Infektion eine Zunahme der zellulären Proteasommenge in Wildtyp-Mäusen festgestellt, die in *lmp7*$^{-/-}$ Mäusen nicht auftritt. Damit konnte ein neuer Mechanismus zur Regulation des zellulären Proteasomgehaltes gezeigt werden, der über die differentielle Expression von β5i gesteuert wird.

Funktionell führt die β5i-Defizienz zu einer verringerten MHC I Oberflächendichte auf antigenpräsentierenden Zellen und zu einer stark verminderten Prozessierung des bakteriellen Antigens $LLO_{296-304}$. Bei der Analyse der $LLO_{296-304}$ spezifischen CD8 T Zell Antwort konnte jedoch kein Unterschied zwischen Wildtyp- und *lmp7*$^{-/-}$ Mäusen festgestellt werden .Die Kontrolle der Infektion in den *lmp7*$^{-/-}$ Mäusen ist jedoch in der Leber verzögert. Dies deutet darauf hin, dass die Erkennung und Elimination infizierter Zellen durch cytotoxische CD8 T Zellen auf Grund der geringeren MHC Klasse I Präsentation bakterieller Antigene behindert wird.

Abstract

The ubiquitin-dependent protein degradation by proteasomes is the main source of peptides for MHC class I antigen presentation. In vertebrates the proteasome-system can be modulated by the expression of different subtypes of the 20S proteasome. The most common subtypes are constitutive proteasomes (c20S) with the catalytic subunits β1, β2 and β5 and immunoproteasomes (i20S) with the immunosubunits β1i, β2i and β5i. Expression of i20s can lead to an improvement of MHC class I antigen presentation by increasing the generation of peptides with high affinity to MHC class I molecules.

Currently, the formation of i20S is thought to be regulated by cooperative proteasome assembly, a principle that is based on the preferential interaction among the immunosubunits. Here, the assembly of 20S proteasomes was analysed in β5i deficient mice (*lmp7*$^{-/-}$ mice) during an ongoing infection with the intracellular bacterium *Listeria monocytogenes*. In this model, no preferential interactions among constitutive subunits or immunosubunits could be determined. Instead, the results show that the integration of constitutive subunits or immunosubunits is regulated by direct competition during proteasome assembly. Further, an increase in cellular proteasome quantity was observed in infected wild-type mice, that was absent in *lmp7*$^{-/-}$ mice. This finding reveals a novel mechanism for the regulation of cellular proteasome quantity that is based on the differential expression of β5i.

Functionally, the deficiency in β5i results in a reduced MHC class I cell surface expression on professional antigen presenting cells and a drastically diminished processing of the bacterial antigen $LLO_{296-304}$. However, the analyses of $LLO_{296-304}$ specific CD8 T cells did not reveal differences in the frequencies of these T cells between wild-type and *lmp7*$^{-/-}$ mice. Still, the control of infection in the liver of *lmp7*$^{-/-}$ mice was delayed. This phenotype suggests that the recognition and elimination of infected target cells by cytotoxic CD8 T cells is constrained due to the low MHC class I presentation of bacterial antigens.

1 Introduction

1.1 The proteasome system

Proteasomes are found in all three domains of life: prokaryots, archaea and eukaryots. They are multimeric protein complexes with varying complexity that possess protein-hydrolyzing activity. While proteasomes may not be important for survival of prokaryotic cells, their function is crucial for the survival of eukaryotic cells (Baumeister, et al., 1998). They are localized in the nucleus and the cytosol and can make up to 1% of cellular protein content (Gerards, et al., 1998).

Besides their housekeeping function in protein turnover and disposal of damaged proteins, they are involved in a variety of cellular processes, e.g. cell cycle control, apoptosis, transcriptional regulation, protein translation, chromatin remodelling, DNA repair and MHC class I antigen presentation. (Baugh and Pilipenko, 2004; Baumeister, et al., 1998; Chang, et al., 1998; Coux, et al., 1996; Goldberg, et al., 2002; King, et al., 1996)

1.1.1 The ubiquitin-proteasome pathway

The major pathway of non-lysomal protein degradation in eukaryotic cells is the ubiquitin-proteasome pathway (Rock, et al., 1994). It is an energy dependent pathway, which involves a complex ubiquitin ligation system and the function of 26S proteasomes. Besides the disposal of damaged proteins, this pathway regulates the cellular content of certain proteins and by that modulates their activity (Kornitzer and Ciechanover, 2000).

Covalent ligation of ubiquitin marks proteins for targeted degradation by proteasomes. Ubiquitin is a highly conserved protein of 76 amino acids. The linkage of ubiquitin to its target protein requires three catalytic steps. First, ubiquitin needs to be activated at its carboxy-terminal (C-terminal) glycine residue in an ATP dependent step by a specific activating enzyme, E1. This step involves formation of an intermediate complex in which ubiquitin is bound to a cysteine residue of E1 via a thiolesther linkage. Thereafter, ubiquitin is transferred to a cysteine residue in the active site of an ubiquitin-carrier protein, E2. Finally, a ubiquitin ligase, E3, takes up ubiquitin from E2 and catalyses an amide isopeptide linkage of the C-terminal glycine of ubiquitin to an ε-amino group of the target protein (Kornitzer and

Ciechanover, 2000). While usually only one E1 is expressed, various species of E2 and multiple families of E3 exist. The E3 proteins confer substrate specificity either by direct binding to a substrate or due to recruitment by other proteins (Hershko and Ciechanover, 1998).

Once a target protein is marked by ubiquitin, polyubiquitin chains form by further ligation of ubiquitins to a specific lysine residue, most commonly Lys^{48}. The resulting polyubiquitinylated proteins are recognized by 26S proteasomes by binding to UBA (ubiquitin associated domains) or UBL (ubiquitin like) domains. This is followed by deubiquitination of the substrate, which is necessary for ubiquitin recycling. Subsequently, the target protein is unfolded and translocated into the proteasome complex where it is hydrolized to peptides. It is still unclear, which steps require ATP in this process. However, the protein hydrolysis itself is energy independent. Thus, ATP is thought to be necessary for substrate unfolding, translocation and deubiquitination (Demartino and Gillette, 2007; Hershko and Ciechanover, 1998).

1.1.2 Proteasome structure

The variety of proteasome complexes found within eukaryotic cells is based on a central 20S core that is bound to different regulators. The 20S core is composed of two identical 16S half-proteasomes. Each half proteasome contains 14 different subunits, which can be grouped in α- or β-type subunits by sequence homology. The particular subunits α1-α7 and β1-β7 are arranged in heptameric α- and β-rings, respectively. In the 20S complex two 16S complexes form a barrel-shaped structure built of two central β-rings and two outer α-rings (Coux, et al., 1996; Groll, et al., 1997). Inside this cylinder three cavities are formed: two antechambers between the α- and β-rings of each 16S half and the central cavity between the two adjacent β-rings. As a mechanism of self-compartementalization, substrate access to the proteolytically active sites in the central cavity is gated by narrow channels, which enables controlled protein degradation (Baumeister, et al., 1998).

Each β-ring contains three catalytically active subunits. An amino-terminal (N-terminal) threonine residue is essential for peptide hydrolysis by a nucleophilic attack (Arendt and Hochstrasser, 1997; Chen and Hochstrasser, 1996; Dick, et al., 1997; Kisselev, et al., 1999; Schmidtke, et al., 1996).

In mammals, two major forms of 20S proteasomes can be distinguished according to the incorporated catalytic β-subunits. The constitutive proteasome (c20S) contains the constitutive subunits β1 (Y), β2 (Z) and β5 (X). By the use of fluorogenic peptide substrates caspase-like (peptidylglutamyl peptide hydrolizing), trypsin-like and chymotrypsin-like activity could be assigned to β1, β2 and β5, respectively (Groll, et al., 1997). Following IFNγ stimulation, mammalian cells express the immunosubunits β1i (LMP2), β2i (MECL1) and β5i (LMP7) (Glynne, et al., 1991; Groettrup, et al., 1996; Hisamatsu, et al., 1996; Nandi, et al., 1996). Incorporation of these subunits results in the formation of immunoproteasomes (i20S), which display increased chymotrypsin-like and reduced caspase-like activity compared to c20S. i20S reveal altered cleavage site specificity, which is commonly thought to improve MHC class I antigen presentation (Groettrup, et al., 2001).

20S proteasomes associate with different types of regulators, which can be bound to either one or both endplates of the outer α-rings. Generally, they are thought to control access to the active sites of the 20S complex inside the central cavity (Baumeister, et al., 1998).

The most abundant regulator of proteasomes is the 19S complex (PA700), which in combination with the 20S complex forms the 26S proteasome. As described previously, the 26S proteasome is the central enzymatic complex of the ubiquitin-proteasome pathway (Hershko and Ciechanover, 1998). 19S complexes include at least 15 different subunits. Six of these are ATPases, which form a hexameric ring that is in direct contact with the α-ring of the 20S complex. The exact ATP consuming steps catalized by these proteins are not identified, but are most likely associated with substrate unfolding, control of substrate access, product release and substrate translocation through the cavities of the 20S complex. Some of the non-ATPase subunits recognize polyubiquitinated substrates and bind them for degradation via UBA or UBL domains. Other components possess deubiquitinating activity and cleave polyubiquitin conjugates of the target proteins for ubiquitin recycling (Baumeister, et al., 1998; Coux, et al., 1996).

The 11S regulator (PA28) is described as an ATP independent activator of proteasomes, which accelerates the peptidase activity of 20S complexes (Dubiel, et al., 1992). However, it does not stimulate the degradation of ubiquitinated proteins. It is a multimer composed of the IFNγ inducible subunits PA28α and PA28β (Realini, et al., 1994). It is thought that 11S regulators open the entry in the α-ring, thus improving substrate access to and product release from the catalytic centre of the 20S complex (Stohwasser, et al., 2000).

Further, the formation of so-called hybrid proteasomes, which contain a 19S regulator and an 11S regulator at opposing sites of the 20S complex, were described. As they combine the ability of the 19S complex to degrade ubiquitinated substrates with increased substrate turnover by the 11S regulator, they are discussed as optimal complexes in protein processing (Tanahashi, et al., 2000).

Additional regulators increase the complexity of the proteasome system. PA28γ, whose regulation is unknown, forms a homoheptamer, that similar to 11S complexes binds to the α-ring. Although the exact function is not clear, PA28γ deficiency in mice results in a growth defect and increased susceptibility to apoptosis. In addition, PA200 can accelerate proteasome activity by opening the occlusions of the α-rings at the 20S complex. It has been associated with DNA repair and cellular stress responses. In contrast, PI31 and Pr39 down-modulate the activity of the proteasome by replacing the activating regulators and obstructing the substrate access (Demartino and Gillette, 2007).

1.1.3 Proteasome assembly

The neogenesis of the 20S proteasome with its 28 subunits involves a series of consecutive events of which the initial steps remain largely elusive (Schmidt, et al., 1997). Recently, the proteasome assembling chaperones, PAC1, PAC2, PAC3 and PAC4, have been identified in mammalian cells. They provide a molecular scaffold, which facilitates the correct formation of a complete α-ring. The proteins PAC1 and PAC2 as well as PAC3 and PAC4 form heterodimers, respectively. While PAC1/PAC2 is bound to the α-ring until formation of the 20S complex is completed, PAC3/PAC4 dissociates of the assembling complex during 16S half proteasome formation (Fig. I A-B). The PAC proteins are not degraded during proteasome neogenesis indicating that they can be recycled (Hirano, et al., 2006; Hirano, et al., 2005; Le Tallec, et al., 2007).

The β-subunits use the α-ring as a matrix and are assembled in a sequential manner. First, the early subunits β2 or β2i, β3, β4 and β1i are bound resulting in an intermediate 13S complex. This is followed by the integration of the residual subunits β1, β5 or β5i, β6 and β7, which leads to the formation of a 16S half proteasome (Nandi, et al., 1997) (Fig. I B).

The proteasome maturation factor POMP (proteassemblin/ Ump1p/ hUmp1) is a component of 13-16S complexes (Burri, et al., 2000; Griffin, et al., 2000). Recently, it was shown that

POMP interacts with most β-subunits and some α-subunits, indicating that it recruits the β-subunits to the α-ring. Further, POMP binds to endoplasmatic reticulum (ER) membranes and by that promotes coordinated proteasome formation at the ER (Fricke, et al., 2007). In addition, it mediates the assembly of two 16S complexes to a 20S proteasome and is therefore essential for the maturation of proteasomes (Fig. I B-C). After completion of assembly it becomes the initial substrate, thus POMP turnover is an indicator for the rate of proteasome neogenesis (Heink, et al., 2005; Ramos, et al., 1998; Witt, et al., 2000).

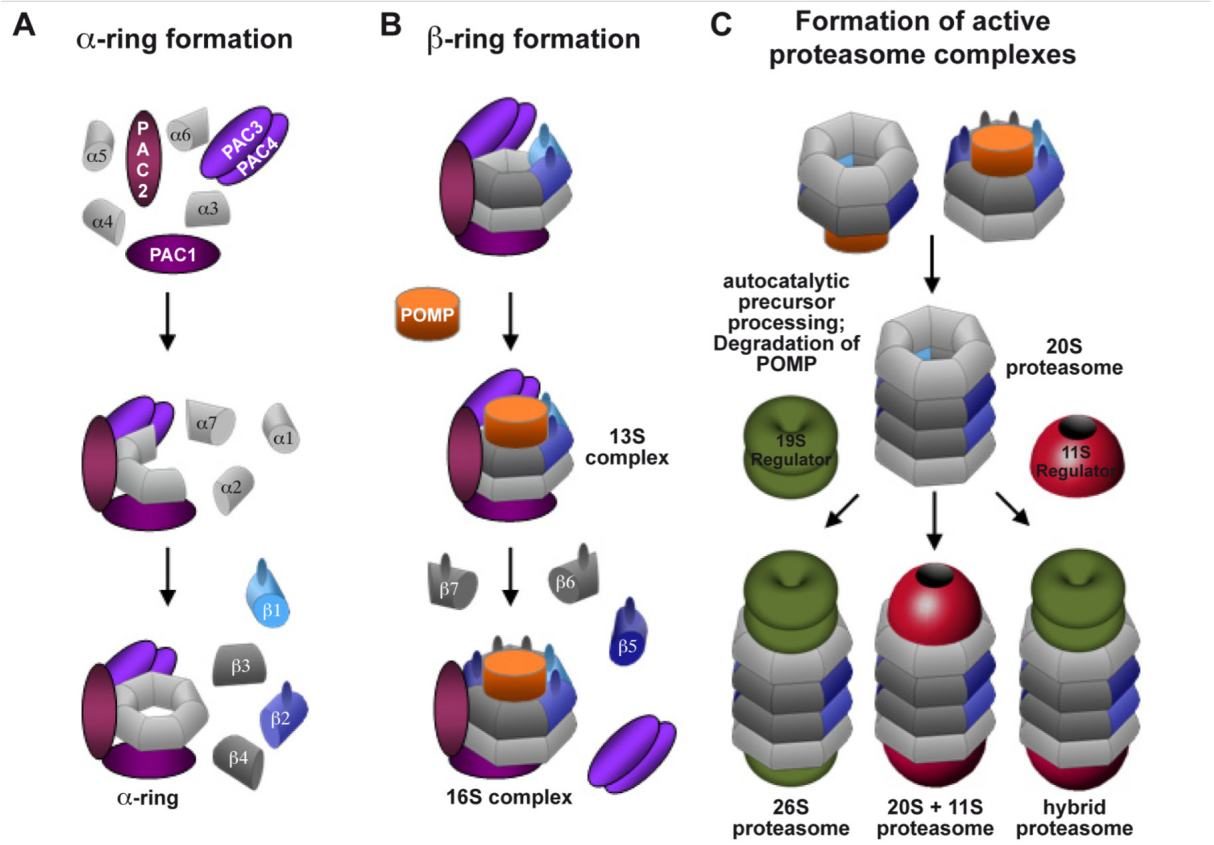

Figure I. Schematic diagramm of the consecutive steps in proteasome assembly
The diagramm schematically illustrates the consecutive steps in proteasome assembly and the known factors involved in this process. α-subunits are displayed in light grey, structural β-subunits in dark grey. The catalytic β-subunits, irrespective if immuno- or constitutive subunits are depicted in blue.

With the exeption of β3 and β4, the β-subunits are integrated as precursor subunits with N-terminal propeptides. The prosequence protects the N-terminal threonine residue of the catalytic subunits from chemical modifications, which is essential to maintain their catalytic activity (Arendt and Hochstrasser, 1999). The prosequences of the proteolytic subunits are

autocatalytically cleaved while the residual β-subunits are most likely processed by the adjacent catalytic subunits (Chen and Hochstrasser, 1996; Schmidtke, et al., 1996). The maturation of precursor β-subunits occurs in 13-16S complexes and is completed upon formation of 20S proteasomes (Frentzel, et al., 1994). This prevents premature proteolytic activity until self-compartmentalization of the active sites in the cavity of the 20S core is achieved (Baumeister, et al., 1998).

Further, information within the sequence of propeptides facilitates efficient integration into 20S proteasomes. While deletion of the β1i-propeptide still allows integration of β1i, the addition of charged residues to the prosequence inhibits its integration (Schmidt, et al., 1999). The propeptides of β2 and β2i were shown to provide differential integration efficiency to their carrying subunits. Especially the β2i-propeptide improved the integration when fused to β2 (De, et al., 2003). Similar results were obtained, when the propeptides of β5 and β5i were exchanged. While fusion of β5i improves the integration of β5, the combination of the β5-propeptide with β5i diminishes its integration (Kingsbury, et al., 2000). Although deletion of the β5i-prosequence still allows integration of β5i, maturation of proteasomes is impaired (Witt, et al., 2000). In summary, these findings underline the importance of the propeptides in the regulation of proteasome assembly.

Following the assembly of 20S proteasomes various regulators, which have been described above, bind to the endplates of the α-rings (Fig I C).

Interestingly, the rate of 20S proteasome assembly is not constant. Recently, it was shown that expression of β5i accelerates the rate of proteasome neogenesis (Heink, et al., 2005). Further, treatment of cells with irreversible proteasome inhibitors induces the concerted expression of proteasomal subunits to allow rapid regeneration of the proteasome pool (Meiners, et al., 2003). This is achieved by activation of the Nrf2-Keap1 signalling pathway, which leads to enhanced transcription of most proteasomal subunit genes via antioxidative response elements (ARE) in their promoters (Kwak, et al., 2002).

1.1.4 Regulation of proteasome composition

Despite the theoretical possibility of multiple combinations of constitutive and immunosubunits, the most abundant forms of 20S proteasomes are c20S or i20S. According to current opinion, formation of c20S or i20S is achieved by cooperative assembly of constitutive or immunosubunits, respectively. In this model, β5 preferentially interacts with β1 and β2 containing precursor proteasomes resulting in c20S, while β5i predominantly pairs with β1i and β2i to form i20S (Fig. II).

The cooperative model of proteasome assembly is based on observations in T2 cells, which carry a deletion in the MHC class II locus covering the genes *lmp2* and *lmp7* encoding for β1i and β5i, respectively. Following reconstitution of T2 cells with *lmp2* but not *lmp7*, pre-β1i and pre-β2i accumulate in precursor proteasomes. This finding suggests that β5i is crucial for efficient maturation of β1i and β2i containing proteasomes, while β5 integrates only inefficiently into these complexes. The specific interaction of immunosubunits is thought to be an intrinsic function of their propeptides (De, et al., 2003; Kingsbury, et al., 2000). In conclusion, formation of mixed proteasomes (m20S) with β1i/β2i/β5 or β1/β2/β5i stoichiometry is supposed to be a rare event (Griffin, et al., 1998) (Fig. II). Cooperative integration was further shown for β1i and β2i, which mutually facilitate their integration into 20S proteasomes (Groettrup, et al., 1997).

By now the stringent model of cooperative proteasome assembly has been enervated due to the identification of various proteasome subtypes with combinations of constitutive and immunosubunits. However, the formation of m20S with β1i/β2i/β5 stoichiometry is still regarded as highly inefficient (De, et al., 2003; Drews, et al., 2007; Kingsbury, et al., 2000; Klare, et al., 2007).

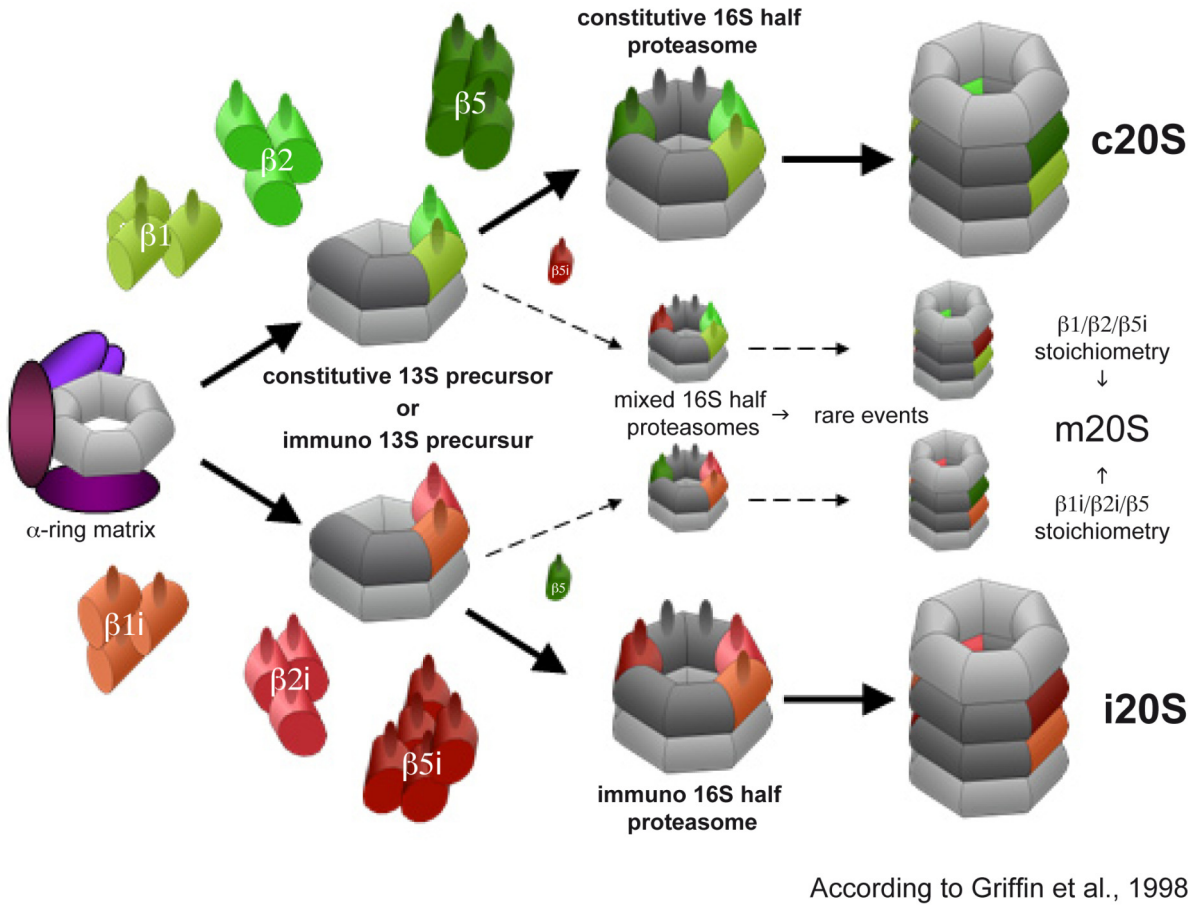

Figure II. Model of cooperative proteasome assembly
Schematic model of proteaome assembly according to Griffin et al., 1998. Constitutive subunits are coloured in green, immunosubunits in red. Specific integration of β5 into β1 and β2 containing precursor proteasomes results in formation of c20S, while β5i predominantly integrates into β1i and β2i containing precursor complexes forming i20S. However, formation of m20S is a rare event indicated by dotted arrows.

1.2 The function of proteasomes in the immune response

1.2.1 The MHC class I pathway of antigen presentation

The function of the major histocompatibility class I (MHC class I) pathway of antigen presentation is to allow the discrimination between immunological self and non-self. The peptide array presented by MHC class I molecules on the cell surface is scanned by $CD8^+$ T cells via their T cell receptor (TCR). Presentation of foreign or tumor antigens results in the rapid elimination of the respective cells by $CD8^+$ T cells (Elliott, 2006). The ubiquitin-proteasome pathway is the major source of peptides for MHC class I antigen presentation (Rock, et al., 1994). Thus, the peptides for MHC class I presentation usually arise from cytosolic proteins. An important source of peptides is defective ribosomal products (DRiPs), which summarize abnormal protein products resulting from defective translation, RNA splicing, folding or posttranslational modification. The use of DRiPs as a source of peptides couples antigen presentation with protein neosynthesis, which is believed to assure rapid presentation of new antigens, e.g. following viral infections (Yewdell, et al., 2001).

Peptides suitable for MHC class I presentation are translocated into the ER by the transporter associated with antigen presentation (TAP). Inside the ER lumen, the TAP complex is associated with the peptide loading complex, which contains the chaperones tapasin, calreticulin and ERp57 (Rock and Goldberg, 1999).

The MHC I molecule is a heterodimer consisting of a heavy chain and a β_2-microglobulin (β_2M). Assembly of this heterodimer is achieved by the action of the chaperones calnexin or BiP (immunglobulin binding protein) and ERp57. Upon association of the MHC class I heavy chain with β_2M calnexin is exchanged against calreticulin resulting in the peptide loading complex. MHC class I molecules associated to the peptide loading complex bind to the TAP complex via interaction with tapasin. Binding of a fitting peptide to the MHC binding grove stabilizes the MHC class I molecule, which is than transported to the cell surface (Antoniou, et al., 2003).

However, the peptides presented by this pathway have to comply with the requirements of the TAP complex and the structure of MHC class I molecules. The TAP complex preferentially transports peptides of 7-15 amino acids (Rock and Goldberg, 1999). Dependending on the haplotype of MHC class I molecules, binding is restricted to peptides of 8-10 amino acids (Rammensee, et al., 1993). Two defined anchor residues within the peptide sequence

additionally determine the stability of peptide binding to the MHC binding grove. Especially at the C-terminus of an epitope, exclusively basic or hydrophobic amino acids are accepted as anchor residues (Heemels and Ploegh, 1995).

The peptides generated by 26S proteasomes have a size range of 4-20 amino acids, of which less than 15% have the correct size for MHC class I binding (Kisselev, et al., 1999). Proteasomes usually generate the correct C-terminus of an epitope and the majority of peptides is produced as N-terminally extended precursors (Cascio, et al., 2001). These precursor epitopes are subjected to post-proteasomal processing either in the cytosol or the ER (Rock, et al., 2004). The cytosolic tripeptidylpeptidase II (TPPII) is involved in this trimming process, because it acts as an exoprotease that cleaves tripeptides from the N-terminus (Reits, et al., 2004). In addition, TPPII can directly process antigens by its endoproteolytic activity and thus complements proteasome function (Kloetzel, 2004; Seifert, et al., 2003). In the ER, especially the ER aminopeptidase 1 (ERAP1) is responsible for trimming of precursor epitopes (York, et al., 2002).

An important mechanism in MHC class I presentation is cross-presentation of particulate or extracellular antigens on professional antigen presenting cells (APCs), e.g. derived from apoptotic cells, which are initially taken up by phagocytosis. Although phagolysosomes are equipped with multiple proteases themselves, efficient cross-presentation of antigens on MHC class I molecules involves the transfer of proteasome substrates to the cytosol (Norbury, et al., 2004). The Sec61 translocon, which is found in phagolysosomal membranes following fusion with ER membranes, is involved in such retrograde transport of proteasomal substrates (Ploegh, 2004). Consequently, cross-presentation involves the classical MHC class I pathway of antigen presentation.

Besides the classical MHC class I pathway described above, formyl-methione containing peptides are presented by non-classical MHC class Ib molecules such as H2M3 in mice. These peptides are directly released into the cytosol by pathogenic bacteria and are independent of further processing. They directly enter the ER via the TAP complex, where they are bound to empty MHC class Ib molecules, which are stored in the ER due to a lack of endogenous peptides (Pamer, 2004). Presentation of bacterial antigens on MHC class Ib molecules plays a crucial role in early adaptive immune responses (Kerksiek, et al., 1999; Seaman, et al., 2000).

1.2.2 The influence of proteasome composition on epitope processing

The MHC class I pathway of antigen presentation is a remarkably inefficient process. As already described, less than 15% of peptides generated by 26S proteasomes have the correct size of 8-10 amino acid residues for MHC class I binding. Although N-terminally extended precursor epitopes can be processed to proper $CD8^+$ T cell epitopes, most of them are degraded to free amino acids by other aminopeptidases in the cytosol before they reach the ER lumen. Further, the enzymes involved in antigen processing can also destroy epitopes by unspecific cleavages. Consequently, less than 0.01% percent of the generated epitopes are presented on MHC class I molecules on the cell surface (Yewdell, et al., 2003). Indeed, the activity of proteasomes was shown to be limiting for MHC class I presentation (Benham and Neefjes, 1997).

The expression of β1i, β2i and β5i and subsequent formation of i20S is generally believed to improve the efficiency of MHC class I presentation. In agreement with this, β1i and β5i are encoded in the MHC class II locus adjacent to the genes of TAP, suggesting a role in antigen presentation (Glynne, et al., 1991). Accordingly, replacement of constitutive subunits by immunosubunits modifies the specificity and activity of 20S proteasomes:

Replacement of β1 by β1i especially reduces the caspase-like activity and thus limits the amount of peptides with acidic C-termini that are incompatible with the MHC class I binding grove. Instead, integration of β1i enhances the chymotrypsin-like activity, which results in the generation of peptides with hydrophobic C-termini optimal for MHC class I binding (Groettrup, et al., 2001).

The impact of the exchange of β2 by β2i is unclear. Both subunits possess trypsin-like activity, which produces peptides with basic C-termini, necessary for the generation of some $CD8^+$ T cell epitopes. Overexpression of an catalytically inactive β2i subunit results in complete loss of trypsin-like activity (Salzmann, et al., 1999). However, the trypsin-like activity in *mecl1*$^{-/-}$ mice is unaltered compared to WT mice, showing that β2 can completely substitute for β2i (Basler, et al., 2006).

Overexpression of β5i increases the chymotrypsin-like and the trypsin-like activity, indicating enhanced substrate turnover by the resulting proteasomes and consequently improved MHC class I presentation (Gaczynska, et al., 1994). In agreement with this finding, the MHC class I surface density on various cell types of *lmp7*$^{-/-}$ mice was found to be 25-50% reduced due to a

lack of generated epitopes (Fehling, et al., 1994). Further, *lmp7*$^{-/-}$ cells present a substantially different peptide repertoire on MHC class I molecules suggesting that the presence of β5i modifies epitope quantity and quality (Toes, et al., 2001). In addition, Heink et al. demonstrated that expression of β5i increases the rate of proteasome neogenesis enabling rapid formation of i20S in infection and inflammation (Heink, et al., 2005). These findings collectively underline the special importance of this immunosubunit for efficient MHC class I antigen presentation.

In summary, these observations suggests that immunosubunits are adapted to the requirements of MHC class I presentation. Indeed, processing of a variety of $CD8^+$ T cell epitopes is substantially facilitated in the presence of i20S (Kuckelkorn, et al., 2002; Sijts, et al., 2000; Sijts, et al., 2000; Strehl, et al., 2006; Toes, et al., 2001; Van den Eynde and Morel, 2001).
In contrast, some tumor- and subdominant viral epitopes are also destroyed by the action of i20S while others are not affected by the proteasome composition at all (Basler, et al., 2004; Chapiro, et al., 2006; Kloetzel, 2001; Morel, et al., 2000). Still, the increased output of epitopes with hydrophobic and basic C-termini strongly suggests that i20S improve the processing of the majority of $CD8^+$ T cell epitopes. This is not only caused by increased substrate turnover, but also by modified cleavage site specificity. Accordingly, it was shown for some epitopes that i20S can specifically increase the rate of cleavages, which result in the correct C-terminus of an epitope, while destructive cleavages within an epitope are reduced (Strehl, et al., 2008). In conclusion, i20S facilitate MHC class I presentation by enhanced quantity and quality of $CD8^+$ T cell epitopes.
Besides i20S, the expression of the 11S regulator increases the overall peptidase activity of proteasomes irrespective of the subunit composition of the associated 20S complex. As the maximal proteasome activity remains unaffected by 11S regulators, it is suggested that they accelerate substrate access and product release (Groettrup, et al., 1996; Schwarz, et al., 2000; Stohwasser, et al., 2000). However, the 11S complex can also specifically improve the processing of some $CD8^+$ T cell epitopes without affecting substrate turnover (Dick, et al., 1997; van Hall, et al., 2000).
In summary, the IFNγ inducible i20S and 11S regulators cooperatively improve epitope processing especially in infection and inflammation. Further, they are constitutively expressed in lymphoid tissues, especially in professional APCs, which is commonly thought to assure optimal MHC class I antigen presentation (Kuckelkorn, et al., 2002; Li, et al., 2001; Macagno, et al., 1999; Macagno, et al., 2001).

1.2.3 Function of $CD8^+$ T cells

The MHC class I restricted $CD8^+$ T cells represent a major arm of the adaptive immune response. Their main function is the recognition of infected or tumor cells. The specific recognition of antigenic epitopes is mediated by the TCR, which is a heterodimer of a α- and β- or γ– and δ- chain. The diversity of TCRs is achieved by random rearrangement of a variety of gene segments encoding fragments of the different chains (Janeway, et al., 2001).
The education of immature T cells occurs in the thymus by positive and negative selection. T cells that can bind with low affinity to self-antigens presented by thymic cortical epithelial cells are positively selected. In contrast, T cells that strongly react against self-antigens presented on medullary thymic epithelial cells, thymic dendritic cells (DCs) or Macrophages (Mϕ) are deleted. T cells that survive the thymic selection process egress to the periphery and contribute to the T cell repertoire that can react against foreign antigens (von Boehmer, et al., 2003).
Naive $CD8^+$ T cells reside within peripheral lymphoid tissues, until they encounter a foreign antigen presented on activated, professional APCs like DCs or Mϕ. The combination of TCR stimulation and costimulatory signals activates naive $CD8^+$ T cells. Following activtion, they start to proliferate and develop into cytotoxic $CD8^+$ effector T cells, a process known as T cell priming. Important costimulatory signals are provided by CD28 or CD137-ligand on $CD8^+$ T cells binding to CD80/CD86 (B7.1/B7.2) or CD137 on the APCs (Shedlock, et al., 2003; Whitmire and Ahmed, 2000). The proliferation is driven by the secretion of Interleukin 2 (IL-2) and simultaneous upregulation of IL-2-receptor, which results in autocrine stimulation (Wong and Pamer, 2004).
Further, priming results in down-regulation of the adhesion molecule CD62L (L-selectin) and the chemokine receptor CCR7, which retain naive $CD8^+$ T cells in the lymphoid compartment. Consequently, $CD8^+$ effector T cells egress to the periphery where they detect infected or inflamed tissues by recognition of adhesion molecules, such as ICAM-1 or VCAM-1, on endothelial cells. Due to these danger signals they adhere to the endothelium and transmigrate from the blood vessels into the infected or inflamed tissue (Weninger, et al., 2002).
When $CD8^+$ effector T cells recognize their cognate antigen on infected or tumor cells, they can mediate cytolysis by two distinct mechanisms. First, by secretion of cytotoxic granules, which contain the pore-forming perforin and proteolytic granzymes. On the one hand this

induces uncontrolled ion leakage and on the other hand the transferred granzymes activate caspases, which leads to apoptosis of the target cell. The second mechanism induces apoptosis by Fas/Fas-ligand interactions between $CD8^+$ T cells and the target cell. Lysis of infected target cells exposes intracellular pathogens to the extracellular space, where they can be attacked by innate defence mechanisms. Further, apoptosis of target cells allows cross-presentation by professional APCs and subsequent cross-priming of more $CD8^+$ T cells. In addition, activated $CD8^+$ effector T cells secrete IFNγ and TNFα, which promote inflammation resulting in enhanced recruitment of lymphocytes (Janeway, et al., 2001).
Although a variety of epitopes of a given antigen are presented to $CD8^+$ T cells, the majority reacts against a few selected epitopes, a phenomenon described as immunodominance. Among these few epitopes the response is skewed to a large fraction of $CD8^+$ T cells that react against one or two immunodominant epitopes, while few $CD8^+$ T cells are directed against subdominant epitopes resulting in a defined immunodominance hierarchy. Immunodominance is influenced by many factors: The stability of a given peptide MHC class I complex; the efficiency of antigen-processing, the strength of the TCR-MHC class I interaction, the frequency of naive $CD8^+$ T cells in the T cell repertoire and suppression of subdominant by immunodominant T cell responses (Chen, et al., 2000; Yewdell and Bennink, 1999).

1.2.4 The impact of proteasome subunit composition on $CD8^+$ T-cell responses

Efficient $CD8^+$ T cell priming and expansion requires a certain treshold of MHC class I antigen presentation on professional APCs. Beyond that treshold, the magnitude of the $CD8^+$ T cell response is largely independent of antigen quantity (Vijh, et al., 1998; Wong and Pamer, 2003). Further, the kinetics with which an antigen is presented on the cell surface critically influences priming of $CD8^+$ T cells (Badovinac, et al., 2002; Mercado, et al., 2000; Williams and Bevan, 2004). Both, quantity as well as processing kinetics of an antigen is influenced by the proteasome subunit composition as described previously. Different proteasome types were also shown to be involved in thymic selection, indicating that proteasomes already influence early $CD8^+$ T cell development (Murata, et al., 2007; Nil, et al., 2004).

Experiments with immunosubunit deficient mice confirmed that proteasome composition influences the development of $CD8^+$ T cell responses *in vivo.* Alterations in the $CD8^+$ T cell repertoire due to differential thymic selection have been detected in *mecl1*$^{-/-}$, *lmp2*$^{-/-}$ and *lmp7*$^{-/-}$ mice (Basler, et al., 2006; Chen, et al., 2001; Osterloh, et al., 2006; Toes, et al., 2001). Further, differences in immunodominance hierachies of $CD8^+$ T cells responding to viral infections were found in *lmp2*$^{-/-}$ and *lmp7*$^{-/-}$ mice (Chen, et al., 2001; Nussbaum, et al., 2005; Robek, et al., 2007).

In addition, impaired priming and expansion of $CD8^+$ T cells directed against i20S dependent epitopes was recently reported in immunosubunit deficient mice (Deol, et al., 2007; Palmowski, et al., 2006; Robek, et al., 2007). However, $CD8^+$ T cell responses directed against some of the examined epitopes were unaffected by immunosubunit deficieny (Chen, et al., 2001; Deol, et al., 2007; Nussbaum, et al., 2005). In conclusion, this indicates that immunosubunit deficiency specifically affects $CD8^+$ T cell responses directed against epitopes whose processing is dependent on i20S activity. Further, this suggests that the activity of i20S can, but must not necessarily, be critical to achieve the treshold of antigen presentation required for efficient $CD8^+$ T cell priming.

Although these reports focused on the analysis of $CD8^+$ T cell responses, the impact of immunosubunit deficiency on control of infections was rarely determined. Only for the lymphocytic choriomeningitis virus (LCMV) it was shown, that viral clearance is not affected in *lmp2*$^{-/-}$ and *lmp7*$^{-/-}$ mice (Nussbaum, et al., 2005). However, the influence of proteasome subunit composition on control of a bacterial infection that depends on the action of $CD8^+$ T cells, like *Listeria monocytogenes*, has not been considered so far.

1.2.5 The infection model of *Listeria monocytogenes*

Listeria monocytogenes (Listeria) is a gram-positive bacterium known as a food borne pathogen in humans. Infection of mice is a well characterized model of systemic bacterial infection (Pamer, 2004).

Listeria can enter their host cells by expression of the surface proteins internalin A (InlA) and internalin B (Inl B). While InlA binds to epithelial cadherin (E-cadherin) and promotes entry into epithelial cells, InlB interacts with the hepatocyte growth factor receptor for invasion of hepatocytes. Once taken up by a cell, Listeria express the major virulence factor Listeriolysin O (LLO), which disrupts the phagosomal membrane and allows the bacteria to escape into the

cytosol, where they start to replicate. Further, they express the actin-assembly-inducing protein A (ActA). ActA utilizes Actin of the host cell and mediates transport of the bacteria to neighbouring cells. By this mechanism Listeria can spread from cell to cell, without being exposed to the extracellular space (Pamer, 2004).

Following intravenous (i.v.) infection, the majority of Listeria are filtered from the bloodstream in the liver. Extracellular bacteria are initially bound to Kupffer cells, the tissue resident Mϕ of the liver, and are subsequently killed by immigrating neutrophils (Gregory, et al., 1996). Listeria, that survived the early innate immune defence invade hepatocytes, in which they start to replicate. However, activation of Kupffer cells and neutrophils results in the release of proinflammatory cytokines such as IL-1, IL-6, IL-12 and TNFα as well as nitric oxide (NO). This results in lymphocyte recruitment to the site of infection. Among infiltrating lymphocytes, NK and NKT cells are activated by the cytokine milieu as well as bacterial components and consequently secrete IFNγ (Cousens and Wing, 2000; Ranson, et al., 2005). IFNγ, IL-6 and TNFα synergistically induce the NADPH oxidase $p47^{phox}$ in hepatocytes resulting in the production of reactive oxygene intermediates (ROI) (Gregory and Wing, 1993; Szalay, et al., 1995). Further, IFNγ activates infiltrating Mϕ, which subsequently secrete reactive nitrogen intermediates (RNI) produced by the inducible nitric oxide synthase (iNOS) (MacMicking, et al., 1995).

In spleen and lymph nodes, Listeria are predominantly taken up by Mϕ and DCs (Conlan and North, 1994). Besides activated Mϕ, a population of TNFα and iNOS producing DCs (TipDCs) was found to exert substantial antilisterial activity in the spleen (Serbina, et al., 2003).

In summary, the oxidative burst restricts the replication of Listeria in liver and spleen, which consequently reaches a plateau 3-4 days after infection until onset of adaptive immunity (Gregory, et al., 1992; Mackaness, 1962).

The adaptive immune response against Listeria is of the T helper type 1 (Th1) phenotype. Secretion of IL-12, IL-18 and IFNγ by cells of the innate immune system is responsible for the polarization of naive, MHC class II restricted $CD4^+$ T cells to the Th1 phenotype (Seki, et al., 2000). $CD4^+$ Th1 cells secrete IFNγ, which contributes to the activation of $CD8^+$ effector T cells. The $CD8^+$ T cell response can be devided in two overlapping waves; the MHC class Ib restricted and the classical MHC class I restricted $CD8^+$ T cells.

The MHC class Ib restricted $CD8^+$ T cells represent an early arm of adaptive immunity, important for the early control of Listeria 3-7 days post infection. Three dominant n-formyl-

methionine containing peptides presented on the MHC class Ib molecule H2M3 are recognized by those $CD8^+$ cells (Kerksiek, et al., 1999; Seaman, et al., 2000).
In contrast, the classical MHC class I restricted $CD8^+$ T cell response peaks 7-10 days following infection with Listeria. They are crucial for the complete irradication of infected cells from the tissue. The major antigens for MHC class I restricted $CD8^+$ T cells are derived from the secreted proteins LLO and murein hydrolase p60 (Pamer, 2004). In mice with the $H2^b$ haplotypic background, the $CD8^+$ T cell response is distributed against a variety of epitopes with no clear immunodominance hierarchy. However, among these, the strongest $CD8^+$ T cell response is elicited against the epitope $LLO_{296-304}$ (Geginat, et al., 2001). Previously, we demonstrated that efficient processing of this epitope depends on the specific activity of i20S (Strehl, et al., 2006).

1.2.6 Putative influences of the proteasome subunit composition on innate immune defence mechanisms

Transcription factors of the NF-κB family are central regulators of innate and inflammatory immune responses, as they control the expression of proinflammatory cytokines, chemokines, costimulatory and adhesion molecules. Activation of NF-κB is a two-step process, which involves degradation of the inhibitory IκB proteins and processing of the NF-κB precursors p105 or p100 to the mature subunits p50 or p52, respectively. This allows the formation of active NF-κB heterodimers (p65/p50, cRel/p50 or RelB/p52), which enter the nucleus and activate gene transcription. The IκBs and the NF-κB precursors are targeted for degradation by ubiquitination. Accordingly, 26S proteasomes are involved in both steps of NF-κB activation (Bonizzi and Karin, 2004). However, it has also been shown that 20S proteasomes can cleave IκB or p105 independent of ubiquitination (Alvarez-Castelao and Castano, 2005; Moorthy, et al., 2006). Especially the chymotryptic activity is essential for efficient processing of p105 and degradation of IκBα by 20S proteasomes (Petrof, et al., 2004). Thus it is conceivable that i20S with their increased chymotrypsin-like activity facilitate NF-κB activation. Indeed, it was reported in different model systems that i20S can promote NF-κB activation (Fitzpatrick, et al., 2006; Hayashi and Faustman, 1999; Hayashi and Faustman, 2000; Visekruna, et al., 2006).

1.3 Aims of this study

The subunit composition of the 20S proteasome strongly influences its activity and specificity. Consequently, cells lacking IFNγ inducible subunits generate different peptide pools presented by MHC class I molecules, which can have functional consequences for $CD8^+$ T cell responses. The aim of this study is to analyse the structural and functional impact of β5i-deficiency in *lmp7*$^{-/-}$ mice during *Listeria monocytogenes* infection.

It is suggested that β5i is crucial for the efficient maturation of β1i and β2i containing precursor proteasomes. Due to this model of cooperative proteasome assembly it is claimed that the integration of β1i and β2i in *lmp7*$^{-/-}$ mice is largely aborted. (Fig.II) (Griffin, et al., 1998; Kingsbury, et al., 2000). In contrast, integration of β1i and β2i in proteasomes of *lmp7*$^{-/-}$ splenocytes has been observed previously (Stohwasser, et al., 1996), but the rate of their integration has not been analysed in detail. Thus, major aims of this study regarding the structural analysis of proteaomes are:

- Quantitative and qualitative analysis of the maturation of β1i and β2i in lymphoid and non-lymphoid tissues of *lmp7*$^{-/-}$ mice infected with Listeria;
- Determination of the actual impact of β5i deficieny on proteasome maturation *in vivo*.

In addition, the functional consequences of β5i-deficiency on antilisterial immunity were analyzed. Our previous work demonstrated, that efficient generation and consequently presentation of the Listeriolysin O derived MHC class I epitope $LLO_{296\text{-}304}$ depends on the presence of i20S (Strehl, et al., 2006). Hence, we expect that processing of this model epitope is impaired in *lmp7*$^{-/-}$ mice. As reduced antigen presentation can affect priming and expansion of $CD8^+$ T cells as well as recognition of infected target cells, we aimed to investigate:

- Processing of the $LLO_{296\text{-}304}$ epitope by 20S proteasomes isolated from *lmp7*$^{-/-}$ mice;
- the $LLO_{296\text{-}304}$ specific $CD8^+$ T cell response in *lmp7*$^{-/-}$ mice;
- the impact of β5i-deficiency on bacterial control during the course of Listeria infection.

2 Material and Methods

2.1 Methods

2.1.1 Mice

2.1.1.1 Breeding of mice

Mice were kept under special pathogen free conditions (spf) with a 12 h day light cycle. C57Bl6/N mice were obtained from Elevage Janvier (Le Genest Saint Isle, France). Homozygous colonies of *lmp7*$^{-/-}$ mice on C57Bl6/N background and 129Ola WT mice were bred at the animal breeding facility of the Max Planck Institute for Infection Biology (MPIIB, Berlin-Marienfelde, Germany). *lmp7*$^{-/-}$ mice on 129Ola background and breeding pairs of *lmp7*$^{-/-}$ mice on C57Bl6/N background were kindly provided by Prof. Dr. Hans Joerg Schild (Johannes Gutenberg University, Mainz, Germany)

2.1.1.2 Infection of mice with Listeria monocytogenes

For the maintenance of bacterial virulence, infection stocks of *Listeria monocytogenes* EGD (Listeria) were generated by passage through C57Bl6/N mice. Briefly, mice were infected intravenously (i.v.) with 5 x 10^3 colony forming units (cfu) of Listeria and sacrificed two days later. Spleens were homogenized and inoculated in Tryptic Soy Broth at 37°C. Listeria were grown to a density of 1-2 x 10^8 cfu/ml; aliquots were frozen in liquid nitrogen and stored at -80°C. CFU counts were determined by plating serial dilutions on Palcam Agar Plates according to van Netten et al., 1989 (Merck, Darmstadt, Germany). For infection experiments, Listeria stocks were thawed and diluted in 1x phosphate buffered saline (PBS). 8-16 weeks old male mice were i.v. infected via the tail vein with 1-5 x 10^3 cfu of Listeria in a volume of 200 µl. The infection experiments were performed at the S2 animal facility of the MPIIB (Berlin-Mitte, Germany).

2.1.1.3 Determination of bacterial titers

Following infection with Listeria, mice were sacrificed by cervical dislocation. Organs were homogenized in 1 ml sterile icecold PBS. 10fold serial dilutions were plated on Palcam Agar Plates according to van Netten et al. and incubated at 37°C. Bacterial colonies were counted 24-48 h later.

2.1.2 Cell culture

2.1.2.1 Phoenix E cells

Phoenix E cells, for ecotrophic packaging of retroviral vector constructs, were kept in Dubelcos Modified Eagle Medium (DMEM, Gibco, Carlsbad, CA, USA) with 10% fetal calf serum (FCS), 1 mM L-Glutamin, 1 mM Sodium-Pyruvate, 1x Pencillin/Streptomycin solution (Gibco). For passaging, cells were trypsinized in 1x Trypsin-EDTA solution (Gibco).

2.1.2.2 Preparation of murine embryonic fibroblasts (MEFs)

13-14 days old embryos were decapitated and inner organs were removed. The residual tissue was minced in 10 ml 1x trypsin-EDTA solution (Gibco) and incubated for 15 min at 37°C. Then, pieces of tissue were dissociated by pipetting. 15 ml of fresh 1x trypsin-EDTA solution were added and cells were incubated for another 15 min at 37°C. Following incubation, the residual peaces of tissue were dispersed and the resulting cell solution was transferred to a 50 ml reaction tube. 20 ml of D10 medium (DMEM (Gibco), 10% FCS, 1 mM L-Glutamin, 1 mM Sodium-Pyruvat, 1x Pencillin/Streptomycin solution (Gibco) were added and cells were sedimented by centrifugation at 1500 rpm for 5 min. The supernatant was discarded, cells were washed in 20 ml D10 medium and centrifuged at 1500 rpm for 5 min. 1 x 10^7 cells were seeded in a 150 cm^2 tissue culture flask in D10 medium and kept in a 37°C incubator with 5% CO_2. Medium was renewed the next day to remove non-adherent cells. MEFs were passaged by trypsinization in 1x trypsin EDTA solution. Spontanious immortalization of MEFs was achieved by frequent passaging. Following 16-18 passages the MEFs were regarded as immortalized cell lines.

2.1.2.3 Preparation of bone-marrow derived macrophages (BM-Mϕ)

Femurae and tibiae were prepared from 10-16 week old male mice. The bones were washed in 70% ethanol for 1 min to kill attached cells, before they were put in D10 medium. Then, the epiphyses were cut off and the bone marrow was flushed out in 1x PBS with a syringe. Bone-marrow cells were resuspended to a single cell solution and centrifuged for 5 min at 1500 rpm. Subsequently, bone marrow cells were resuspended in BM-Mϕ medium (DMEM (Gibco), 10% FCS, 5% horse serum, 20% cell culture supernatant of macrophage colony stimulating factor (M-CSF) producing L929-CSF cells (MPIIB, Berlin, Germany), 1 mM L-Glutamine, 1 mM Sodium-Pyruvate, 1x Penicillin/Streptomycin solution). 5 x 10^6 bone marrow cells were seeded per cell culture dish with 10 cm diameter in 10 ml BM-Mϕ medium and incubated at 37°C, 5% CO_2. After 5 days 5 ml of fresh BM-Mϕ medium were added per cell culture dish. Following 7-8 days of culture in BM-Mϕ medium the bone marrow cells were differentiated into BM-Mϕ.

2.1.3 Biochemical methods

2.1.3.1 Preparation of organ lysates

Murine organs frozen in liquid nitrogen were homogenzid to powder with mortar and pestle. An equal volume of Native Lysis Buffer (1x NativePAGE™ Sample Buffer (Invitrogen, Carlsbad, CA, USA), 0,5% DDM, 0,2 mM Sodium Vanadate, 5 mM Sodium Fluoride, 1 mM PMSF, 1 mM Pefabloc® SC (Roche Applied Science, Mannheim, Germany), 1x Complete protease inhibitor cocktail (Roche Applied Science)) or Lysis Buffer (20 mM Tris HCl pH 7,2, 50 mM NaCl, 1 mM EDTA, 1 mM NaN_3, 1 mM DTT, 0,1% Nonidet P40, 0,2 mM Sodium Vanadate, 5 mM Sodium Fluoride, 1 mM PMSF, 1 mM Pefabloc® SC (Roche Applied Science), 1x Complete protease inhibitor cocktail (Roche Applied Science)) was added for 2D Two colour Fluorescent Western Blot analysis or Two colour Fluorescent Western Blot analysis, respectively. Samples were mixed until the powder was thawed. Following three freeze thaw cycles with freezing in liquid nitrogen and thawing on ice, samples were centrifuged for 30 min at 13.000 rpm and 4°C in a Microfuge. For Two colour Fluorescent Western Blot analysis supernatants were aliquoted, frozen in liquid nitrogen and stored at -80°C for further use. Supernatants for 2D Two colour Fluorescent Western Blot analysis were centrifuged for another 20 min at 50.000 rpm and 4°C. The clear supernatants were frozen in liquid nitrogen. The protein concentration in the lysates was measured with Protein-Assay solution (Bio-Rad, Hercules, CA, USA) according to manufacturers instructions against a standard row of bovine serum albumin (BSA).

2.1.3.2 Preparation of cell lysates

MEFs were harvested by trypsinization and washed in icecold 1x PBS. Sedimented cells were resuspended in icecold Lysis Buffer (see 2.1.3.1). Following three freeze thaw cycles with freezing in liquid nitrogen and thawing on ice, cellular debris was sedimented for 30 min at 13.000 rpm and 4°C in a Microfuge. The cleared supernatants were frozen in liquid nitrogen and stored at -80°C. The protein concentration in the lysates was measured with Protein-Assay solution (Bio-Rad, Hercules, CA, USA) according to manufacturer`s instructions against a standard row of bovine serum albumin (BSA).

2.1.3.3 Two Colour Fluorescent Western Blot analysis

25-50 µg total protein per lane of organ lysates and 10-25 µg per lane of cell lysates denaturated in 1x Laemmli Buffer were seperated by SDS-PAGE. Tris-Glycine buffered SDS-polyacrylamide gels with 5% stacking gel and 15% resolving gel according to (Laemmli, 1970) were used. Gels were run in Tris-Glycine Running Buffer (25 mM Tris, 250 mM Glycine, 0,1% (w/v) SDS) at 10-15 V/cm for 70-90 min. Following SDS-PAGE

proteins were transferred to Immobilon-FL PVDF (Millipore, Billerica, MA, USA) or nitrocellulose membrane (Pierce, Rockford, IL, USA) with 0,45 µm poresize by electroblotting. Protein transfer was performed in a Mini Transblot Cell (Biorad) at 400 mA in Transfer Buffer (50 mM Tris, 40 mM Glycine, 0,037% (w/v) SDS, 20% (v/v) Methanol) for 70 min at 4°C. Following protein-transfer, membranes were blocked in Odyssey Blocking Reagent (Licor Bioscience, Lincoln, NE, USA) for 1 h at room temperature or at 4°C over night. Then, membranes were successively stained with rabbit or chicken polyclonal antibodies against proteasomal subunits or POMP; mouse monoclonal GAPDH-antibodies as a loading control; anti-rabbit IgG AlexaFluor680 or anti-chicken IgG IrDye700 conjugated secondary antibodies, respectively, and at last with anti-mouse IgG IrDye800 labelled secondary antibodies. All antibodies were diluted in Odyssey Blocking Reagent at an assay depend dilution (see 2.2.1) and incubated for 1 h at room temperature or over night at 4°C. Membranes were washed thrice for 5 min with 1x PBS, 0.05% Tween20 following each staining. In the end membranes were scanned with the Odyssey® Infrared Imaging system (Licor Biosciences). AlexaFluor680 and IrDye700 conjugated secondary antibodies were detected in the 700 nm channel (red signals) and IrDye800 conjugated secondary antibodies in the 800 nm channel (green signals). Densitometric analysis was performed with the Odyssey® Image Analyser Software Vers.1.2 (Licor Biosciences). Normalized band intensities were calculated by deviding the band intensity of the analysed protein through the band intensity of the loading control GAPDH.

2.1.3.4 2D Two Colour Fluorescent Western Blot analysis

In the first dimension, protein complexes were separated by Blue Native PAGE according to (Camacho-Carvajal, et al., 2004). Briefly, 50-100 µg total protein per lane of organ lysates in 1x Native Lysis Buffer (see 2.1.3.1) supplemented with 0,125% (v/v) NativePAGE™ G-250 Sample Additive (Invitrogen) were loaded on NativePAGE™ Novex 4-16% Bis-Tris Gels (Invitrogen). Gels were run in an XCell *SureLock™* Mini-cell (Invitrogen) with 1x NativePAGE™ Running Buffer (Invitrogen) as Anode Buffer and 1x Dark-Blue Cathode Buffer (1x NativePAGE™ Running Buffer, 1x Cathode Buffer Additive (Invitrogen)). Following 30 min of electrophoresis at 150 V, the Dark-Blue Cathode Buffer was exchanged against the Light-Blue Cathode Buffer (1x NativePAGE™ Running Buffer, 0.1x Cathode Buffer Additive) and gels were run for another 60 min. Following electrophoresis, gels were sliced into single lanes. For the second dimension, the protein complexes were denaturated by equilibration of the gel slices in 2x Laemmli Buffer (Laemmli, 1970) for 30 min at room temperature. Subsequently, the gel slices were placed in a preparative slot of a SDS-PAGE with 5% stacking and 15% resolving gel. SDS-PAGE, protein transfer to Immobilon-FL PVDF membranes and blocking was performed as described previously (see 2.1.3.3). All membranes were stained against proteasome subunit α3 with a mouse monoclonal antibody (Calbiochem, Darmstadt, Germany) and IrDye800 conjugated anit-mouse IgG secondary

antibodies. As α3 is a component of early to late proteasome complexes this staining indicates the positions of different proteasome complexes according to their separation in the first dimension. Further, membranes were stained against other proteasomal subunits and POMP with rabbit or chicken polyclonal antibodies (see 2.2.1) and anti-rabbit IgG AlexaFluor680 or anti-chicken IgG IrDy700 labelled secondary antibodies, respectively. Staining of membranes was performed as described previously (2.1.3.3). In the end, membranes were scanned and evaluated with the Odyssey® Infrared Imaging system (Licor Biosciences).

2.1.3.5 Coimmunoprecipitation analysis

WT MEFs stably overexpressing β5 or β5i with a C-terminal Flag-tag (DYKDDDDK) were generated by retroviral transduction (see 2.1.4.4-2.1.4.6). WT MEFs transduced with an empty vector construct were used as a negativ control. The MEFs were either left untreated or cultured for 4 days in the presence of 100 U/ml IFNγ (Strathmann Biotec, Hannover, Germany) in D10 medium. Cell lysates were prepared as previously described (2.1.3.2). Anti-Flag® M2 Affinity Gel (Sigma-Aldrich, Munich, Germany) was washed twice in TBS (25 mM TrisHCl pH 7.2, 50 mM NaCl) before use according to manufacturers instructions. 500 µg total protein diluted in 1 ml Lysis Buffer (see 2.1.3.2) were mixed with 40 µl Anti-Flag® M2 Affinity Gel and shaked head over tail at 4°C for 2 h. Subsequently, the gel matrix was sedimented by centrifugation for 30 sec at 8000 xg and the supernatant was discarded. Than, the gel matrix was washed 3 times with 0,5 ml TBS. In the end the matrix was resuspended in 1x Laemmli Buffer (Laemmli, 1970) and incubated at 95°C for 2 min. Coimmunoprecipitation of β1, β2, β1i and β2i with β5- or β5i-Flag, respectively, was analysed by Two Colour Fluorescent Western Blot Analysis (see. 2.1.3.3).

2.1.3.6 20S proteasome activity assay

The proteolytic activity of 20S proteasomes was measured with fluorogenic peptide substrates. The chymotrypsin-like activity was routinely assayed with the substrate Suc-LLVY-AMC (Biomol, Hamburg, Germany). 1 µg purified 20S proteasomes or 10 µl of fractions from the purification of 20S proteasomes (2.1.3.7) were added to 100 µl reaction buffer (50 mM TrisHCl pH7.5, 10 mM NaCl, 30 mM KCl, 0,1 mM EDTA, 20 µM Suc-LLVY-AMC) and incubated at 37°C for 1 h in the dark. For the determination of background proteolytic activity each sample was measured in presence or absence of 10 µM of the proteasome inhibitor MG132 (Sigma-Aldrich). Following incubation, the resulting fluorescence was detected with a Fluoroscan Ascent microplate reader (Thermo Labsystems, Waltham, MA, USA) at 355 nm excitation and 460 nm emission wavelength.

2.1.3.7 Purification of 20S proteasomes

Organs were homogenized in Lysis Buffer (see 2.1.3.1) with a T8 basic Ultra-Turrax® (ISA® Maschinenbau, Staufen, Germany). The tissue homogenate was further broken up with a douncer and cleared by centrifugation at 17000 rpm for 30 min at 4°C. The organ lysates were mixed with DEAE Sephacel (GE Healthcare, Buckinghamshire, UK) eqilibrated in 2x TEAD (40 mM TrisHCl pH7.2, 2 mM EDTA, 2 mM NaN_3, 2 mM DTT) and shaken head over tail for 1 h at 4°C. The loaded DEAE Sephacel was transferred to a column and washed with 10-15 column volumes icecold 1x TEAD (20 mM TrisHCl pH7.2, 1 mM EDTA, 1 mM NaN_3, 1 mM DTT) supplemented with 50 mM NaCl until the flow through exhibited an absorbtion at A=280 nm below 0,08. This washing step was repeated with 1x TEAD, 150 mM NaCl. Subsequently, proteins were eluted with 1x TEAD, 350 mM NaCl and fractions with high chymotrypsin-like activity (2.1.3.6) were pooled. Then, a fractionated ammonium-sulfate precipitation was performed. First, ammonium sulfate was added to a final concentration of 35% (w/v) under constant stirring on ice. The precipitated proteins were sedimented at 25000 xg for 10 min at 4°C. The pellet was discarded and ammonium sulfate was added to the supernatant to a final concentration of 70% (w/v). Precipitated proteins were centrifuged at 19000 xg for 20 min at 4°C. The supernatant was discarded; the pellet was solved in 600 µl 1x TEAD, 50 mM NaCl and cleared by centrifugation at 19000 xg for 10 min at 4°C. The clear supernatant was loaded on 10-40% sucrose gradients, which were centrifuged at 2.8 x 10^5 xg for 16 h at 4°C. The resulting fractions with highest chymotrypsin-like activity (2.1.3.6) were pooled and diluted 1 in 10 in Buffer A (1x TEAD, 100mM NaCl), filtered and subjected to FPLC. Proteins were loaded on a MonoQ HR 5/5 column (GE Healthcare) at a flow rate of 1 ml/min. The NaCl concentration during FPLC was increased stepwise at a flow rate of 1 ml/min with 5 min 0-20% Buffer B (1x TEAD, 1 M NaCl), 20 min 20-35% Buffer B, 2 min 35-100% Buffer B and 5 min 100% Buffer B. Fractions with high protein concentration according to absorption at A=280 nm and high chymotrypsin-like activity (2.1.3.6) were pooled. For further use, the buffer was exchanged against 1x TEAD, 50 mM NaCl and 20S proteasomes were concentrated on Amicon Ultra spin columns with 10 kDa cut-off (Millipore) according to manufacturers instructions.

2.1.3.8 Digestion of peptide substrates with purified 20S proteasomes

To determine proteasome-mediated processing of a LLO peptide substrate, 3 µg of a synthetic 27mer derived from the LLO sequence ($LLO_{291–317}$: AYISSVAYGRQVYLKLSTNSHSTK VKA) were incubated at 37°C for 2–4 h with 1 µg of purified 20S proteasomes (see 2.1.3.6) in 100 µl of digestion buffer (HEPES/KOH pH 7.8, 2 mM magnesium-acetate, and 2 mM DTT). Reactions were stopped by adding trifluoroacetic acid to a final concentration of 0.1%.

2.1.3.9 Identification of proteasomal cleavage products

Digestion products (see 2.1.3.7) were identified and quantified by liquid chromatography-electrospray ionization-ion trap mass spectrometry (LC-ESI-MS) according to (Sijts, et al., 2000). For statistical analysis, ion counts of each reaction were normalized to the internal standard 9GPS, a peptide (YPHFMPTNLGPS), which was added in equal amounts to each stopped reaction, and the mass of which does not interfere with the masses of any proteasomal cleavage product derived from $LLO_{290–317}$. Two replicates were averaged.

2.1.3.10 Measurement of cytokine secretion by BM-Mϕ

2×10^5 BM-Mϕ (see 2.1.2.3) per well of a 96well cell culture plate were seeded in D10 medium and stimulated with 100 U/ml IFNγ (Strathmann) over night at 37°C and 5% CO_2. Next day, the medium was exchanged against 100 µl/well D10 medium and cells were either left untreated or were infected with Listeria at a MOI of 1 for 1h at 37°C. Then, Gentamycin (Gibco) was added to a final concentration of 50 µg/ml to kill extracellular bacteria. The cell culture supernatants were harvested at different time points, frozen in liquid nitrogen and stored at -20°C. The concentrations of IL-6 and TNFα in the supernatants were determined with the Bioplex Cytokine Bead Array System (Bio-rad) according to manufacturer`s instructions. The cytokine secretion was measured from three independent BM-Mϕ preparations per group and time point.

2.1.4 Molecular biological methods

2.1.4.1 RNA isolation

Organs were homogenized in TRIZOL® Reagent (Invitrogen) with a T8 basic Ultra Turrax. 200 µl Chloroform per ml TRIZOL® Reagent were added and samples were shaken for 30 sec; incubated for 5 min at room temperature and then centrifuged at 13000 rpm for 15 min at 4°C in a microfuge. Subsequently, the aqueous phase was transferred to a new reaction tube and 500 µl isopropanol, 120 µl 5 M ammonium acetate and 10 µl 0.5% (w/v) Glycogen were added per ml TRIZOL® Reagent. RNA was precipitated for 15 min at -20°C and sedimented by centrifugation at 13000 rpm for 15 min at 4°C in a microfuge. The supernatant was discarded and the pellet was washed with icecold 70% ethanol. The samples were centrifuged at 8000 rpm for 5 min at 4°C in a microfuge; the supernatants were discarded and the pellet was dried at the air. Then, the pellet was solved in deionized water and RNA concentration and quality were determined with a 2100 Bioanalyzer (Agilent Technologies, Santa Clara, CA, USA).

2.1.4.2 cDNA synthesis

2 µg total RNA per sample were transcribed to cDNA with random hexamer primers and SuperScript™ II Reverse Transcriptase (Invitrogen according) according to manufacturer´s instructions.

2.1.4.3 Semi-quantitative Real-Time RT PCR

Semi-quantitative Real-Time RT PCR reactions contained 1x SYBR Green mix (Applied Biosystems, Foster City, CA, USA), 10 pmol forward-primer, 10 pmol reverse-primer and 5 µl cDNA template (2.1.4.2) diluted 1:10 to 1:50 in UltraPure Water (Millipore) in a total volume of 30 µl. The amplification was performed with an ABI Prism 7000 sequence detection system (Applied Biosystems) with the following programm: 2 min 50°C, 10 min 95°C and 40 cycles with 15 sec 95°C and 15 sec 60°C. The runs were evaluated with the SDS2.2.2 Software (Applied Biosystems). Specificity of the products was assured by measurement of the products melting points. Amplification of PCR products derived from contaminating genomic DNA was excluded by the use of intron-exon spanning primer pairs (see 2.2.2). The expression of Ribosomal Protein Subunit 9 (RPS9) was used for standardization. The relative expression was calculated with the ΔΔCT method. Relative expression values of proteasomal catalytic β-subunits and POMP were determined from 3 mice per group and time point.

2.1.4.4 Molecular Cloning of vector constructs for retroviral transduction

The vector pDest-Super used for retroviral transduction of MEFs (2.1.2.2) was provided by David Ermert (MPIIB). It is a hybrid plasmid, in which the MultiSite Gateway® Three Fragment recombination site from pDest™R4-R3 (Invitrogen) substitutes the cloning site of pSuper.retro.puro (OligoEngine, Seattle, WA, USA), which provides the flanking long terminal repeats (LTR) of MSCV and puromycin resistance. DNA-sequences encoding β5 and β5i with C-terminal Flag-tag were amplified from a murine liver cDNA library (2.1.4.2) by nested PCR with Expand™ High Fidelity Polymerase (Roche Applied Science). First, inserts were amplified using primer pairs β5-start-for/β5-Flag-rev and lmp7-start-for/lmp7-Flag-rev (see 2.2.2) for β5- and β5i-Flag, respectively. The PCR products from the first reaction were used for further amplification with attB1- and attB2-adapter primers. Inserts with an IRES-eGFP sequence were amplified from a plasmid provided by Marcus Koch (MPIIB) with primers IRES-eGFP-for/IRES-eGFP-rev (see 2.2.2). The inserts were purified by electrophoresis on a 1% Agarose Gel in 1x TAE (40 mM Tris-acetate pH8.5, 2 mM EDTA) and the QuiaQuick Gel Extration Kit (Quiagen, Düsseldorf, Germany) according to manufacturer's instructions. Purified β5- and β5i-Flag inserts were subcloned into the entry

vector pDONR™221 (Invitrogen) and IRES-eGFP inserts into pDONR™P2R-P3 (Invitrogen) with the BP-recombination reaction according to the MultiSite Gateway® Three-Fragment Vector Construction Kit Manual. The pDONR™P4-P1R-EF-1α entry vector containing the sequence of the EF-1α-promoter was provided by David Ermert (MPIIB). Final expression vectors were generated by a LR-recombination reaction between pDest-Super, pDONR™P4-P1R-EF-1α, pDONR™221-β5-Flag or pDONR™221-β5i-Flag and pDONR™P2R-P3-IRES-eGFP according to manufacturer´s instructions resulting in the expression vectors pEX-EF-1α-β5-Flag-IRES-eGFP and pEX-EF-1α-β5i-Flag-IRES-eGFP, respectively. One Shot® TOP10 chemically competent *E. coli* (Invitrogen) were transformed with the plasmids according to manufacturer's instructions. Ampicillin resistant, Chloramphenicol sensitive clones were verified as positive clones by colony PCR with primers β5-for/β5-rev and β5i-for/β5i-rev for pEX-EF-1α-β5-Flag-IRES-eGFP and pEX-EF-1α-β5i-Flag-IRES-eGFP, respectively. Verified clones were cultured and the plasmids were purified with the QuiaPrep Spin Miniprep Kit (Quiagen) according to manufacturer's instructions.

2.1.4.5 Preparation of retroviral particles

The vector pEX-EF-1α-eGFP, which was provided by David Ermert (MPIIB) expressing eGFP from the EF-1α promoter, was used as empty vector control in the following experiments. Packaging of the expression vectors pEX-EF-1α-β5-Flag-IRES-eGFP, pEX-EF-1α-β5i-Flag-IRES-eGFP and pEX-EF-1α-eGFP into ecotrophic retroviral particles was achieved by transient transfection of Phoenix E cells (2.1.2.1) by Ca-phosphate precipitation. 2 x 10^6 Phoenix E cells were seeded per cell culture dish with 10 cm-diameter. Next day, Ca-phosphate-DNA precipitates were generated by mixing 20 µg plasmid DNA (2.1.4.4) with 32 µl 2 M $CaCl_2$ and 300 µl 2x HBS Buffer (Clontech, Saint-Germain-en-Laye, France) adjusted to a final volume of 600 µl with deionized water. The mixture was incubated for 30 min at room temperature and the resulting precipitates were cautiously dispersed on the 60-70% confluent monolayers of Phoenix E cells. 24 h later the medium was exchanged against fresh D10 medium. The supernatants containing retroviral particles were harvested 24 and 48 h later, filtered through a sterile filter with 0,45 µm pore-size and polybrene was added to a final concentration of 4 µg/ml.

2.1.4.6 Retroviral transduction of MEFs

For retroviral transduction 2 x 10^4 MEFs (2.1.2.2) were seeded per well of a 6well cell culture plate. 24 h later the medium was removed and 2 ml/well of the supernatants containing retroviral particles (2.1.4.5) were added to the MEFs. Plates were then centrifuged for 30 min at 2000 rpm and 30°C. The supernatants were removed 24 h later and the transduction was repeated with fresh supernatants. Another 24 h later the supernatants were exchanged against

D10 medium containing 10 µg/ml Puromycin (Sigma-Aldrich) for selection of transduced MEFs. Following 2-4 weeks of culture under puromycin selection eGFP expressing cells were repeatedly sorted with a DIVA cell sorter (BD Biosciences) until a purity of >98% of eGFP high expressing MEFs was achieved.

2.1.5 Flow cytometry

2.1.5.1 Isolation of lymphocytes for flow cytometry

Spleens were pressed through a metal wire with 120 µm pore size. Splenocytes were resuspended in RPMI medium (RPMI 1640 (Gibco), 10% FCS, 1 mM L-glutamine, 1 mM sodium pyruvate, 100 U/ml penicillin, and 100 µg/ml streptomycin) and sedimented by centrifugation at 1500 rpm for 5 min at 4°C.
Liver lymphocytes were prepared by pressing livers through a metal wire with 120 µm pore size. Then, cells were resupended in RPMI medium and centrifuged for 30 sec at 18 xg to remove hepatocytes and tissue debris. The pellet was discarded and the supernatant was again centrifuged at 18 xg for 30 sec. The lymphocytes in the supernatant were sedimented by centrifugation at 1500 rpm for 5 min at 4°C.
Splenocytes and liver lymphocytes were resuspended in Erythrocyte Lysis Buffer (155 mM NH_4Cl, 0,1 mM EDTA) and incubated for 3-4 min at room temperature. Lysis was stopped by adding 20 ml of RPMI medium. Following sedimentation at 1500 rpm for 5 min at 4°C the cells were resuspended in FACS buffer (1x PBS, 0.1% (w/v) BSA, 2 mM NaN_3) for direct staining of cell surface markers (2.1.5.2) or in RPMI medium for ICS (2.1.5.3).

2.1.5.2 Flow cytometric analysis of MHC class I surface expression

First, 2 x 10^6 splenocytes per sample were resuspended in 200 µl FC-receptor block (1 µg/ml CD16 and 1 µg/ml CD32 antibodies (MPIIB) diluted in FACS buffer) and incubated for 5 min at room temperature. Then, either CD11b-Pe-Cy7 (BD Pharmingen, Heidelberg, Germany), CD11c-Biotin (MPIIB), $H2K^b$-Pe (BD Pharmingen), $H2D^b$-Cy5 (MPIIB) and MHC class II-FITC (MPIIB) or CD11b-Pe-Cy7, CD11c-Biotin, MHC II-FITC and polyclonal hamster H2M3 antibodies were added to a final concentration of 2 µg/ml each and cells were stained for 15 min at 4°C in the dark. Cells were washed with FACS Buffer, centrifuged at 1500 rpm for 5 min at 4°C and supernatants were discarded. The cells were resuspended in 200 µl FACS Buffer containing 2 µg/ml Streptavidin-APC-Cy7 (BD Pharmingen). Further, 2 µg/ml anti hamster IgG-Cy5 conjugated secondary antibodies (BD Pharmingen) were added to the stainings against H2M3. Cells were incubated for 15 min at 4°C in the dark. Cells were washed with FACS Buffer and resuspended in 0.5 ml FACS Buffer for flow cytrometric analysis on a FACS CANTO (BD Biosciences, Heidelberg, Germany). Data analysis was

performed with FCS express 3 (De Novo Software, Los Angeles, CA, USA). Briefly, $CD11b^{high}$ $MHCII^{high}$ and $CD11c^{high}$ $MHCII^{high}$ were regarded as Mϕ or DCs, respectively. Relative surface density of MHC class I molecules on these cell types was determinded by mean fluorescence intensity (MFI) in the respective fluorescence channel. The MFI was measured on 3-4 splenocyte preparations per group and time point.

2.1.5.3 Intracellular cytokine staining (ICS)

Splenocytes and liver lymphocytes were cultured in RPMI medium. 5 x 10^5 cells per well of a 96well plate were incubated in the presence or absence of 1 µg/ml $LLO_{296–304}$ peptide (VAYGRQVYL). After 45 min of stimulation at 37°C and 5% CO_2, brefeldin A (Sigma-Aldrich) was added to a final concentration of 10 µg/ml, and the cells were cultured for another 3–4 h. Following stimulation, cells were washed with 1x PBS and centrifuged for 5 min at 1100 rpm. Cells were resuspended in 100 µl FC-receptor block (1 µg/ml CD16 and 1 µg/ml CD32 antibodies (MPIIB) diluted in FACS buffer) and incubated at room temperature for 5 min. Subsequently, CD8-PE-Cy7 (BD Pharmingen) and CD62L-PE (MPIIB) antibodies diluted in FACS buffer were added to a final concentration of 1 µg/ml each and samples were incubated for 15 min at 4°C. Thereafter, cells were washed with 1x PBS and fixed in 4% (w/v) paraformaldehyde in 1x PBS for 20 min at room temperature. Fixation was stopped by washing with FACS buffer. Fixed cells were permeabilized for 5 min in saponin buffer (1x PBS, 0.5% (w/v) saponin (Sigma-Aldrich), 0.1% (w/v) BSA) before adding IFNγ-FITC antibodies (MPIIB) to a final concentration of 2 µg/ml. Following incubation for 15 min at 4°C, cells were washed with FACS buffer, and samples were measured on a FACS CANTO (BD Biosciences). The resulting data were analyzed using FCS Express 2 software (De Novo Software).

2.2 Materials

2.2.1 Antibodies

Antibodies used for Western Blot Analysis				
specificity	host species	clone	used dilution	supplier
GAPDH	mouse	6C5	1:2500	Calbiochem, Darmstadt, Germany
β1	rabbit	polyclonal (K43)	1:5000	Institute for Biochemistry, Charité, Berlin, Germany
β2	chicken	polyclonal	1:5000	Abcam, Cambridge, UK
β5	rabbit	polyclonal	1:5000	Abcam, Cambridge, UK
β1i	rabbit	polyclonal	1:5000	Abcam, Cambridge, UK
β2i	rabbit	polyclonal	1:2500	Biomol, Exeter, UK
β5i	rabbit	polyclonal (K63)	1:10000	Institute for Biochemistry, Charité, Berlin, Germany
α3	mouse	MCP257	1:5000	Calbiochem, Darmstadt, Germany
POMP (HSPC014)	chicken	polyclonal	1:1000	Abcam, Cambridge, UK
PA28α	rabbit	polyclonal	1:5000	Institute for Biochemistry, Charité, Berlin, Germany
19S subunit S4	rabbit	polyclonal	1:5000	Institute for Biochemistry, Charité, Berlin, Germany
20S proteasome	rabbit	polyclonal (MP3)	1:5000	Institute for Biochemistry, Charité, Berlin, Germany
rabbit IgG-AlexaFluor680	goat	polyclonal	1:5000	Molecular Probes, Eugene, OR, USA
chicken IgY-IrDye700	goat	polyclonal	1:5000	Rockland, Gilbertsville, PA, USA
mouse IgG-IrDye800	goat	polyclonal	1:5000	Rockland, Gilbertsville, PA, USA

Antibodies used for Flow Cytometry				
specificity	host species	clone	used dilution	supplier
CD11b-Pe-Cy7	rat	M1/70	2 µg/ml	BD Biosciences, Heidelberg, Germany
CD11c-Biotin	mouse	N418	2 µg/ml	MPIIB, Berlin, Germany
$H2K^b$-Pe	mouse	AF6-88.5	2 µg/ml	BD Biosciences, Heidelberg, Germany
$H2D^b$-Cy5	mouse	HB27	2 µg/ml	MPIIB, Berlin, Germany
H2M3	armenian hamster	clone130	2 µg/ml	BD Biosciences, Heidelberg, Germany
MHC II	mouse	Tib120	2 µg/ml	MPIIB, Berlin, Germany
hamster IgG-Cy5	mouse	G70-204/ G94-90.5	2 µg/ml	BD Biosciences, Heidelberg, Germany
CD8-Pe-Cy7	rat	53-6.7	2 µg/ml	BD Biosciences, Heidelberg, Germany
CD62L-Pe	rat	Mel14	2 µg/ml	MPIIB, Berlin, Germany
IFNγ-FITC	mouse	XMG1.2	2 µg/ml	MPIIB, Berlin, Germany

2.2.2 Primer-sequences

primer	sequence (5’ to 3’)*
β1-for	TGACCAAGGACGAATGTCTG
β1-rev	GATTTGGTCTCCCAAAAGCA
β2-for	CTGTCTTGGAAGCGGATTTC
β2-rev	GCAACAACCATCCCTTCAGT
β5-for	GTGAATCAGCACGGGTTTT
β5-rev	AATCCGCTGCAACAATGACT
β1i-for	CATCATGGCAGTGGAGTTTGAC
β1i-rev	ACCTGAGAGGGCACAGAAGATG
β2i-for	CAGCCAAACATGACGCTGG
β2i-rev	CAGTGATCACACAGGCATCCAC
β5i-for	ACCACACTCGCCTTCAAGTTC
β5i-rev	GCCAAGCAGGTAAGGGTTAATC
POMP-for	AACATCCAGGGTCTGTTTGC
POMP-rev	TCGTTGCCCCTCAAAATATC
RPS9-for	CTGGACGAGGGCAAGATGAAGC
RPS9-rev	TGACGTTGGCGGATGAGCACA
β5-start-for	AAAAAGCAGGCTCCACCATGGCGCTGGCTAGCGTG
β5-Flag-rev	AGAAAGCTGGGTCTCAGATCTTATCGTCGTCATCCTTG-TAATCGGGGACAGATACACTAC
lmp7-start-for	AAAAAGCAGGCTCCACCATGGCGTTACTGGATCTGTG
lmp7-Flag-rev	AGAAAGCTGGGTCTCAGATCTTATCGTCGTCATCCTTG-TAATCCAGAGCGGCCTCTCCG
attB1-for	GGGGACAAGTTTGTACAAAAAAGCAGGCT
attB2-rev	GGGGACCACTTTGTACAAGAAAGCTGGGT
IRES-eGFP-for	GGGGACAGCTTTCTTGTACAAAGTGGTCAGCTTCGAATTCTGCAGTCG
IRES-eGFP-rev	GGGGACAACTTTGTATAATAAAGTTGCTTACTTGTACAGCTCGTCCATGC

*All primers were obtained from TIB Molbiol, Berlin, Germany.

3 Results

3.1 Analysis of 20S proteasome assembly in *Listeria monocytogenes* infected *lmp7*$^{-/-}$ mice

According to the current model of cooperative proteasome assembly, β1i and β2i require β5i for efficient maturation in i20S. This model is based on observations in T2 cells, which carry a deletion in the MHC class II locus covering the genes encoding for β1i and β5i. When these cells are reconstituted with β1i but not β5i, the maturation of β1i and β2i is almost aborted (Fig. II; Griffin et al., 1998).

To analyse the impact of β5i-deficiency on proteasome assembly *in vivo,* we infected *lmp7*$^{-/-}$ mice i.v. with Listeria. Due to the targeted deletion of the *lmp7* gene, the expression of β1i and β2i was expected to remain unaffected. In addition, this system allows the analysis of proteasome maturation in lymphoid or non-lymphoid tissues with either constitutive or IFNγ induced immunosubunit expression, respectively.

3.1.1 The abundance of catalytic β-subunits in Listeria-infected WT and *lmp7*$^{-/-}$ mice

The abundance of the proteasomal catalytic β–subunits in spleen and liver of C57Bl6/N (WT) and *lmp7*$^{-/-}$ mice was analysed by Two-Colour Fluorescent Western Blot analysis following infection with Listeria (Fig.1; Fig.2).

As expected, we observed a constitutive, high abundance of the immunosubunits in the spleen of naïve WT animals (Fig. 1A). Densitometric analysis revealed that the abundance of β1i and β5i was unaffected by infection, while β2i was about 2fold increased (Fig. 1B). The usage of the constitutive subunits β1, β2 and β5 was generally low in the spleen of WT animals and was not influenced by infection (Fig. 1A-B).

In the absence of β5i in *lmp7*$^{-/-}$ mice, maturation of β1i and β2i was impaired as seen by accumulation of precursor proteins, pre-β1i and pre-β2i, respectively. Surprisingly, the majority of β1i and β2i subunits occurred as mature subunits, showing more efficient processing of these subunits in the absence of β5i than expected (Fig. 1 A+B).

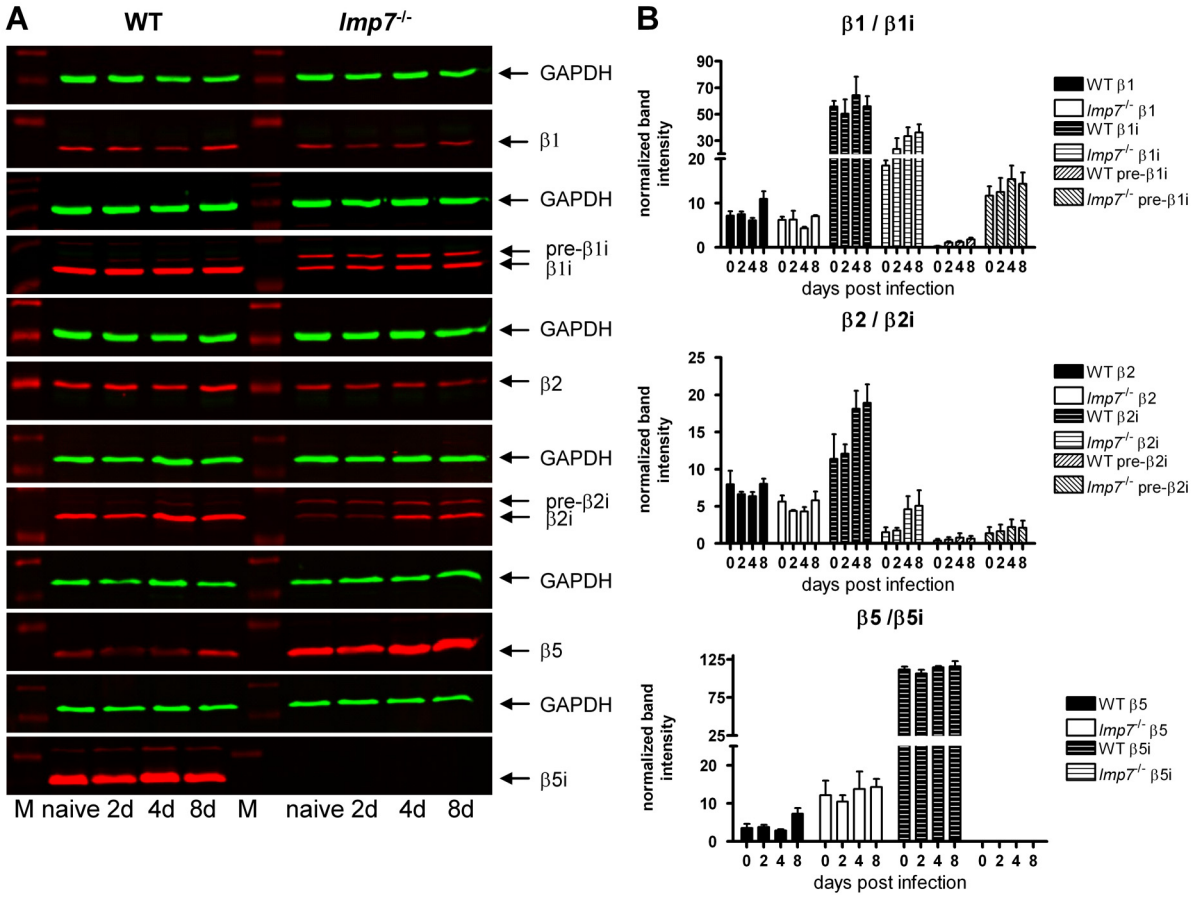

Figure 1. Protein abundance of catalytic β-subunits in the spleen following infection with Listeria
Spleens of naïve and infected WT and *lmp7*$^{-/-}$ mice were isolated at the indicated time points post infection. Mice were infected i.v. with 5 x 10^3 cfu of Listeria and organs were pooled from 3-4 mice per group. Organ lysates were separated by SDS-PAGE and subjected to Two-Colour Fluorescent Western Blot analysis. Each membrane was stained against GAPDH for standardization. Further, membranes were stained with antibodies specific for the six catalytic β-subunits. Representative blots of 4 experiments are shown (A). Densitometric analysis was performed using the Odyssey Image Analyser software. Standardized band intensity was calculated as follows: (β-subunit signal / GAPDH-signal) x 100. The given results are means of two independent experiments, each analysed in duplicates (B).

In contrast to WT spleen, the abundance of mature β1i and β2i subunits was approximately 2fold increased following infection of *lmp7*$^{-/-}$ mice indicating enhanced integration into 20S proteasomes.

The usage of β5 was 3-4fold increased in *lmp7*$^{-/-}$ mice as compared to WT mice, presumably to compensate the lack of β5i. Interestingly, the constitutive, high abundance of β5 in *lmp7*$^{-/-}$ spleen was not further increased following infection. The prevalence of β1 and β2 remained unaltered in *lmp7*$^{-/-}$ mice during infection despite increased maturation of β1i and β2i. However, their abundance appeared 15-30% lower compared to WT mice at all time points analysed (Fig. 1B).

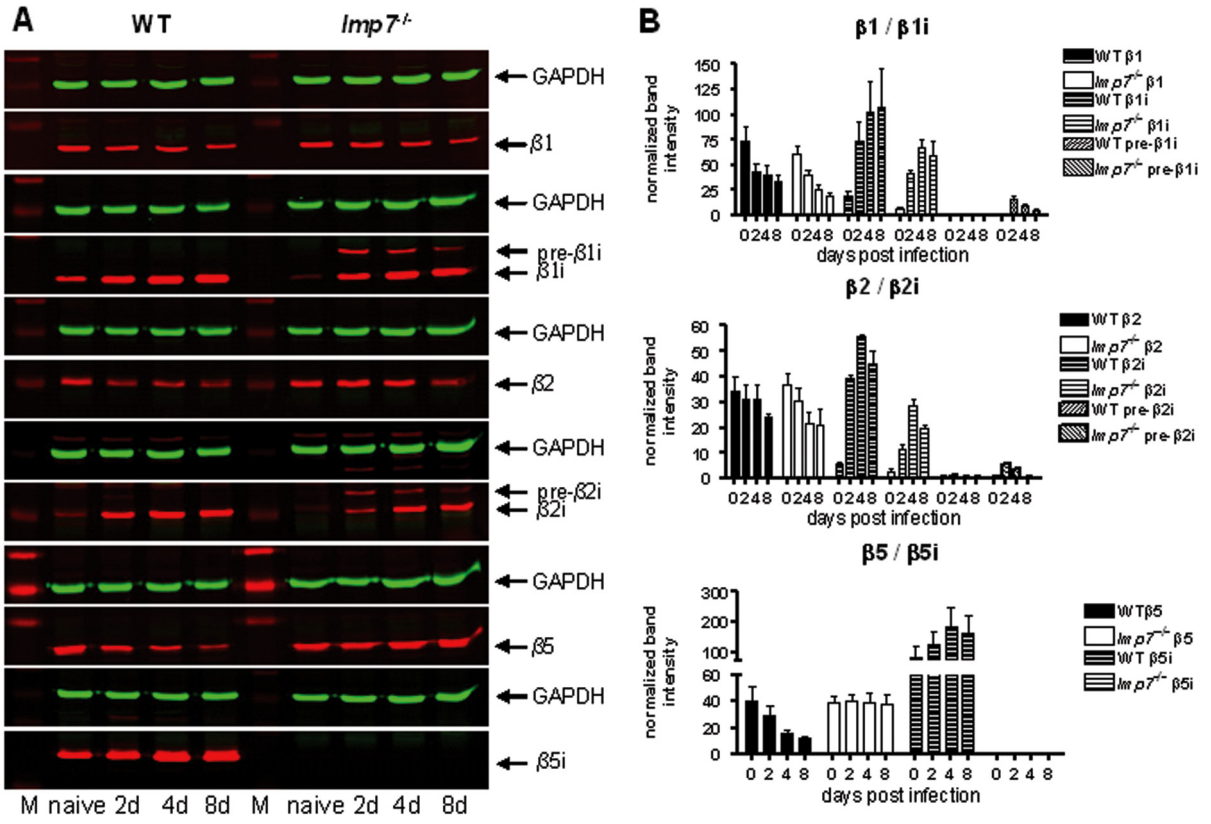

Figure 2. Protein abundance of catalytic β-subunits in the liver following infection with Listeria
Livers of naïve and infected WT and *lmp7*$^{-/-}$ mice were isolated at the indicated time points post infection. Mice were infected i.v. with 5 x 10^3 cfu of Listeria and organs were pooled from 3-4 mice per group. Organ lysates were separated by SDS-PAGE and subjected to Two-Colour Fluorescent Western Blot analysis. Each membrane was stained against GAPDH for standardization. Further, membranes were stained with antibodies specific for the six catalytic β-subunits. Representative blots of 4 experiments are shown (A). Densitometric analysis was performed using the Odyssey Image Analyser software. Standardized band intensity was calculated as follows: (β-subunit signal / GAPDH-signal) x 100. The given results are means of two independent experiments, each analysed in duplicates (B).

In the liver of naïve WT and *lmp7*$^{-/-}$ mice, we observed high abundance of β1, β2 and β5 (Fig. 2A). In contrast, the abundance of β1i and β2i was low in naïve WT and *lmp7*$^{-/-}$ animals and revealed an 8-10fold increase upon infection. Interestingly, β5i was readily detectable in naïve WT animals and its amount was only 2fold enhanced following infection, which revealed constitutive integration of this subunit in the liver (Fig. 2A-B).

The abundance of β1 and β2 decreased with comparable kinetics in WT and *lmp7*$^{-/-}$ liver, indicating their replacement by β1i and β2i (Fig. 2B). Further, this demonstrates that competition between β1 and β2 with β1i and β2i occurs at similar rates in WT and *lmp7*$^{-/-}$ mice during proteasome assembly.

Like in the spleen, maturation of β1i and β2i was impaired in the liver of *lmp7*$^{-/-}$ mice. The incidence of pre-β1i and pre-β2i in *lmp7*$^{-/-}$ mice peaked 2 days after infection and gradually

declined during the course of infection, while the abundance of mature subunits increased. Suprisingly, the ratio of pre-β1i and pre-β2i to mature β1i and β2i was much lower in the liver compared to the spleen (Fig 2 A-B). Eight days after infection less than 10% of total β1i and β2i were found as precursor subunits. This reveals that immunosubunits in *lmp7*$^{-/-}$ mice can efficiently pair with β5 to form mixed proteasomes (m20S). However, the pool of m20S increases with slower kinetics as compared to i20S in WT mice.

Further, we observed a replacement of β5 in infected WT liver due to increasing β5i levels (Fig. 2B). In contrast, in *lmp7*$^{-/-}$ mice the abundance of β5 remained constant during the course of infection (Fig. 2 A-B). This suggests that the usage of β5 in *lmp7*$^{-/-}$ liver is already maximal and cannot be further enhanced to counterbalance β5i-deficiency. Still, high constitutive expression of β5 in the liver of *lmp7*$^{-/-}$ mice seems to allow more efficient integration of β1i and β2i as compared to the spleen.

In summary, these findings show that β5 can compensate for the lack of β5i in *lmp7*$^{-/-}$ mice with unexpected efficiency, especially in the liver. Still, impaired maturation of β1i and β2i shows, that β5 is a limiting factor for assembly of m20S in infection.

3.1.2 Analysis of proteasome assembly in WT and *lmp7*$^{-/-}$ mice

To verify that the maturation of β1i and β2i in *lmp7*$^{-/-}$ mice (Fig.1, Fig. 2) results in the formation of m20S in association with β5, we employed 2D-Two-Colour Fluorescent Western Blot analysis. The combination of 2D gelelectrophoresis with the Two Colour Fluorescent Western Blot technology allowed us to analyse proteasome assembly without previous purification of the complexes. Membranes were stained for proteasome subunit α3 as it is a component of assembly intermediates as well as mature proteasome complexes. Thus, α3 indicates the positions of the various complexes following their separation according to molecular weight in the first dimension. The positions of 13-16S precursor proteasomes, 20S proteasomes or 20S proteasomes bound to 11S and/or 19S regulatory complexes were confirmed by the presence of pre-β1i and staining for the 11S subunit PA28α or the 19S subunit S4, respectively (Fig. 3).

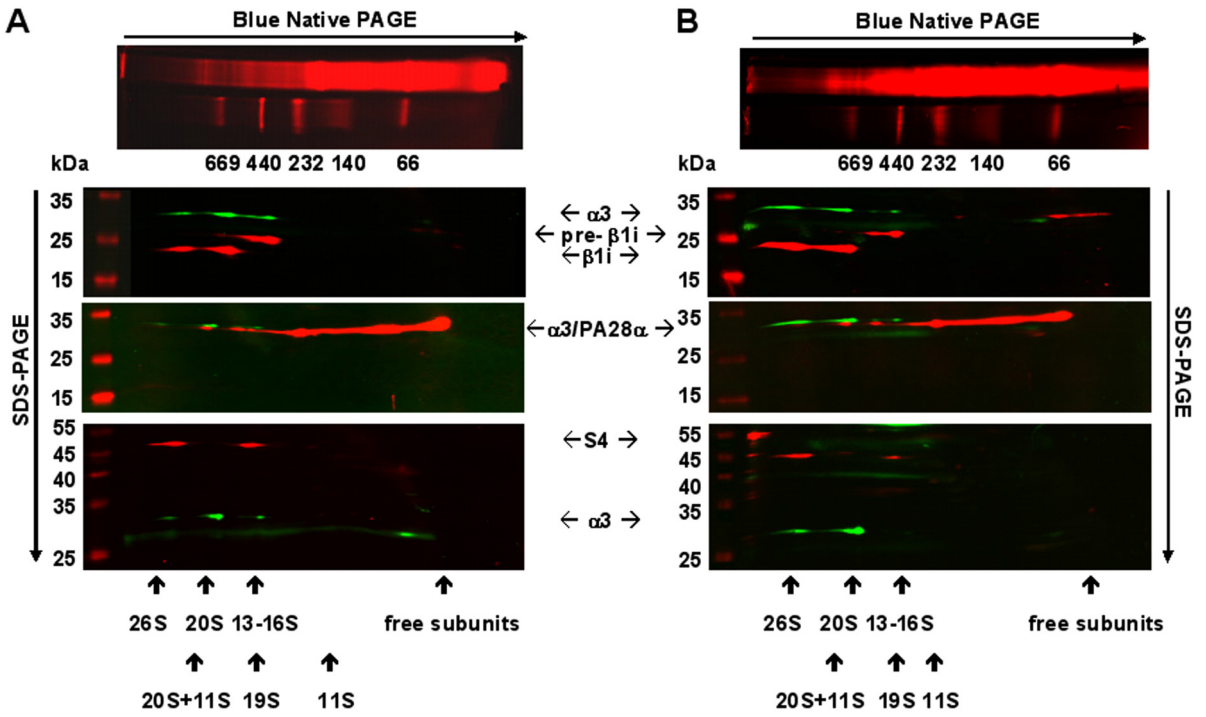

Figure 3. Analysis of proteasome assembly by 2D Two Colour Fluorescent Western Blot Analysis
Organ-lysates of spleen (A) and liver (B) of *lmp7*$^{-/-}$ mice, which were infected i.v. with 5 x 10^3 cfu of Listeria 4 days before, were prepared in native lysis buffer and analysed by 2D Two Colour Fluorescent Western Blot analysis. First, protein complexes were separated by Blue Native-PAGE. In the second dimension single lanes of the Blue Native-PAGE were subjected to SDS-PAGE followed by Two Colour Fluorescent Western blot analysis. Each membrane was stained for α3 (green signal). Besides the molecular weight difference of the complexes in the first dimension, α3 is a marker for the presence and positions of 13-16S, 20S, 20S + 11S and 26S complexes in the second dimension. The complexes were confirmed by staining against 19S ATPase subunit S4, 11S subunit PA28α or presence of pre-β1i-subunits (red signals). Arrows indicate the positions of the observed proteasome complexes. Organs of 3-4 mice per group were pooled for the analysis.

In the spleen of naïve and infected WT mice, catalytic β-subunits were exclusively detected in mature proteasome complexes, either as free 20S proteasomes or bound to 11S and/or 19S regulatory complexes (Fig. 4). Further, mature proteasome fractions in WT mice predominantly contained β5i and only low amounts of β5, which reflects the results of the densitometric analysis of conventional Western-Blots (Fig. 1B).

Substantial amounts of β1i and β2i subunits in mature proteasomes were also detected in the spleens of naïve and infected *lmp7*$^{-/-}$ mice (Fig. 4). This demonstrates that mature β1i and β2i subunits previously observed by conventional Western Blot analysis (Fig. 1A) are integrated into 20S proteasomes. In contrast to WT mice, we further detected high amounts of β5 in mature proteasomes of *lmp7*$^{-/-}$ mice, which confirms that β5 can efficiently pair with β1i and β2i to form m20S.

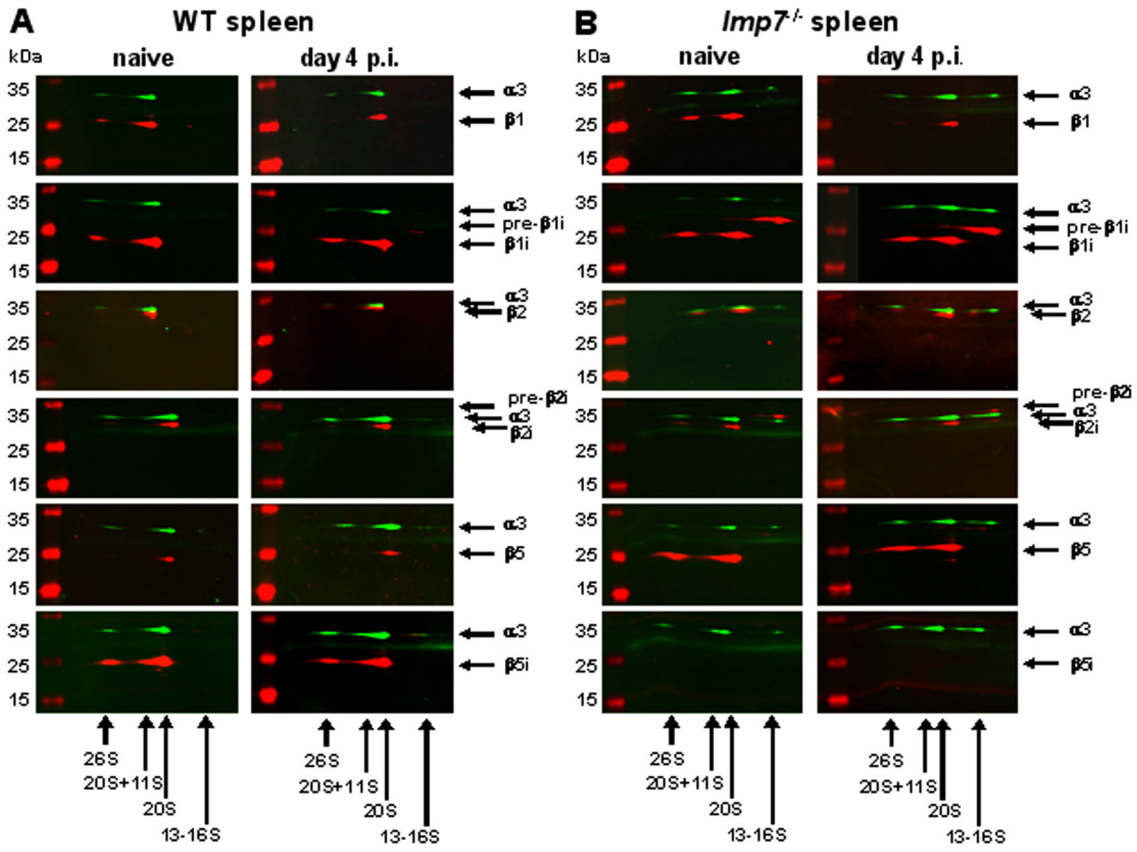

Figure 4. Analysis of proteasome assembly in the spleen following Listeria infection of WT and *lmp7*$^{-/-}$ mice

Organ-lysates of the spleen were analysed by 2D Two Colour Fluorescent Western Blot analysis. First, protein complexes were separated by Blue Native-PAGE. In the second dimension single lanes of the Blue Native-PAGE were subjected to SDS-PAGE followed by Two Colour Fluorescent Western blot analysis. Each membrane was stained for proteasome subunit α3 (green signal). Besides the molecular weight difference of the complexes in the first dimension, α3 is a marker for the positions of 13-16S, 20S, 20S + 11S and 26S complexes in the second dimension. Further, membranes were stained for the catalytic β-subunits (red signals). This allows identifying, in which proteasome fractions the subunits are present in the spleen of naïve and infected WT (A) and *lmp7*$^{-/-}$ mice (B). Arrows indicate the observed proteasome complexes. Mice were infected i.v. with 5 x 10^3 cfu Listeria and sacrified 4 days post infection. Organs of 3-4 mice per group were pooled for the analysis.

In the livers of WT mice, catalytic β-subunits were predominantly detected in mature proteasome fractions with increasing amounts of IFNγ inducible subunits in infected compared to naïve mice. Only marginal amounts of pre-β1i were found in precursor proteasome complexes of WT mice (Fig.5).

Also in the livers of *lmp7*$^{-/-}$ mice, β1i and β2i incorporation into proteasome complexes was strongly enhanced upon infection. Interestingly, the majority of β1i and β2i subunits were detected in mature proteasome complexes, while only a small fraction was found in 13-16S assembly intermediates (Fig.5). This confirms that β1i and β2i are more efficiently integrated in the liver of *lmp7*$^{-/-}$ mice as compared to spleen.

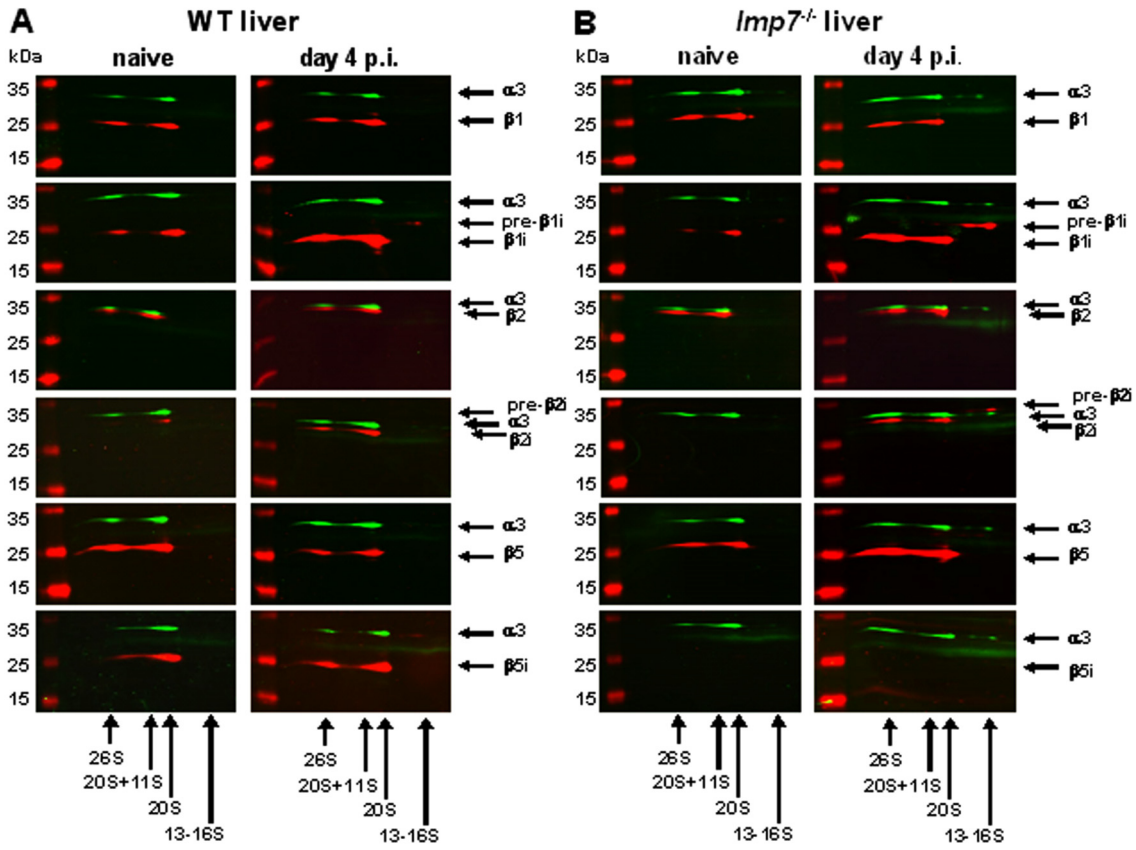

Figure 5. Analysis of proteasome assembly in the liver following Listeria infection of WT and *lmp7*$^{-/-}$ mice
Organ-lysates of the liver were analysed by 2D Two Colour Fluorescent Western Blot analysis. First, protein complexes were separated by Blue Native-PAGE. In the second dimension single lanes of the Blue Native-PAGE were subjected to SDS-PAGE followed by Two Colour Fluorescent Western blot analysis. Each membrane was stained for proteasome subunit α3 (green signal). Besides the molecular weight difference of the complexes in the first dimension, α3 is a marker for the positions of 13-16S, 20S, 20S + 11S and 26S complexes in the second dimension. Further, membranes were stained for the catalytic β-subunits (red signals). This allows identifying, in which proteasome fractions the subunits are present in the liver of naïve and infected WT (A) and *lmp7*$^{-/-}$ mice (B). Arrows indicate the observed proteasome complexes. Mice were infected i.v. with 5 x 10^3 cfu Listeria and sacrified 4 days post infection. Organs of 3-4 mice per group were pooled for the analysis.

Still, the presence of pre-β1i and pre-β2i in precursor proteasomes of naïve and infected *lmp7*$^{-/-}$ mice reveals impaired maturation of 20S proteasome complexes (Fig. 4 and 5). Because β5 was predominantly found in mature proteasome complexes in *lmp7*$^{-/-}$ mice, but only traces were detectable in the accumulated 13-16S complexes, we suggest that integration of β5 is a rate-limiting step for proteasome maturation in these mice. Thus, the neosynthesis of 20S proteasomes in the absence of β5i seems to directly correlate with the availability of β5.

3.1.3 mRNA expression of the catalytic β-subunits in WT and *lmp7*$^{-/-}$ mice

We performed semi-quantitative Real-Time RT-PCR analysis to determine the impact of β5i-deficiency on the expression of the remaining catalytic β-subunits following Listeria infection.

The kinetics of β1i and β2i expression were comparable in WT and *lmp7*$^{-/-}$ mice in both analysed organs, demonstrating that β5i-deficiency does not influence their expression (Fig. 6 A-B). Also mRNA levels of β1 and β2 were similar in both groups of mice. Noteworthy, the expression of β1 and β2 remained constant following infection (Fig 6B), although their protein abundance declined in the liver (Fig. 2B), indicating that the down-regulation of constitutive subunits is not transcriptionally regulated. Instead, induction of IFNγ inducible subunits results in the replacement of constitutive subunits at protein level, indicating competitive integration of catalytic β- subunits during proteasome assembly.

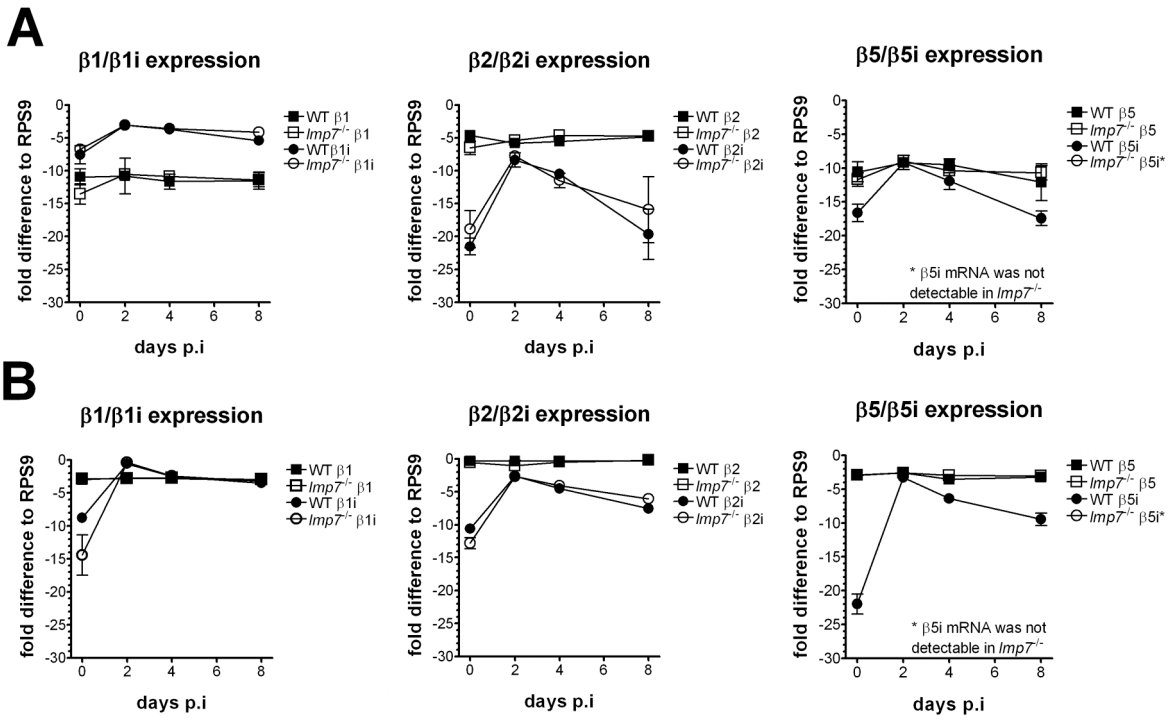

Figure 6. mRNA expression of the catalytic β-subunits during Listeria infection
Total RNA of spleen (A) and liver (B) of naïve and Listeria-infected WT and *lmp7*$^{-/-}$ mice was isolated at the indicated time points and semi-quantitative Real Time RT PCR analysis was performed. The results were calculated as relative mRNA expression levels compared to the expression of the internal standard ribosomal protein subunit 9 (RPS9) by the ΔΔCT method. Each value represents mean and standard error of three individual mice. The data shown are representative for two independent experiments. The values of β1, β2 and β5 are marked by filled squares in WT and open squares in *lmp7*$^{-/-}$ mice, respectively, while the values for β1i, β2i and β5i are indicated by filled circles for WT mice and open circles for *lmp7*$^{-/-}$ mice.

Interestingly, the mRNA expression of β5 was not influenced by infection and no differences between WT or *lmp7*$^{-/-}$ mice could be detected, neither in spleen nor liver (Figure 6A-B). The fact, that the mRNA expression of β5 was not increased in *lmp7*$^{-/-}$ mice shows, that the deficiency of β5i is not compensated at the transcriptional level.

In contrast to similar β5 mRNA levels, the protein abundance of β5 in *lmp7*$^{-/-}$ mice was constitutively increased in the spleen and remained constant in infected liver, while it was decreased in WT mice (Fig.1; Fig.2). Further, despite increasing amounts of β1i and β2i proteins in infected *lmp7*$^{-/-}$ mice, the abundance of β5 was not further enhanced, suggesting that the usage of β5 in *lmp7*$^{-/-}$ mice is maximal. In conclusion, the constant mRNA expression of β5 seems to limit its availability during infection and is not sufficient to compensate β5i-deficiency. We thus speculate, that precursor proteasomes containing pre-β1i and pre-β2i cannot be completed due to shortage of free β5 subunits and therefore accumulate in *lmp7*$^{-/-}$ mice.

3.1.4 Quantification of 20S proteasomes in Listeria infected WT and *lmp7*$^{-/-}$ mice

Our assumption that β5 is a rate-limiting factor for proteasome assembly in *lmp7*$^{-/-}$ mice raised the question, if the cellular proteasome content might be reduced in these mice. Thus, we aimed to quantify the total amount of proteasome complexes in organ lysates of WT and *lmp7*$^{-/-}$ mice during the course of infection. For this purpose, we employed the Two Colour Fluorescent Western Blot analysis with subsequent densitometry.

For the detection of proteasomal subunits a polyclonal rabbit serum specific for murine 20S proteasomes was used. With this serum, termed MP3, multiple bands in a molecular weight range of 20-35 kDa according to the sizes of α- or β-type subunits were detected (Fig.7 A, B). One prominent band was identified as structural subunit α3, as seen by complete overlay with the α3 staining in 2D Two Colour Fluorescent Western Blot Analysis (Fig.7 E-F). It was not further characterized, which other subunits are detected by MP3. However, the band patterns observed by Western Blot analysis were identical in samples of WT and *lmp7*$^{-/-}$ mice (Fig. 7 A, B).

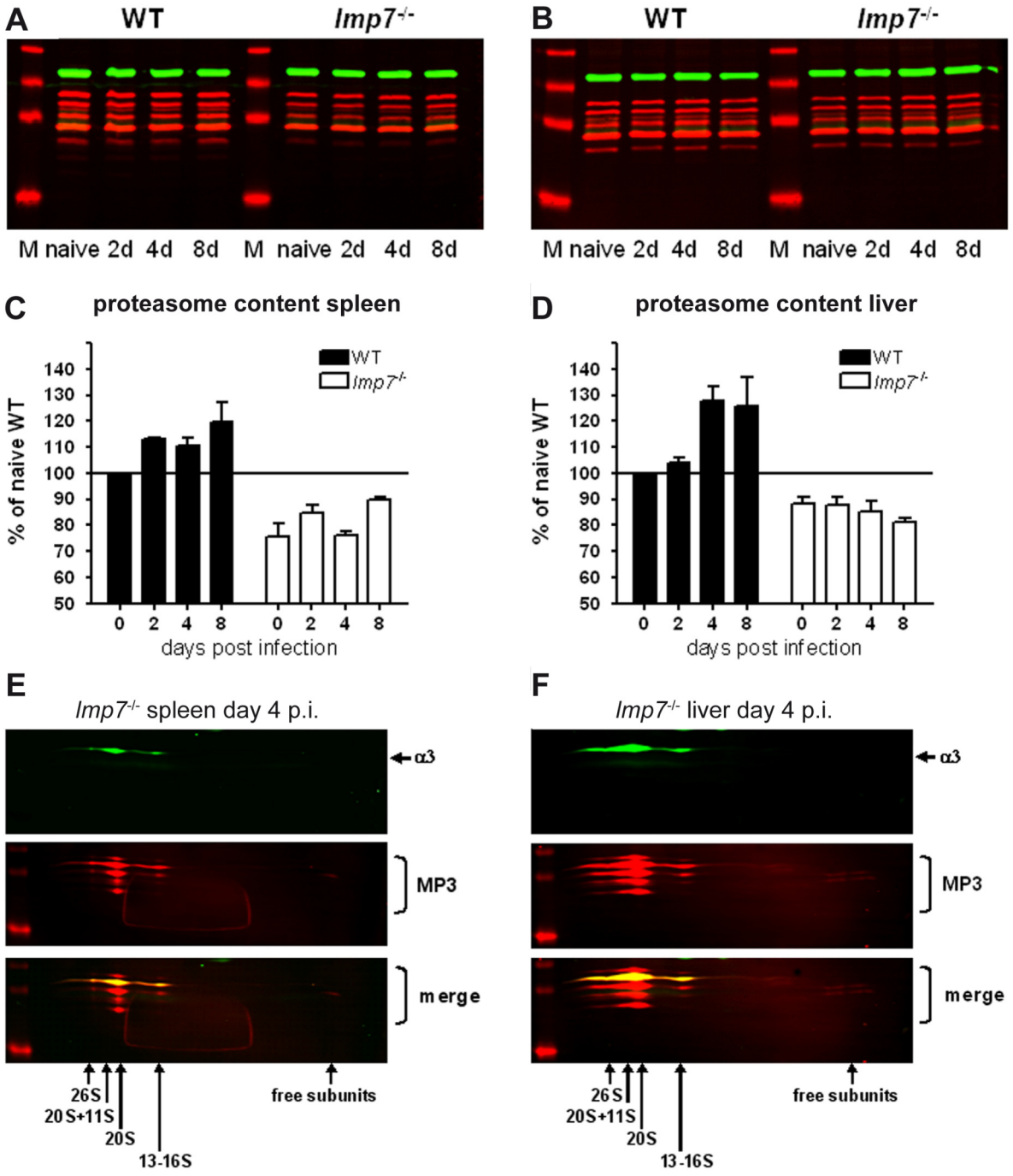

Figure 7. Quantitative analysis of the proteasome content during Listeria infection
Organ lysates of naïve and infected spleen (A) and liver (B) of WT and *lmp7*$^{-/-}$ mice were analysed by Two Colour Fluorescent Western Blot. The intensity of the proteasome subunit band pattern between 20-35 kDa (red signals) was quantified by densitometry and normalized to the band intensity of GAPDH (green signals). For the comparison of proteasome content between naïve and infected WT and *lmp7*$^{-/-}$ mice, the normalized band intensity of naive WT mice was set to 100% (C, D). The densitometric analysis was performed in duplicates from two independent experiments. 3-4 mice per group and time point were infected i.v. with 5 x 10^3 cfu of Listeria and 2D Two Colour Western Blot analysis of *lmp7*$^{-/-}$ spleen (E) and liver lysates (F) was performed to analyse, which proteasome complexes are stained by antibody MP3. The membranes were further stained for α3 as a marker for the occurring proteasome complexes, which are indicated by arrows.

This indicates, that differences in the overall band intensity do not simply rely on varying amounts of catalytic β-subunits as previously shown (Fig1; Fig.2). Hence, it was concluded that MP3 predominantly stains structural subunits and that the quantification of the observed band pattern is a good correlate of the proteasomal content.

For the comparison of proteasome amounts, the overall band intensity of the proteasome subunit pattern per lane was quantified and normalized to the internal standard GAPDH. The normalized band intensity of naïve WT mice was set to 100%. By this, it became obvious that in naïve spleens of *lmp7*$^{-/-}$ mice the proteasome content was about 25% reduced (Fig.7 A, C), while in naïve liver of *lmp7*$^{-/-}$ mice the proteasome content was decreased about 10% as compared to WT mice (Fig.7 B, D). This might be explained by the fact that β5i is constitutively present in both organs of naive WT mice (Fig. 1 and 2).

Interestingly, in both organs of WT mice, the proteasome content increased following infection. In striking contrast, the proteasome amount remained constant in infected *lmp7*$^{-/-}$ mice (Fig. 7 C, D).

In spleens of WT mice, the proteasome amount was raised up to 20% after infection, which augmented the difference to *lmp7*$^{-/-}$ mice up to 30-40% (Fig. 7B). In the liver of WT mice, the increase in proteasome content reached up to 30% with a maximal difference of 40% to *lmp7*$^{-/-}$ mice (Fig. 7D).

However, the antibody MP3 used for the quantification of proteasomes also stained subunits present in 13-16S precursor proteasomes of *lmp7*$^{-/-}$ mice (Fig. 7 E, F). If these proteasome fractions could be excluded from the quantification, the difference in 20S proteasome content between WT and *lmp7*$^{-/-}$ mice is expected to be even more pronounced.

In summary, the results suggest that the concerted expression of all three immunosubunits is necessary to enhance the cellular proteasome content in infection. However, the constant amount of proteasomes in *lmp7*$^{-/-}$ mice coincides with the observation that the abundance of β5 remained unchanged through the course of infection. In conclusion, these findings strengthen the hypothesis that impaired maturation of 20S proteasomes in *lmp7*$^{-/-}$ mice is caused by the limited availability of β5, which could be responsible for the reduced amount of catalytically active proteasomes per cell.

3.1.5 Analysis of POMP turnover in *lmp7*$^{-/-}$ mice

Next, turnover of the proteasome maturation protein (POMP) was analysed. POMP is a chaperone that binds to precursor proteasomes and directly interacts with β5 and β5i (Fricke, et al., 2007; Heink, et al., 2005). It is a component of 13-16S precursor proteasomes and is necessary for the assembly of two 16S half proteasomes to a catalytically active 20S proteasome (Fig. I). Because it becomes the first substrate for newly formed 20S proteasomes (Ramos, et al., 1998), the degradation of POMP can be regarded as a marker for the rate of proteasome assembly.

It was shown, that POMP mRNA expression is inducible by IFNγ *in vitro* presumably to support the rapid neosynthesis of i20S. Further, expression of β5i is sufficient to increase POMP turnover (Heink, et al., 2005). Thus, we wanted to analyse how β5i-deficiency influences the expression of POMP and its turnover in infection.

The analysis of POMP by Two Colour Fluorescent Western Blot revealed that it accumulates in naïve and infected spleens of *lmp7*$^{-/-}$ mice and that its abundance is constitutively about 5fold enhanced compared to WT mice (Fig. 8 A-B). In the liver of *lmp7*$^{-/-}$ mice the abundance of POMP increased upon infection with Listeria. Its incidence peaked at day 2 after infection with a 4fold increase compared to WT mice and than gradually declined up to day 8. In contrast, POMP was barely detectable in spleens and livers of WT animals, indicating its rapid turnover in infection (Fig 8 C-D).

However, POMP mRNA expression was comparable between WT and *lmp7*$^{-/-}$ mice in spleen and liver (Fig. 8 E -F). Interestingly, in both organs the transcription of POMP was not significantly induced following infection. This was against our expectation, as POMP mRNA was shown to be inducible by IFNγ *in vitro* and infection with Listeria results in systemic secretion of this cytokine (Strehl, et al., 2006). In addition, this shows that the accumulation of POMP in *lmp7*$^{-/-}$ mice occurs at protein level.

As degradation of POMP correlates with the neosynthesis of 20S proteasomes, the low levels of POMP coincide with the accelerated proteasome formation observed in infected WT mice. In contrast, the accumulation of POMP reflects the reduced neosynthesis of proteasomes in *lmp7*$^{-/-}$ mice (Fig. 7).

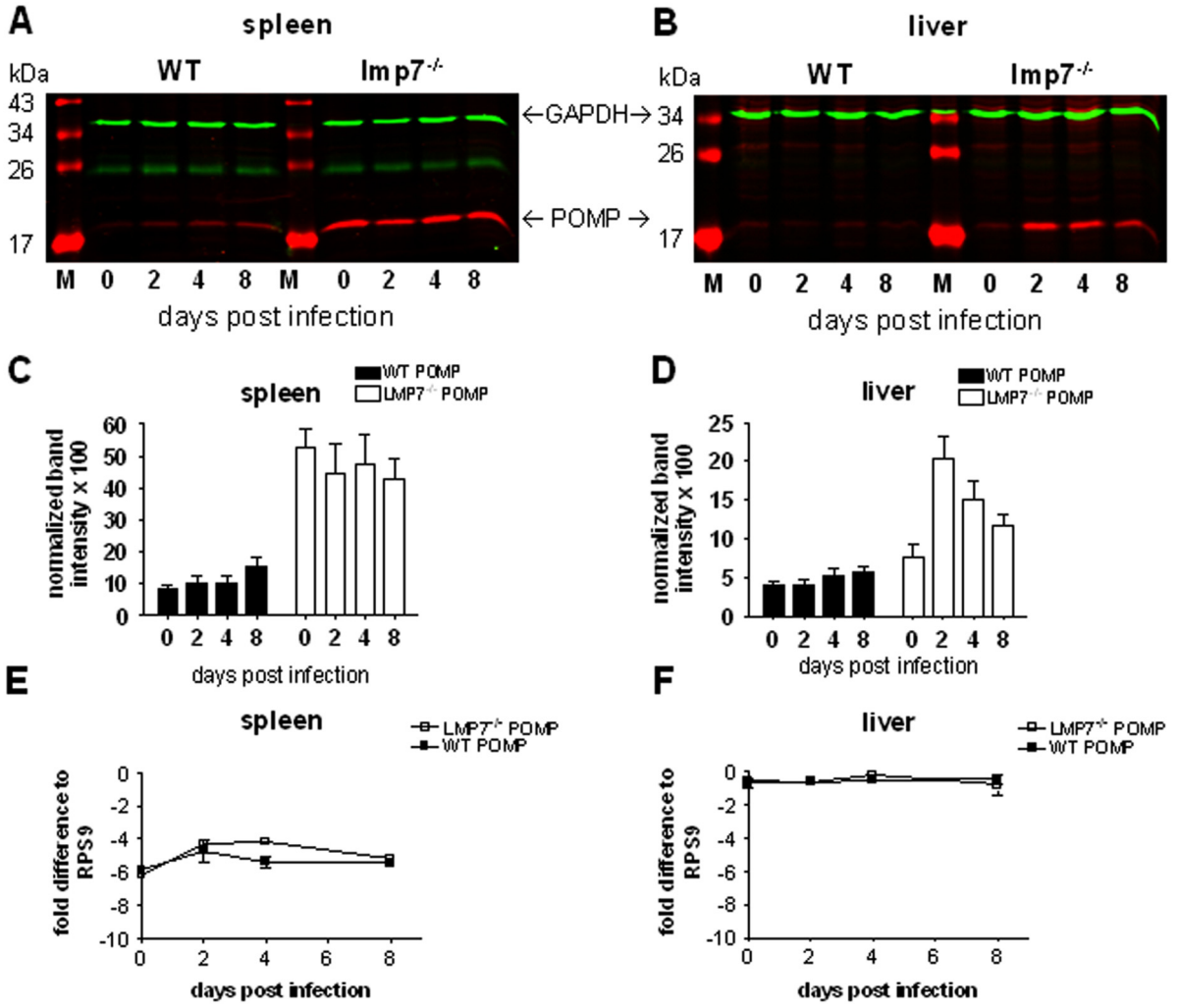

Figure 8. POMP expression at protein and mRNA level following Listeria infection
The abundance of POMP in organ lysates of naïve and infected spleen (A) and liver (C) of WT and *lmp7*$^{-/-}$ mice was analysed by Two Colour Western Blot analysis. POMP was stained with a polyclonal antibody raised in chicken and anti chicken IgY IRDye700 labelled secondary antibodies. As a loading control membranes were further stained with mouse monoclonal anti-GAPDH antibodies and anti-mouse IgG IRDye800 labelled secondary antibodies. For densitometric analysis band intensities of POMP were normalized to the corresponding GAPDH signal. The quantification was performed in duplicates from two independent infections with 3-4 mice per group (B and D). mRNA expression of POMP in spleen (F) and liver (F) was measured by semi quantitative Real Time RT-PCR analysis. Expression levels of POMP were calculated as fold difference to the mRNA of the internal standard RPS9. Shown results are mean values ± standard error of 3 individual mice per time point. Given results are representative of two measurements from independent infections. Mice were infected i.v. with 5 x 10^3 cfu of Listeria.

The increased amounts of POMP in *lmp7*$^{-/-}$ mice raised the question wether it is associated with precursor proteasome complexes or whether it is found as free protein. This question was addressed by 2D Two Colour Fluorescent Western Blot Analysis. We found that POMP is bound to the 13-16S precursor proteasome fractions of naïve and infected *lmp7*$^{-/-}$ spleen as well as in infected *lmp7*$^{-/-}$ liver, whereas free subunits could not be detected. As expected, POMP was not visible in proteasome complexes of WT spleen and liver (Fig. 9 A-B).

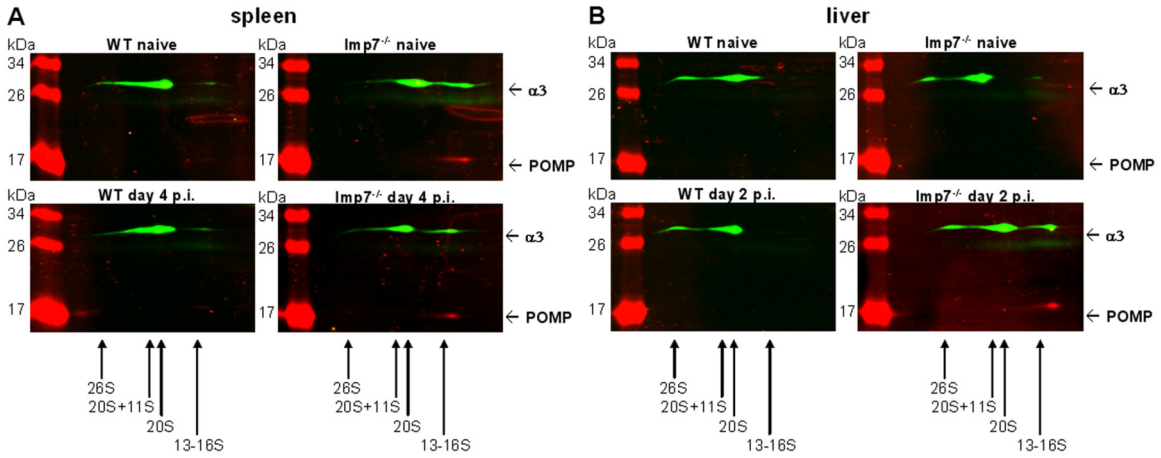

Figure 9: 2D-Two Colour Western Blot analysis of POMP in proteasome complexes
The appearance of POMP in precursor proteasome complexes was analysed by 2D-Two Colour Western Blot. Organ lysates of naïve WT and *lmp7*$^{-/-}$ spleen (A) and liver (B) as well as Listeria infected spleen and liver, 4 days and 2 days post infection respectively, were separated by blue native PAGE. Single lanes were subjected to SDS PAGE in the second dimension and proteins were transferred to PVDF membrane. Membranes were stained with a polyclonal chicken antibody against POMP and IRDye700 conjugated secondary antibodies (red signals) as well as mouse monoclonal antibodies against α3 and anti mouse IgG IRDy800 conjugated secondary antibodies (green signal). Arrows indicate the different proteasome complexes. Mice were infected with 5 x 10^3 cfu of Listeria and organs were pooled of 3-4 mice per group.

In conclusion, accumulation of POMP proteins in *lmp7*$^{-/-}$ mice is caused by its stabilization in precursor proteasomes. Further, this demonstrates that POMP is a component of precursor proteasomes before β5 or β5i are integrated, as these subunits were absent in the observed precursor fractions (Fig. 4, 5). It is known, that β5 or β5i belong to the last subunits that are integrated in precursor proteasomes and that both subunits interact with POMP (Heink, et al., 2005; Nandi, et al., 1997; Witt, et al., 2000). This confirms that the interaction of β5 or β5i with POMP is involved in their recruitment to precursor proteasomes as reported recently (Fricke, et al., 2007). Hence, accumulation of POMP in *lmp7*$^{-/-}$ mice might be an indicator for a shortage of β5 subunits that can be recruited to complete proteasome assembly.

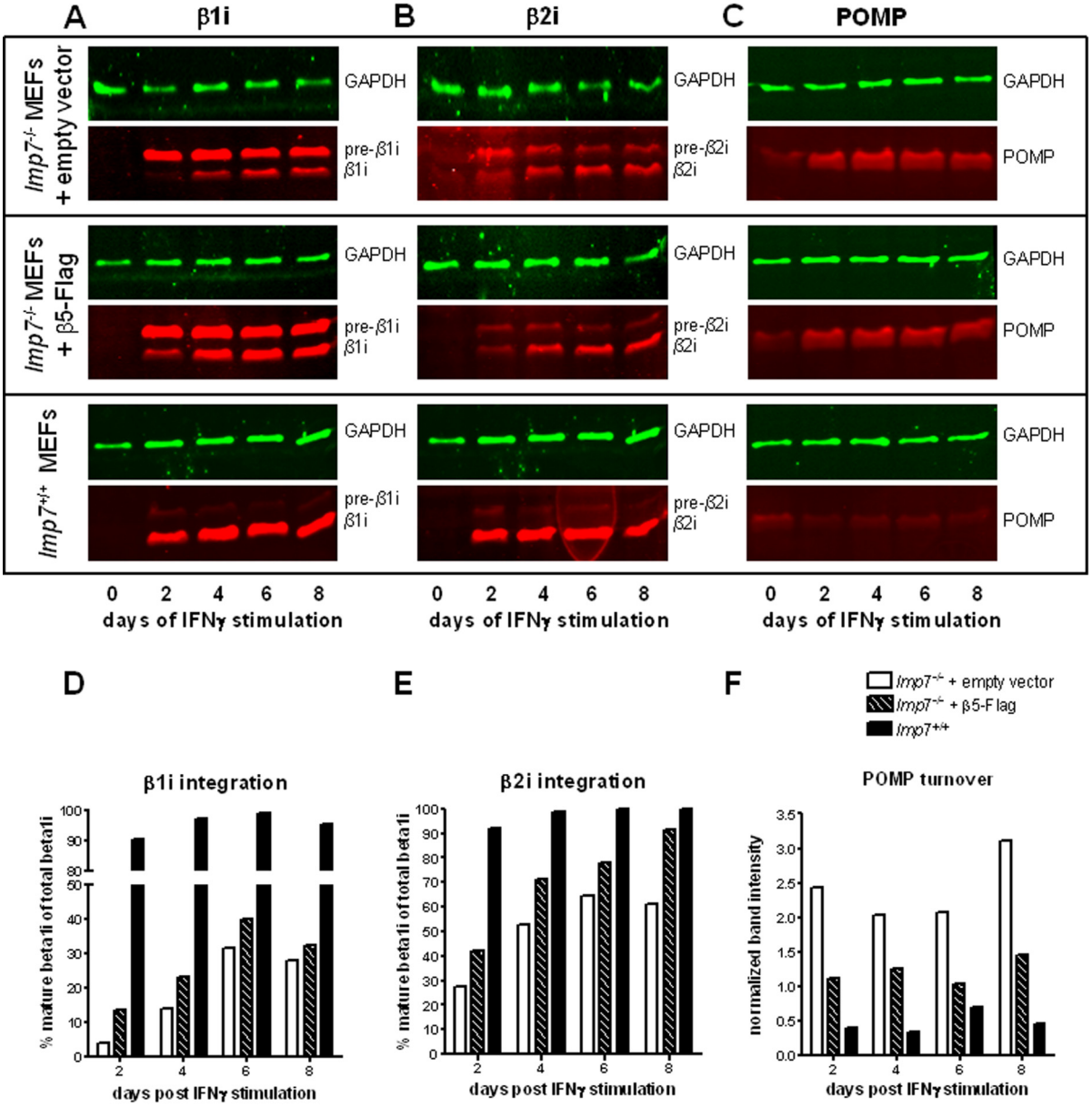

Figure 10. Maturation of β1i and β2i in *lmp7*$^{-/-}$ MEFs overexpressing β5

Overexpression of a β5-Flag fusion protein was achieved by retroviral transduction of *lmp7*$^{-/-}$ MEFs. The integration of β1i and β2i as well as the turnover of POMP was analysed in *lmp7*$^{-/-}$ MEFs overexpressing β5-Flag compared to *lmp7*$^{-/-}$ MEFs transduced with empty vector or *lmp7*$^{+/+}$ (WT) MEFs. Cell lines were either left untreated or stimulated with 50 U/ml IFNγ for the indicated time periods. To determine the abundance of pre-β1i and pre-β2i subunits or mature β1i and β2i as well as POMP, protein lysates of these cells were subjected to Two Colour Fluorescent Western Blot analysis. Membranes were stained for β1i (A), β2i (B) and POMP (C) as well as GAPDH for standardization. The percentages of mature β1i (D) or β2i (E) were calculated as normalized band intensity of β1i or β2i devided through the total pre-β1i + β1i or pre-β2i + β2i signals multiplied with 100. To compare the degradation of POMP in the different cell lines, normalized band intensities measured following IFNγ stimulation are shown (F).

3.1.6 Overexpression of β5 in *lmp7*$^{-/-}$ MEFs

According to our previous results, we wondered whether shortage of β5 is responsible for impaired maturation of β1i and β2i in IFNγ stimulated *lmp7*$^{-/-}$ cells. For this purpose, we generated retrovirally-transduced *lmp7*$^{-/-}$ MEFs overexpressing a β5-Flag fusion protein under control of the constitutive EF1α promoter (*lmp7*$^{-/-}$ MEFs + β5-Flag). We achieved a 7,8fold increased expression of β5 compared to *lmp7*$^{-/-}$ MEFs transduced with an empty vector construct (Table 1). Improved maturation of β1i and β2i under these conditions would support the assumption that the quantity of β5 is a limiting factor following IFNγ stimulation of *lmp7*$^{-/-}$ cells.

However, when we analysed the integration of β1i and β2i in *lmp7*$^{-/-}$ MEFs + β5-Flag at various time points after IFNγ stimulation, only a slight increase in mature β1i subunits was detected as compared to empty vector controls. In average, the abundance of mature β1i was 10% increased and maximally 40% of total β1i was integrated. This was still far beyond WT MEFs, in which more than 90% of total β1i was found in its mature form (Fig. 10 A, D). Interestingly, the integration of β2i could be enhanced up to 30% in *lmp7*$^{-/-}$ MEFs + β5-Flag. Albeit with slow kinetics, up to 90% of total β2i were integrated after IFNγ stimulation, which is close to the maximal integration of WT MEFs (Fig.10 B, D). The strong integration of β2i compared to β1i is surprising, as it was reported that they mutually require each other for efficient maturation (Groettrup, et al., 1997). Further, this finding is in contrast to the efficient integration of both subunits in the liver of *lmp7*$^{-/-}$ mice (Fig. 2B), but might be explained by the artificially high IFNγ concentrations used for *in vitro* experiments.

The degradation of POMP correlates with neosynthesis of 20S proteasomes (Heink, et al., 2005; Ramos, et al., 1998). Compared to WT MEFs and *lmp7*$^{-/-}$ MEFs transduced with an empty vector, we observed an intermediate degradation of POMP in *lmp7*$^{-/-}$ MEFs + β5-Flag. Taken together with the increased maturation of β1i and β2i, this finding underlines that the maturation of 20S proteasomes is improved by enhanced expression of β5.

In summary, overexpression of β5 in *lmp7*$^{-/-}$ MEFs increases the integration of β1i and β2i. Still, the maturation of β1i is drastically impaired and β2i is integrated with much slower kinetics in *lmp7*$^{-/-}$ MEFs + β5-Flag as compared to WT MEFs. In conclusion, this suggests that it is not only the quantity that limits the integration of β5. Instead, we assume that the slower rate of proteasome assembly that was reported in the presence of β5 limits the maturation of m20S in *lmp7*$^{-/-}$ mice, which might explain the accumulation of precursor proteasomes in these mice or IFNγ-treated *lmp7*$^{-/-}$ MEFs (Heink, et al., 2005).

MEF cell line:	β5 x expression	β5i x expression
WT MEFs + empty vector	1x	1x
WT MEFs + β5-Flag	33,2x	0,3x
WT MEFs + β5i-Flag	1,4x	3281x
lmp7$^{-/-}$ MEFs + empty vector	1x	n.d.
lmp7$^{-/-}$ MEFs + β5-Flag	7,8x	n.d.

Table 1: Expression levels of β5 and β5i in retrovirally transduced MEFs
The mRNA expression of β5 and β5i in the retrovirally transduced MEF lines was analysed by Real-Time RT-PCR. The expression of RPS9 was used for normalization. The fold-expression values of β5 and β5i were calculated by equating the corresponding empty vector controls to 1x expression. n.d.: not detectable

3.1.7 Overexpression of β5 in WT MEFs

According to the model of cooperative proteasome assembly, β5i predominantly interacts with β1i/β2i containing precursor proteasomes, while β5 preferentially integrates into β1/β2 containing precursor proteasomes. However, our results so far suggest, that integration of β5 or β5i is a competitive event, rather than a cooperative interaction of constitutive or immunosubunits.

To follow up this question, we constructed retroviral vectors for constitutive overexpression of β5 or β5i fused to a C-terminal Flag-tag. The C-terminal fusion tag does not interfere with integration of the subunits and allows specific immunoprecipitation of proteasome complexes as has been shown previously (De, et al., 2003). This approach is employed to test whether β5 or β5i specifically interact with constitutive or immunsubunits, respectively, or if their integration is competitive.

The WT MEFs express β1i and β2i, but also endogenous β5i exclusively following IFNγ stimulation. This allows analysing whether the overexpressed β5-Flag or β5i-Flag proteins interact with β1 and β2 in unstimulated WT MEFs or with β1i and β2i in IFNγ treated cells.

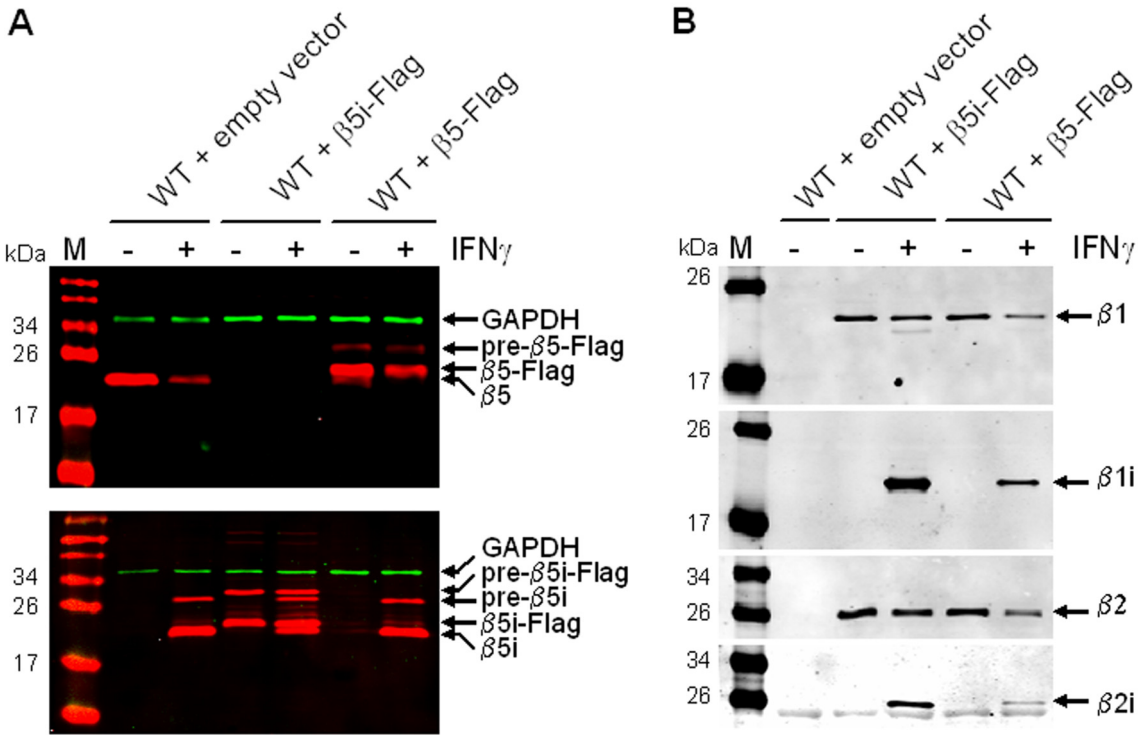

Figure 11. Coimmunoprecipitation analysis in β5-Flag and β5i-Flag overexpressing WT MEFs
β5 or β5i with a C-terminal Flag-tag fusion were stably overexpressed in WT MEFs by retroviral transduction. The expression of the Flag-tagged proteins as well as the endogenously expressed β5 and β5i subunits was analysed by Two Colour Fluorescent Western Blots in cell lysates of the indicated WT MEF cell lines. The cells were either left untreated or stimulated with 50 U/ml of IFNγ for 4 days (A). The interaction of β5-Flag and β5i-Flag with β1/β2 or β1i/β2i respectively was analysed by coimmunoprecipitation via the Flag-tag fusion (B).

Although the expression of the β5i-Flag construct was strongly increased compared to the basic expression level in empty vector controls (Table 1), the IFNγ induced expression of endogenous β5i was sufficient to compete with the overexpressed β5i, as seen in the lysates before immunoprecipitation, in which native and Flag-tagged β5i subunits were detectable (Fig. 11A).

However, β5i-Flag completely replaced the endogenous β5 in unstimulated WT MEFs as seen by the absence of β5 in the cell lysates before immunoprecipitation (Fig. 11A). Accordingly, we found that β5i interacts with β1 and β2 in unstimulated WT MEFs. Overexpression of β5i even allowed prolonged integration of β1 and β2 following IFNγ stimulation. In contrast, β1 and β2 were partly replaced in IFNγ stimulated WT MEFs overexpressing β5-Flag. As expected, β1i and β2i coimmunoprecipitated with β5i-Flag in IFNγ treated cells (Fig. 11B).

The expression of β5 in WT-MEFs transduced with β5-Flag was 33,2fold increased compared to empty vector controls. This expression was strong enough to oust the endogenous β5, as predominantly β5-Flag was detectable in the cell lysates (Fig. 11A). As expected, β1 and β2 coimmunoprecipitated with β5-Flag in unstimulated cells (Fig. 11B). However, β1i and β2i coimmunoprecipitated with β5-Flag following IFNγ stimulation of WT MEFs transduced with β5-Flag (Fig. 11B). This demonstrates that β5 can compete with the induced expression of β5i when it is expressed at high levels. Still, the overexpressed β5-Flag was partly replaced by the high expression of endogenous β5i after IFNγ stimulation, but to a lesser extent as compared to WT MEFs transduced with an empty vector construct (Fig. 11A).

In summary, these data challenge the model of cooperative proteasome assembly suggested by Griffin et al., as no preferential integration of β5i in β1i/β2i- or of β5 in β1/β2-containing precursor proteasomes was detected (Griffin, et al., 1998; Kingsbury, et al., 2000). Thus, the results strongly support the hypothesis, that integration of β5 and β5i is predominantly regulated by competition at the protein level. However, in this process β5i has two advantages, which facilitate the displacement of β5 and rapid formation of i20S in lymphoid or infected tissue: First, its strong expression and second its accelerated recruitment by POMP as compared to β5.

3.2 Functional impact of β5i-deficiency on the immune response against *Listeria monocytogenes*

A major aim of this study is the analysis of the immune response against Listeria in *lmp7*$^{-/-}$ mice. As the structure of the 20S proteasome especially influences the peptide pools presented on MHC class I molecules, we focused on possible consequences for the CD8$^+$ T cell response. For our analysis we chose the epitope $LLO_{296-304}$ derived of Listeriolysin O, a major virulence factor of Listeria. It is the strongest antigenic determinant for CD8$^+$ T cells in mice with the MHC class I haplotype H2^b, such as C57Bl6 or 129Ola mice, which were used for this study. Still, the CD8$^+$ T cell frequency directed towards this epitope is low (Geginat, et al., 2001). However, from our previous work we know that processing of $LLO_{296-304}$ is drastically improved in the presence of i20S (Strehl, et al., 2006). Accordingly, processing of this epitope was expected to be decreased in *lmp7*$^{-/-}$ mice and thus, we also anticipated a reduction in the frequency of $LLO_{296-304}$ specific CD8$^+$ T cells. In addition, we analysed the impact of β5i-deficiency on bacterial control.

3.2.1 Determination of MHC class I surface expression on professional APCs of *lmp7*$^{-/-}$ mice

The phenotype of *lmp7*$^{-/-}$ mice is characterized by a 25-50% reduction in MHC class I surface expression on a variety of immune cells, which underlines the importance of β5i for efficient antigen processing and presentation (Fehling, et al., 1994). However, Fehling et al. did not determine the MHC class I surface expression on professional APCs following infection. Thus, we wanted to investigate whether the reduced MHC class I antigen presentation in *lmp7*$^{-/-}$ mice is sustained on dendritic cells (DCs) or macrophages (MΦ) after Listeria infection.

Presentation of antigens on professional APCs in lymphoid tissue within the first 2 days of Listeria infection is essential to elicit a CD8$^+$ T cell response (Mercado, et al., 2000; Wong and Pamer, 2003). Thereafter, proliferation of CD8$^+$ T cells is mostly antigen independent (Wong and Pamer, 2001). Therefore, the MHC class I surface density on professional APC subsets of the spleen was determined in WT and *lmp7*$^{-/-}$ mice before and 2 days after infection.

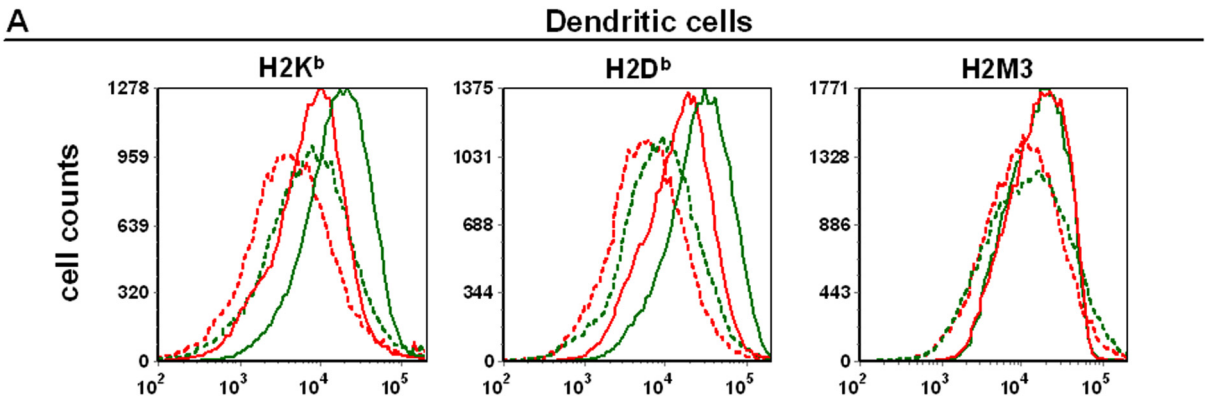

	MFI	MFI normalized to WT	MFI	MFI normalized to WT	MFI	MFI normalized to WT
WT naive	14431 ± 1260	100%	15293 ± 76	100%	18114 ± 574	100%
lmp7$^{-/-}$ naive	9200 ± 440	63,8%	10650 ± 1000	69,6%	18515 ± 877	102%
WT day 2 p.i.	18181 ± 4432	100%	30436 ± 5541	100%	19324 ± 1803	100%
lmp7$^{-/-}$ day 2 p.i.	11081 ± 553	60,9%	20807 ± 967	68,4%	19352 ± 818	100,1%

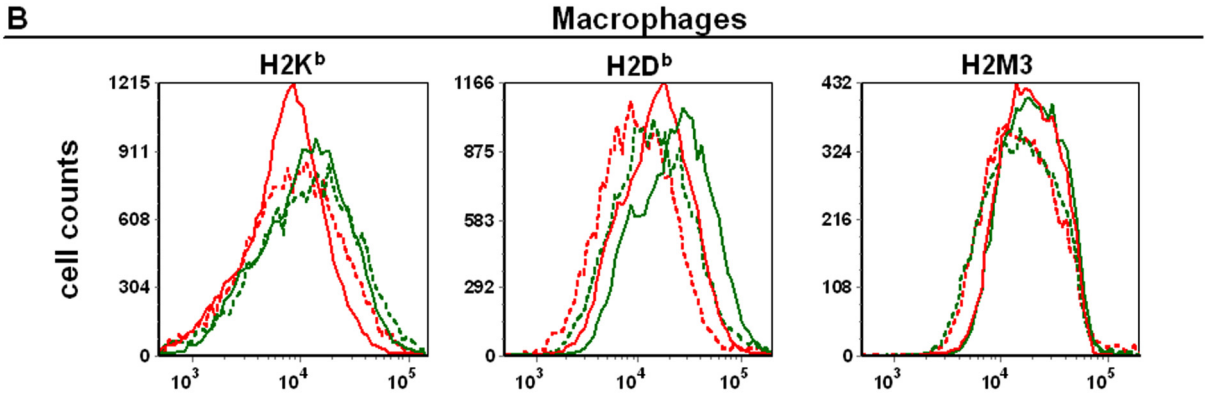

	MFI	MFI normalized to WT	MFI	MFI normalized to WT	MFI	MFI normalized to WT
WT naive	20204 ± 814	100%	21306 ± 866	100%	22439 ± 3163	100%
lmp7$^{-/-}$ naive	15622 ± 1464	77,3%	14000 ± 230	65,7%	22319 ± 3618	99,5%
WT day 2 p.i.	20298 ± 163	100%	35359 ± 1122	100%	23542 ± 2899	100%
lmp7$^{-/-}$ day 2 p.i.	12244 ± 1128	60,3%	22815 ± 1482	64,5%	20721 ± 1871	88%

Figure 12. MHC class I surface expression on professional APCs of Listeria infected WT and *lmp7*$^{-/-}$ mice
Surface expression of MHC class I molecules H2K^b and H2D^b as well as MHC class Ib molecule H2-M3 was measured on APCs by flow cytometry. Splenocytes were prepared of naïve *lmp7*$^{-/-}$ and WT mice or 2 days after i.v. infection with 5 x 10^3 cfu of Listeria. For differentiation of APC subtypes, cells were stained with antibodies for surface markers CD11b, CD11c and MHC class II. Mature, activated dendritic cells (A) or Macrophages (B) were identified as CD11c^{high} MHC class II^{high} expressing and CD11b^{high} MHC class II^{high} expressing cells, respectively. The surface expression of H2K^b, H2D^b and H2-M3 on the APC populations was determined by measurement of the median fluorescence intensity (MFI) of the respective stainings. Shown are representative histograms of naïve WT and *lmp7*$^{-/-}$ mice indicated by green doted and red doted lines, respectively as well as APCs of Listeria-infected WT and *lmp7*$^{-/-}$ mice are indicated by green solid and red solid lines, respectively. The given values of MFI are mean values ± standard deviation of 3-4 mice per group.

As lineage markers for professional APCs, splenocytes were stained with antibodies against CD11c for DCs and CD11b for MΦ. As these markers are also expressed on other cell types, we selected CD11c and CD11b high expressing cells during FACS analysis, which represent predominantly DCs and MΦ, respectively. Further, the cells were stained for MHC class II, as upregulation of this molecule can be used as an activation marker for APCs. Accordingly, the analysis of MHC class I surface expression was focused on $CD11c^{high}$ MHC class II^{high} and $CD11b^{high}$ MHC class II^{high} expressing cells, which represent mature and activated DCs and MΦ, respectively. Although our model epitope $LLO_{296-304}$ is presented via $H2K^b$, we were interested in the overall impact of β5i-deficiency on MHC class I antigen presentation and also measured the surface expression of $H2D^b$ and the non-classical MHC class Ib molecule H2M3.

To quantify the reduction of MHC class I surface expression on APCs of *lmp7*$^{-/-}$ mice, the surface expression of the corresponding APC population in WT mice was set to 100% (Fig. 12). By this calculation we found, that the surface expression of $H2K^b$ and $H2D^b$ on DCs of naïve *lmp7*$^{-/-}$ mice is decreased about 36% and 30%, respectively. This reduction in MHC class I molecules on DCs of *lmp7*$^{-/-}$ mice remained unaltered after Listeria infection, as the average surface expression of $H2K^b$ was 39% and that of $H2D^b$ 31% lower as compared to WT DCs (Fig. 12A).

Similar results were found for MΦ of naïve and Listeria infected *lmp7*$^{-/-}$ mice. The $H2K^b$ surface expression on MΦ of naïve *lmp7*$^{-/-}$ mice was about 23% and the $H2D^b$ surface expression 34% reduced. Accordingly, the average surface density of $H2K^b$ was 40% and that of $H2D^b$ 35% decreased on MΦ of Listeria infected *lmp7*$^{-/-}$ mice (Fig. 12B).

In summary, these data confirm that MHC class I antigen presentation is reduced on professional APCs of *lmp7*$^{-/-}$ mice, which is maintained during Listeria infection. In addition, these findings underline the importance of β5i for efficient antigen processing by professional APCs. As the difference in MHC class I surface expression was found within the first two days of infection, which are critical for $CD8^+$ T cell priming, it is assumed that the $LLO_{296-304}$ specific $CD8^+$ T cell response might be impaired in *lmp7*$^{-/-}$ mice.

Besides presentation of antigens on classical MHC class I molecules, n-formyl methionine containing peptides are presented on non-classical MHC class Ib molecules in bacterial infections. MHC class Ib restricted $CD8^+$ T cells, expand more rapidly compared to classical MHC class I restricted $CD8^+$ T cells. This early arm of adaptive immunity is important for the control of Listeria 3-7 days after infection (Kerksiek, et al., 1999; Seaman, et al., 2000). The

three dominant n-formyl methionine containing peptides of Listeria are directly secreted into the host cell cytosol and are presented on MHC class Ib molecule H2-M3 without further processing (Pamer, 2004). Thus, it was not expected, that their presentation would be affected in *lmp7*$^{-/-}$ mice. Accordingly, when H2-M3 surface expression was determined on DCs (Fig. 12A) and MΦ (Fig. 12B) no differences between WT and *lmp7*$^{-/-}$ mice were detected. This confirms, that presentation of peptides on MHC class Ib molecules is not influenced by β5i-deficiency. Further, this suggests that the function of MHC class Ib restricted CD8^{+} T cells as an effector mechanism of early adaptive immunity against Listeria is not impaired in *lmp7*$^{-/-}$ mice.

3.2.2 Analysis of $LLO_{296-304}$ epitope generation by 20S proteasomes isolated from *lmp7*$^{-/-}$ mice

Recently, we could show that efficient generation of the $LLO_{296-304}$ epitope correlates with the presence of i20S in lymphoid and infected tissues (Strehl, et al., 2006). According to the model of cooperative proteasome assembly, we anticipated that β1i and β2i would be barely integrated in 20S proteasomes of *lmp7*$^{-/-}$ mice, which would consequently result in complete absence of immunosubunits (Griffin, et al., 1998). Thus, we expected impaired processing of $LLO_{296-304}$ in *lmp7*$^{-/-}$ mice. However, the data presented so far, revealed efficient integration of β1i and β2i in *lmp7*$^{-/-}$ mice leading to the formation of m20S. This raised the question, if processing of $LLO_{296-304}$ requires the specific activity of i20S or if the integration of β1i and β2i in m20S is sufficient for efficient processing of $LLO_{296-304}$.

To address this question, 20S proteasomes were isolated from naïve and infected spleen and liver of WT and *lmp7*$^{-/-}$ mice and incubated with a 27mer peptide substrate encompassing the $LLO_{296-304}$ epitope (LLO substrate; Fig. 13A). The cleavage products generated from the LLO substrate were analysed by LC-ESI mass spectrometry. The digestion products detected by mass spectrometry are shown in Fig. 13A. The sequence of the $LLO_{296-304}$ epitope and its precursor $LLO_{294-304}$ are depicted in black. The generation of both, epitope and precursor, was quantified (Fig.13 B-C), because the precursor carries the correct C-terminus of $LLO_{296-304}$ and can be trimmed to the correct epitope by post-proteasomal processing. Thus, the precursor epitopes may contribute to the pool of peptides presented by $H2K^{b}$ molecules.

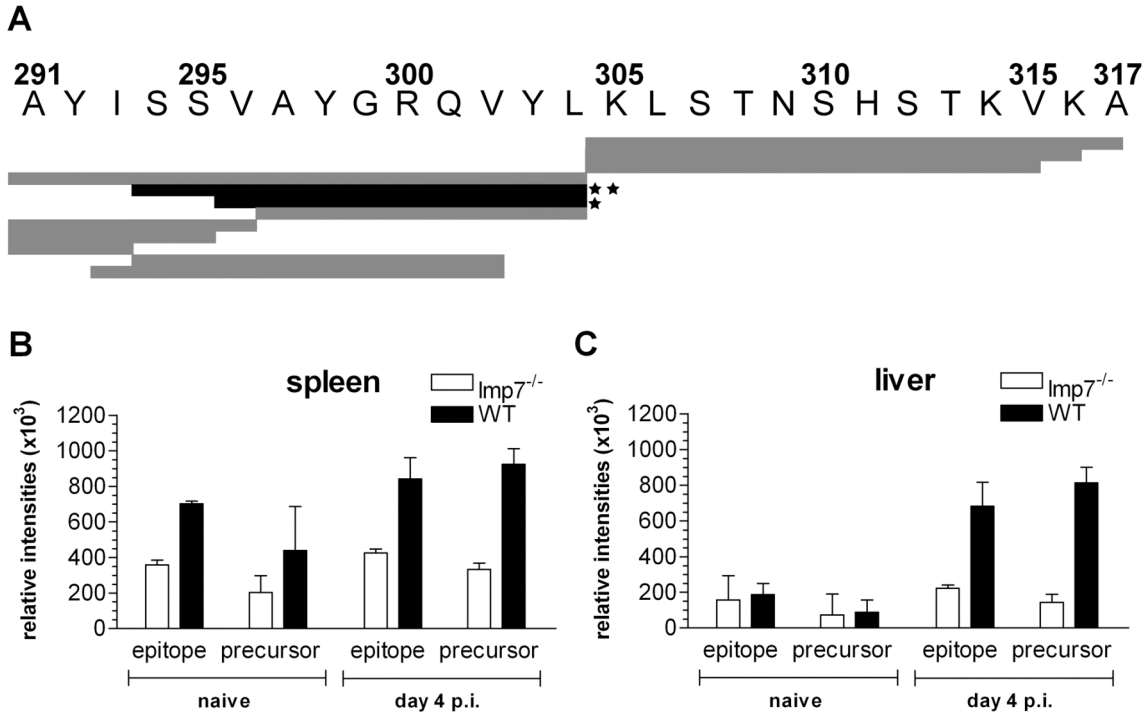

Figure 13. Analysis of $LLO_{296-304}$ epitope generation by isolated 20S proteasomes from WT and *lmp7*$^{-/-}$ mice

20S proteasomes were isolated of naïve or infected spleen and liver of 5 WT and *lmp7*$^{-/-}$ mice per group. Mice were infected i.v. with 5 x 10^3 cfu of Listeria 4 days prior to isolation of 20S proteasomes. The utilized 27mer peptide substrate is derived from the Listeriolysin O sequence and encompasses the $LLO_{296-304}$ epitope (LLO substrate). The LLO substrate was incubated with the different proteasome preparations for 4 h at 37°C. The cleavage products resulting from processing of the LLO substrate were quantified by LC-ESI-mass spectrometry as relative intensities compared to the signal of the standard peptide 9GPS that was added to all reactions in the same concentration. Among the occurring cleavage products the $LLO_{296-304}$ epitope (★) and its precursor $LLO_{294-304}$ (★★) are depicted in black (A). The generation of epitope and precursor by 20S proteasomes from spleen (B) and liver (C) was quantified in duplicates.

The quantification revealed that processing of the LLO substrate by 20S proteasomes isolated from the spleens of WT mice was more efficient as compared to those isolated from *lmp7*$^{-/-}$ mice. Further, processing of the LLO substrate was not significantly enhanced by 20S proteasomes isolated from spleens of infected WT mice, which can be explained by the constitutively high abundance of i20S in WT spleen (Fig. 13B). However, compared to WT mice, proteasome mediated generation of $LLO_{296-304}$ and $LLO_{294-304}$ was about 50% reduced by 20S proteasomes isolated from spleens of naïve or infected *lmp7*$^{-/-}$ mice (Fig 13 B).

20S proteasomes isolated from the livers of naïve WT and *lmp7*$^{-/-}$ mice were inefficient in processing the LLO substrate. This was expected, since naïve livers predominantly contain c20S. However, 20S proteasomes isolated from the liver of infected WT mice revealed 4fold increased $LLO_{296-304}$ epitope processing and 5fold elevated generation of the precursor epitope $LLO_{294-304}$. In contrast, 20S proteasomes prepared from the liver of infected *lmp7*$^{-/-}$ mice did not show increased processing of the LLO substrate. In conclusion, enhanced $LLO_{296-304}$ and

$LLO_{294-304}$ generation coincides with the induction of i20S in the liver of WT mice, but not with the formation of m20S in *lmp7*$^{-/-}$ mice.

Although substantial amounts of β1i and β2i were integrated in m20S of infected *lmp7*$^{-/-}$ mice (Fig. 1-4), processing of the LLO substrate was diminished compared to WT mice. In conclusion, this demonstrates that the activity of m20S cannot compensate the activity of i20S in LLO processing. Still, it cannot be clarified, if generation of $LLO_{296-304}$ or $LLO_{294-304}$ depends on the specific activity of β5i or if it requires the unique, structural features of i20S.

3.2.3 Quantification of $LLO_{296-304}$ specific $CD8^+$ T cells in WT and *lmp7*$^{-/-}$ mice

So far, reduced cell surface expression of MHC class I molecules on professional APCs and decreased generation of the epitope $LLO_{296-304}$ was detected in *lmp7*$^{-/-}$ mice infected with Listeria. To test whether the $CD8^+$ T cell response directed against $LLO_{296-304}$ is affected by the limited antigen presentation in *lmp7*$^{-/-}$ mice, we analysed priming and expansion of $LLO_{296-304}$ specific $CD8^+$ T cells by intracellular cytokine staining (ICS) in WT and *lmp7*$^{-/-}$ mice (Fig. 14).

Following stimulation with the $LLO_{296-304}$ peptide, IFNγ producing $CD8^+$ T cells were detected in lymphocyte preparations of spleen (Fig. 14A) and liver (Fig. 14B) in both groups of mice. In contrast, only background staining for IFNγ was recognized in unstimulated controls in all lymphocyte preparations tested (Fig. 14 A-B). This demonstrates that $LLO_{296-304}$ specific $CD8^+$ T cells could be specifically detected by ICS in WT and *lmp7*$^{-/-}$ mice infected with Listeria.

Further, we used CD62L expression as an activation marker; with $CD62L^{low}$ expressing cells representing recently activated $CD8^+$ effector T cells. Accordingly, $LLO_{296-304}$ specific $CD8^+$ T cell frequencies are expressed as the percentage of $IFN\gamma^+$ cells among $CD62L^{low}$ $CD8^+$ T cells (Fig. 14 C-D).

However, no significant differences in the frequencies of $LLO_{296-304}$ specific effector $CD8^+$ T cells were detected in WT and *lmp7*$^{-/-}$ spleen at any analysed time point after infection. In both groups of mice, the $CD8^+$ T cell frequencies peaked 10 days post infection with an average of 0.35% in WT and 0.25% in *lmp7*$^{-/-}$ mice (Fig. 14C).

Similar results were obtained for the liver, as comparable frequencies of $LLO_{296-304}$ specific $CD8^+$ T cells were found in WT and *lmp7*$^{-/-}$ mice (Fig. 14D). Like in the spleen, $CD8^+$ T cell

frequencies were maximal 10 days post infection with an average of 0.45% in WT and 0.50% in *lmp7*$^{-/-}$ mice.

In conclusion, this demonstrates that impaired processing of $LLO_{296-304}$ and reduced MHC class I antigen presentation on professional APCs of *lmp7*$^{-/-}$ mice is not limiting for priming and expansion of $LLO_{296-304}$ specific $CD8^+$ effector T cells.

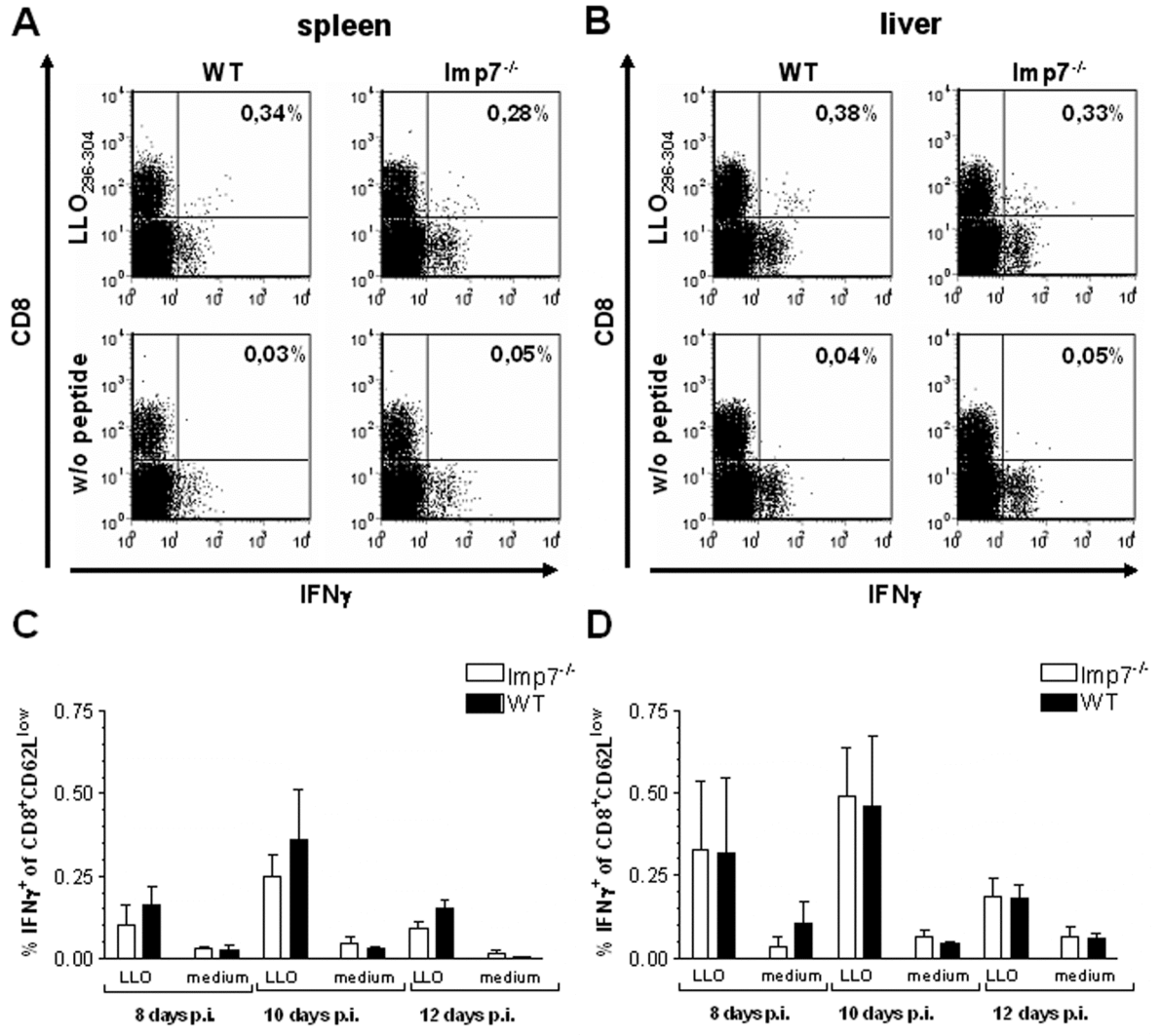

Figure 14. $LLO_{296-304}$ specific $CD8^+$ T cells in WT and *lmp7*$^{-/-}$ mice following infection with Listeria
Lymphocytes of spleen and liver of WT and *lmp7*$^{-/-}$ mice were isolated at indicated time points after i.v. infection with 10^3 cfu Listeria. Lymphocytes were either left untreated or stimulated with 1 µg/ml $LLO_{296-304}$ peptide in the presence of brefeldin A. Following stimulation, cells were subjected to intracellular cytokine staining. Shown are representative FACS dot plots of CD8 vs. IFNγ stainings with lymphocytes of spleen (A) and liver (B) isolated 10 days after infection with Listeria. Frequencies of $LLO_{296-304}$ specific $CD8^+$ T cells in spleen (C) and liver (D) are shown as % $IFN\gamma^+$ cells of $CD8^+$ $CD62L^{low}$ cells following peptide stimulation (LLO) of lymphocytes isolated of WT (black bars) or *lmp7*$^{-/-}$ mice (open bars) at the indicated time points post infection. Background staining is shown as % $IFN\gamma^+$ cells of $CD8^+$ $CD62L^{low}$ cells in unstimulated (medium) controls. $LLO_{296-304}$ specific $CD8^+$ T cell frequencies were measured in 3 individual mice per group. Shown are representative results of two independent experiments.

3.2.4 Analysis of bacterial control in Listeria infected WT and *lmp7*$^{-/-}$ mice

Although we did not detect any significant differences in CD8$^+$ T cell responses directed against our model epitope $LLO_{296-304}$, we were interested whether the control of Listeria infection is affected by β5i-deficiency. Thus, bacterial titers were determined in spleen and liver of WT and *lmp7*$^{-/-}$ mice during the time course of infection.

In the first 2 days after infection bacterial burdens were comparable in spleen and liver of WT and *lmp7*$^{-/-}$ mice showing that early bacterial control was not affected. Unexpectedly, bacterial titers in spleen and liver were significantly increased 3-4 days post infection in *lmp7*$^{-/-}$ compared to WT mice. The median baterial burden was 10fold increased in the spleens and 15fold enhanced in the livers of *lmp7*$^{-/-}$ mice. This defect is independent of MHC class I restricted CD8$^+$ T cell function, because in primary infection CD8$^+$ effector T cells do not mediate significant protection before day 5 after infection. As predominantly innate immune defence mechanisms mediate control of Listeria infection at that time, these results suggest a so far unreported role of β5i in innate immunity.

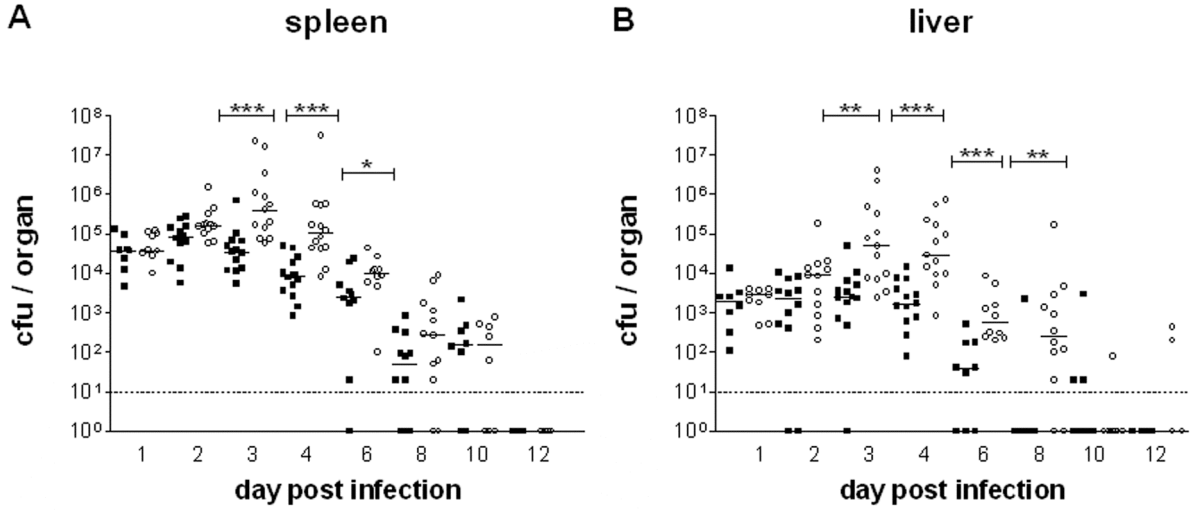

Figure 15. Analysis of bacterial titers in WT and *lmp7*$^{-/-}$ mice during the Listeria infection
WT and *lmp7*$^{-/-}$ mice were infected i.v. with 5 x 10^3 cfu of Listeria and sacrificed at the indicated time points post infection. Organs were homogenized in 1x PBS and serial dilutions were plated on Palcam agar plates. Bacterial titers of spleen (A) and liver (B) were determined in 3-4 individual mice per group and time point from 3 independent experiments. For each group the median is indicated and significance was determined by the Mann-Whitney non-parametric t-test. Significance levels: * p<0,05; ** p<0.01; *** p<0,001.

Bacterial titers in spleens of *lmp7*$^{-/-}$ mice adjusted to the level of WT mice 8 days after infection and the Listeria were cleared with similar kinetics until day 12 post infection (Fig. 15A). This finding indicates, that in the spleen reduced MHC class I surface expression is not limiting for CD8$^+$ T cell mediated clearance of Listeria.

However, compared to WT mice clearance of Listeria from the livers of *lmp7*$^{-/-}$ mice was delayed. While the bacteria were largely eliminated in WT mice 8 days after infection, the median bacterial burden in *lmp7*$^{-/-}$ mice was still above 10^2 cfu. The Listeria were cleared from the livers of *lmp7*$^{-/-}$ mice 10 days after infection, showing that irradication of the bacteria was two days delayed in these mice (Fig. 15B).

Because late control of Listeria depends on adaptive immunity (Ladel, et al., 1994), these results suggest an impaired function of the CD8$^+$ T cell response in liver but not spleen of *lmp7*$^{-/-}$ mice. This was surprising, as reduced MHC class I antigen presentation did not affect CD8$^+$ T cell frequencies neither in spleen nor liver of *lmp7*$^{-/-}$ mice (Fig. 14). Thus, we assume that reduced MHC class I surface expression on infected target cells of *lmp7*$^{-/-}$ mice limits their recognition by CD8$^+$ T cells and is consequently responsible for delayed bacterial clearance. As the control of Listeria was only impaired in the liver, we propose that the reduced MHC class I antigen presentation in *lmp7*$^{-/-}$ mice is especially limiting for recognition of non-lymphoid target cells like hepatocytes.

3.2.5 Proinflammatory cytokine secretion by Listeria-infected *lmp7*$^{-/-}$ macrophages *in vitro*

The analysis of listerial titers revealed an impaired control of the bacteria in spleen and liver of *lmp7*$^{-/-}$ mice 3-4 days post infection (Fig. 15). At that time, anti-bacterial immunity depends on innate immune defence mechanisms. This raised the question, how β5i-deficiency may influence early bacterial control.

MΦ represent a major arm of innate immunity in bacterial infection. Thus, we investigated wether MΦ function might be affected in *lmp7*$^{-/-}$ mice. For this reason, bone marrow derived macrophages (BM-MΦ) were generated from WT and *lmp7*$^{-/-}$ mice and infected with Listeria *in vitro*. The secretion of the proinflammatory cytokines IL-6 and TNFα was measured as an indication for the activation of BM-MΦ following infection.

While the IL-6 production by WT BM-MΦ was maximal 12 h post infection, the secretion of IL-6 by *lmp7*$^{-/-}$ BM-MΦ was induced with slower kinetics (Fig. 16B). Further, TNFα release by *lmp7*$^{-/-}$ BM-MΦ was reduced compared to WT BM-MΦ; most pronounced 6 h after infection (Fig. 16A). These results indicate impaired secretion of proinflammatory cytokines by MΦ of *lmp7*$^{-/-}$ mice and suggest that β5i-deficiency has a so far unreported role in innate immune defence mechanisms.

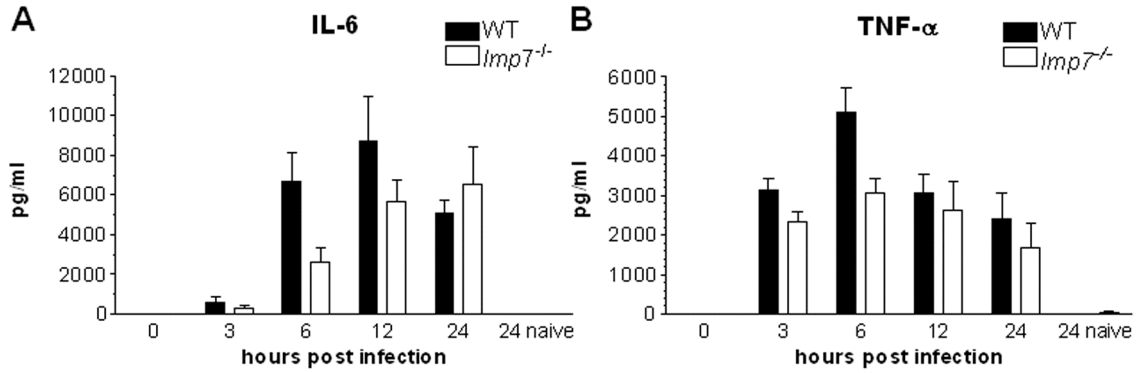

Figure 16. Secretion of proinflammatory cytokines by WT and *lmp7*$^{-/-}$ BM-MΦ infected with Listeria
Bone marrow derived macrophages (BM-MΦ) were generated of WT and *lmp7*$^{-/-}$ mice. 2 x 10^5 BM-MΦ per well were seeded in 96well plates and stimulated over night with 200 U/ml IFNγ for activation. Next day BM-MΦ were infected with Listeria at a MOI =1 and cell culture supernatants were harvested at the indicated time points. Concentrations of proinflammatory cytokines IL-6 and TNFα in the supernatants were measured with the Bioplex cytokine bead array system (Biorad). Secretion of cytokines was measured in three independent preparations of WT and *lmp7*$^{-/-}$ BM-MΦ.

4 Discussion

4.1 The structural impact of β5i-deficiency on 20S proteasome assembly

The role of β5i in proteasome assembly was previously investigated in T2 cells reconstituted with *lmp2* or *lmp2* and *lmp7 in vitro*. In this system, expression of β5i is essential for efficient integration of β1i and β2i in 20S proteasomes, which suggested that immunosubunits form i20S by cooperative assembly (Griffin, et al., 1998).
Here, we determined the impact of β5i-deficiency on integration of β1i and β2i in different organs of Listeria-infected *lmp7*$^{-/-}$ mice. Our results challenge the current model of cooperative assembly, because we found efficient integration of β1i and β2i in m20S in association with β5. In the following, the relevance of our findings with regard to the current opinion is discussed.

4.1.1 Formation of m20S in *lmp7*$^{-/-}$ mice

According to the concept of cooperative proteasome assembly, β5i predominantly interacts with β1i and β2i containing precursor proteasomes to form i20S, while β5 is restricted to β1 and β2 containing precursor proteasomes resulting in c20S (Griffin, et al., 1998). Further, it is claimed that the β5i-prosequence mediates specific interaction with pre-β1i and pre-β2i (Kingsbury, et al., 2000). However, the ability of the β5i-propeptide to interact with β1 and β2 and the influence of subunit quantities was not shown by Kingsbury et al., although it was already suggested that β5i can also pair with β1 and β2. By now, various subtypes of proteasomes with mixtures of constitutive and immunosubunits have been identified. However, formation of m20S with β1i/β2i/β5 stoichiometry is still regarded as highly inefficient (De, et al., 2003; Kingsbury, et al., 2000; Klare, et al., 2007). In contrast, integration of β1i and β2i in 20S proteasomes of *lmp7*$^{-/-}$ splenocytes has been reported previously (Stohwasser, et al., 1996). However, the maturation of β1i and β2i subunits with correlation to their precursors was not quantified in this study.
Here, we found that especially in the liver of infected *lmp7*$^{-/-}$ mice up to 90% of β1i and β2i subunits were found in their mature form. Further, compared to WT mice, β1 and β2 were

replaced with similar kinetics in the liver of *lmp7*$^{-/-}$ mice, which demonstrates that β5 predominantly interacts with β1i and β2i following infection. In addition, we found that β5-Flag protein overexpressed in WT MEFs can also pair with β1i and β2i in competition with IFNγ–induced β5i. Altogether, this demonstrates efficient formation of m20S with β1i/β2i/β5 stoichiometry.

Also when we analysed the interaction of β5i with other catalytic β-subunits, we did not detect a preferential interaction with immunosubunits. Instead, constitutive overexpression of β5i leads to the formation of 20S proteasomes with β1/β2/β5i stoichiometry. Further, we detected high levels of mature β5i in naïve livers of WT mice, while β1i and β2i were barely detectable, which suggests interaction with β1 and β2 also *in vivo*.

Thus, our data challenge the concept of preferential interaction of β5i with β1i and β2i containing precursur proteasomes and the β5i propeptide seems to generally facilitate the integration of this subunit in 20S proteasomes. This is in agreement with other reports that revealed efficient integration of β5i in *lmp2*$^{-/-}$ and *mecl1*$^{-/-}$ mice or formation of various proteasome subtypes with various combinations of β5i with constitutive or immunosubunits (Basler, et al., 2006; Groettrup, et al., 2001; Klare, et al., 2007).

Instead, our results suggest that integration of β5 or β5i is substantially regulated by competition at the protein level. Thus, we propose that simultaneous overexpression of all three immunosubunits in lymphoid or infected tissues is an important mechanism of i20S formation.

However, at mRNA level simultaneous overexpression of all three immunosubunits was only found in infected liver. In the spleen, where i20S are the prevalent proteasome type, (Kuckelkorn, et al., 2002), only β1i revealed constitutively higher mRNA expression compared to β1, while β2i and β5i reached the expression levels of β2 and β5 only after infection. However, Groettrup et al. showed that β1i and β2i mutually improve their integration into i20S (Groettrup, et al., 1997). Hence, high expression of β1i in naive spleens might be sufficient to promote integration of β2i.

In contrast, we observed increased integration of β2i independently of β1i in spleens of infected WT mice. In addition, overexpression of β5 in *lmp7*$^{-/-}$ MEFs substantially improved the integration of β2i while that of β1i was only marginally enhanced. These findings indicate that besides mutual interaction, the integration of β2i is also influenced by competition with β2 at protein level.

Gaczynska et al. demonstrated that overexpression of β1 downregulates the integration of β1i and vice versa, which fits to our model of competitive integration (Gaczynska, et al., 1996). However, this study also reported that overexpression of β5 downregulates the percentage of integrated β1i, which was interpreted as preferential interaction of β5 with β1. But it was shown, that overexpression of β5 increases the total proteasome content per cell (Chondrogianni, et al., 2005; Liu, et al., 2007). Increasing the amount of proteasomes might reduce the competition of β1 and β1i and could allow parallel integration of both subunits, which would consequently decrease the ratio of β1i to β1. Accordingly, we found improved integration of β1i and β2i in IFNγ-stimulated *lmp7*$^{-/-}$ MEFs overexpressing β5 and parallel integration of β1 and β1i in IFNγ-stimulated WT MEFs overexpressing β5i. Thus, the results of Gaczynska et al. can also be explained by our concept of competitive integration of catalytic β-subunits (Fig. III).

On the basis of our data we cannot exclude that higher affinity of immunosubunits to assembling proteasome complexes contributes to the formation of i20S. In agreement with this, β1i is found in earlier assembly intermediates compared to β1 indicating its preferential integration (Nandi, et al., 1997). In addition, we found complete replacement of β5 in WT MEFs constitutively expressing β5i-Flag protein, which supports the idea of preferential integration of immunosubunits. However, according to our concept, higher affinity of immunosubunits would only accelerate the replacement of constitutive subunits and explains why i20S can form rapidly after infection.

In summary, our results demonstrate that the model of cooperative proteasome assembly must be revised. Instead, we suggest that simultaneous overexpression of all three immunosubunits, which consequently leads to the replacement of constitutive subunits at protein level, is an important mechanism of i20S formation. In this competition, high affinity of immunosubunits to assembling proteasome comlexes seems to further facilitate their rapid integration.

4.1.2 β5 is a limiting factor for proteasome maturation in *lmp7*$^{-/-}$ mice

We demonstrated that in infected *lmp7*$^{-/-}$ mice β5 is preferentially integrated into m20S and could not find evidence for specific integration into c20S. Still, the accumulation of precursor proteasomes containing pre-β1i and pre-β2i points at impaired maturation of 20S complexes in lymphoid or infected tissues of *lmp7*$^{-/-}$ mice.

According to cooperative proteasome assembly, β5i deficieny is sufficient to induce an accumulation of precursor proteasomes, because it is crucial for efficient maturation of β1i and β2i in T2 cells (Griffin, et al., 1998; Kingsbury, et al., 2000). However, that the accumulation of precursor proteasomes may be caused by a shortage of β5 subunits in lymphoid or infected tissues has been barely considered.

Here, we provide data suggesting a limitation of β5. First, compared to WT mice the abundance of β5 is constitutively increased in the spleens of *lmp7*$^{-/-}$ mice. Second, the amount of β5 remained constant in the livers of *lmp7*$^{-/-}$ mice, while the abundance of this subunit declined during infection of WT mice. However, in both organs the amount of β5 remained unaltered in infection, indicating that its usage was already maximal. In agreement with this finding, we did not detect free β5 subunits or β5 bound to precursor proteasomes of *lmp7*$^{-/-}$ mice. These results support the assumption that the availability of β5 is a limiting factor for 20S proteasome assembly in *lmp7*$^{-/-}$ mice.

Further, we showed that the mRNA expression of β5 was not upregulated in *lmp7*$^{-/-}$ mice in order to compensate for the deficiency of β5i. However, the transcriptional level of β5 was much higher in the liver as compared to the spleen and may explain, why β1i and β2i were more efficiently integrated in the liver of *lmp7*$^{-/-}$ mice. In conclusion, we assume that the limitation of β5 is set at the transcriptional level, which consequently results in the varying integration-efficiency of β1i and β2i in lymphoid and non-lymphoid tissues of *lmp7*$^{-/-}$ mice. Noteworthy, T2 cells are of lymphoid origin with presumably low expression of β5, which could explain the strong accumulation of pre-β1i and pre-β2i in T2 cells reconstituted with *lmp2* but not *lmp7*.

Also other groups showed that the transcription of β5 is a limiting factor for proteasome assembly, as overexpression of β5 could increase the total amount of proteasomes per cell

(Chondrogianni, et al., 2005; Das, et al., 2007; Liu, et al., 2007). However, the impact of β5 on the integration of β1i and β2i was not analysed in these studies.

Indeed, overexpression of β5 in *lmp7*$^{-/-}$ MEFs facilitates the maturation of β1i and β2i and accelerated proteasome neosynthesis was confirmed by increased POMP turnover. Especially the integration of β2i was substantially improved albeit with slower kinetics than in WT MEFs. In contrast, the integration of β1i was only marginally increased. This is in agreement with the work of Kingsbury et al., who showed that overexpression of β5 in T2 cells reconstituted with *lmp2* cannot substantially improve the integration of β1i. However, the effect on the integration of β2i was not analysed in this study (Kingsbury, et al., 2000).

In summary, our results demonstrate that the availability of β5 in *lmp7*$^{-/-}$ mice is limiting for the integration of β1i but especially of β2i. However, the large proportion of precursor proteasomes in *lmp7*$^{-/-}$ MEFs despite strong overexpression of β5 indicates that other factors than mere quantity must be involved in the regulation of β5-integration in 20S complexes.

4.1.3 POMP regulates the integration efficiency of β5 and β5i

The strong accumulation of precursor proteasomes in *lmp7*$^{-/-}$ cells despite overexpression of β5 raised the question, which factors regulate the differential integration efficiency of β5 and β5i.

In yeast, the proteasome maturation factor Ump1p is required for proper maturation of 20S proteasomes. Interestingly, deficiency in Ump1p allows integration of β5 with a deleted prosequence while presence of Ump1p inhibits it. Therefore, an Ump1p dependent checkpoint in proteasome assembly, which controls the integration of β5 on the basis of its propeptide, has been postulated (Ramos, et al., 1998). In addition, it was recently shown that the interaction of Ump1p with pre-β5 stabilizes the 16S precursor dimer and thus allows efficient maturation of 20S proteasomes (Li, et al., 2007). Hence, it is conceivable that similar to Ump1p its mammalian homologue POMP might regulate the integration of β5 and β5i. Accordingly, POMP was shown to interact with both subunits in mammalian cells (Fricke, et al., 2007; Heink, et al., 2005; Jayarapu and Griffin, 2004; Witt, et al., 2000).

It is known that incorporation of β5 or β5i occurs late in the formation of half proteasomes (Nandi, et al., 1997). We found accumulation of POMP in precursor proteasomes, which were devoid of β5 subunits in *lmp7*$^{-/-}$ mice. This indicates that POMP binds to precursor

proteasomes before β5 or β5i are integrated, which is a prerequisite to control their access to assembling proteasome complexes. Accordingly, it was recently shown that POMP already binds to α-rings and can interact with all β-subunits indicating that it recruits these subunits to assembling proteasome complexes (Fricke, et al., 2007). Thus, we suggest that similar to Ump1p in yeast, POMP controls the integration of β5 and β5i in mammalian cells.

Although β5 and β5i can bind to POMP independent of their propeptides, Heink et al. suggested that the prosequences mediate differential interaction of these subunits with POMP (Heink, et al., 2005). In agreement with this, integration of β5 is improved, when its propeptide is exchanged against that of β5i. In contrast, fusion of the β5-propeptide to β5i diminishes the integration of the chimeric protein (Kingsbury, et al., 2000). Also deletion of the β5i-prosequence results in impaired proteasome maturation (Witt, et al., 2000) and the β5i isoform LMP7E1, which carries a different prosequence compared to the major isoform LMP7E2, is barely integrated into 20S proteasomes (Heink, et al., 2006). In addition, interaction analysis with a yeast two-hybrid screen indicated higher affinity of β5i to POMP compared to β5 (Fricke, et al., 2007).

In summary, it can be concluded that the differential interaction of β5 and β5i with POMP regulates the rate of proteasome assembly, which is most likely a function of their prosequences. In this process, rapid recruitment of β5i by POMP promotes accelerated proteasome assembly and facilitates i20S formation. In contrast, slow recruitment of β5 by POMP limits the assembly rate of m20S in *lmp7*$^{-/-}$ mice and therefore is responsible for the accumulation of precursor proteasomes observed in these mice. Finally, limited recruitment of β5 by POMP might explain why overexpression of this subunit in *lmp7*$^{-/-}$ MEFs can restore integration of β2i only with slow kinetics.

4.1.4 Regulation of the proteasome content

So far, the regulation of the cellular proteasome content in mammalian cells is largely unknown. In yeast, the amount of proteasomes is regulated by the transcription factor Rpn4, which drives the transcription of all proteasomal subunits by a PACE sequence in their promoters. Rpn4 itself is a proteasomal substrate, thus the amount of proteasomes is kept constant by a feedback loop between Rpn4-synthesis and its proteasomal degradation (Dohmen, et al., 2007).

It has been shown that treatment of cell cultures with proteasome inhibitors leads to the concerted expression of proteasomal subunits as well as POMP, which indicates that such a feedback-loop could also exist in mammalian cells (Meiners et al., 2003). Indeed, the transcription factor Nrf2 was shown to induce the transcription of most proteasome subunits via an antioxidant response element (ARE) in their promoters (Kwak, et al., 2002; Kwak, et al., 2003). However, Nrf2 also induced the expression of β1, β2 and β5, while we found unaltered expression of these subunits in infection. This suggests that Nrf2 is not involved in the upregulation of proteasome content in infection.

Our results demonstrate that the induction of β5i is crucial for the upregulation of proteasomal content in WT mice, because the amount of proteasomes remained constant in infected *lmp7*$^{-/-}$ mice. In addition, the proteasome quantity was constitutively decreased in *lmp7*$^{-/-}$ compared to WT mice. This suggests that a feedback-loop like in yeast does not exist in mammals, because it would counterbalance the reduced amount of proteasomes in *lmp7*$^{-/-}$ mice as well as the upregulation of proteasomes in WT mice to maintain proteasome homoeostasis.

Instead, we propose that the high affinity of β5i to POMP does not only mediate accelerated proteasome assembly as reported previously (Heink, et al., 2005), but also drives the upregulation of proteasome content in infection. In contrast, the slow recruitment of β5 by POMP results in a constant turnover of proteasomes resulting in homoeostasis under steady state conditions. Consequently, the balance of POMP and β5 determines the amount of proteasomes under homoeostatic conditions. This is supported by the observation, that overexpression of either β5 or POMP, is capable to increase the cellular proteasome content, because both will shift the balance towards accelerated proteasome assembly (Chondrogianni and Gonos, 2007; Chondrogianni, et al., 2005; Das, et al., 2007; Liu, et al., 2007).

The expression of POMP is IFNγ-inducible *in vitro*, which is thought to promote the rapid neogenesis of i20S (Burri, et al., 2000; Heink, et al., 2005; Witt, et al., 2000). Although we observed an IFNγ dependent upregulation of immunosubunits following Listeria infection (Strehl, et al., 2006), we did not detect a significant increase in POMP mRNA expression neither in spleen nor liver. This demonstrates that induction of POMP is not involved in the upregulation of proteasomal content following infection. Accordingly, reconstitution of T2 cells with β5i is sufficient to increase the rate of proteasome assembly independent of IFNγ (Heink, et al., 2005). Still, it cannot be excluded that simultaneous induction of all three immunosubunits is necessary to increase the amount of proteasomes per cell.

Besides expression of IFNγ inducible subunits, upregulation of the cellular proteasome content requires that either all structural subunits of the 20S complex are constitutively produced in excess or that their expression is induced by infection. However, it was shown that overexpression of β5 is sufficient for the upregulation of proteasome content in different cell types (Chondrogianni et al., 2005; Liu et al., 2007). This implies constitutive overproduction of the structural subunits, which could be a mechanism to allow rapid neogenesis of proteasomes under cellular stress, e.g. in infection.

4.1.5 Model of competitive integration of catalytic β-subunits in 20S proteasome assembly

Although our data strongly challenge the model of cooperative proteasome assembly (Fig.II; (Griffin, et al., 1998; Kingsbury, et al., 2000), we still think that c20S and i20S are the most abundant proteasome forms in WT animals and that only a smaller fraction occurs as mixed 20S proteasomes. In the following, we present a new model of 20S proteasome assembly that explains the formation of c20S or i20S by competitive integration of the catalytic β-subunits. This model further decribes the regulation of the cellular proteasome content by expression of constitutive or immunosubunits (Fig. III).

Naive, non-lymphoid tissues display high expression of the constitutive subunits while that of immunosubunits is low (Kuckelkorn, et al., 2002). Hence, under these conditions predominantly c20S are generated. Further, we assume that POMP controls the rate of β5-integration resulting in a constant turnover of 20S complexes (Fig. IIIA).

In infected or inflamed tissues immunosubunits are simultaneously expressed at high levels, while the expression of the constitutive subunits remains unaltered. This enables the immunosubunits to oust the constitutive subunits, which consequently results in the formation of i20S (Fig. IIIB).

Although we also detected signs of competitive integration in the spleen, mere mass action cannot explain the predominant integration of immunosubunits in lymphoid tissue. Especially, the expression of β2i is low in naive spleens as compared to β2. However, as previously discussed β1i and β2i mutually facilitate their integration in 20S proteasomes (Groettrup, et al., 1997). Thus, we propose that the high constitutive expression of β1i promotes the integration of β2i in lymphoid tissue.

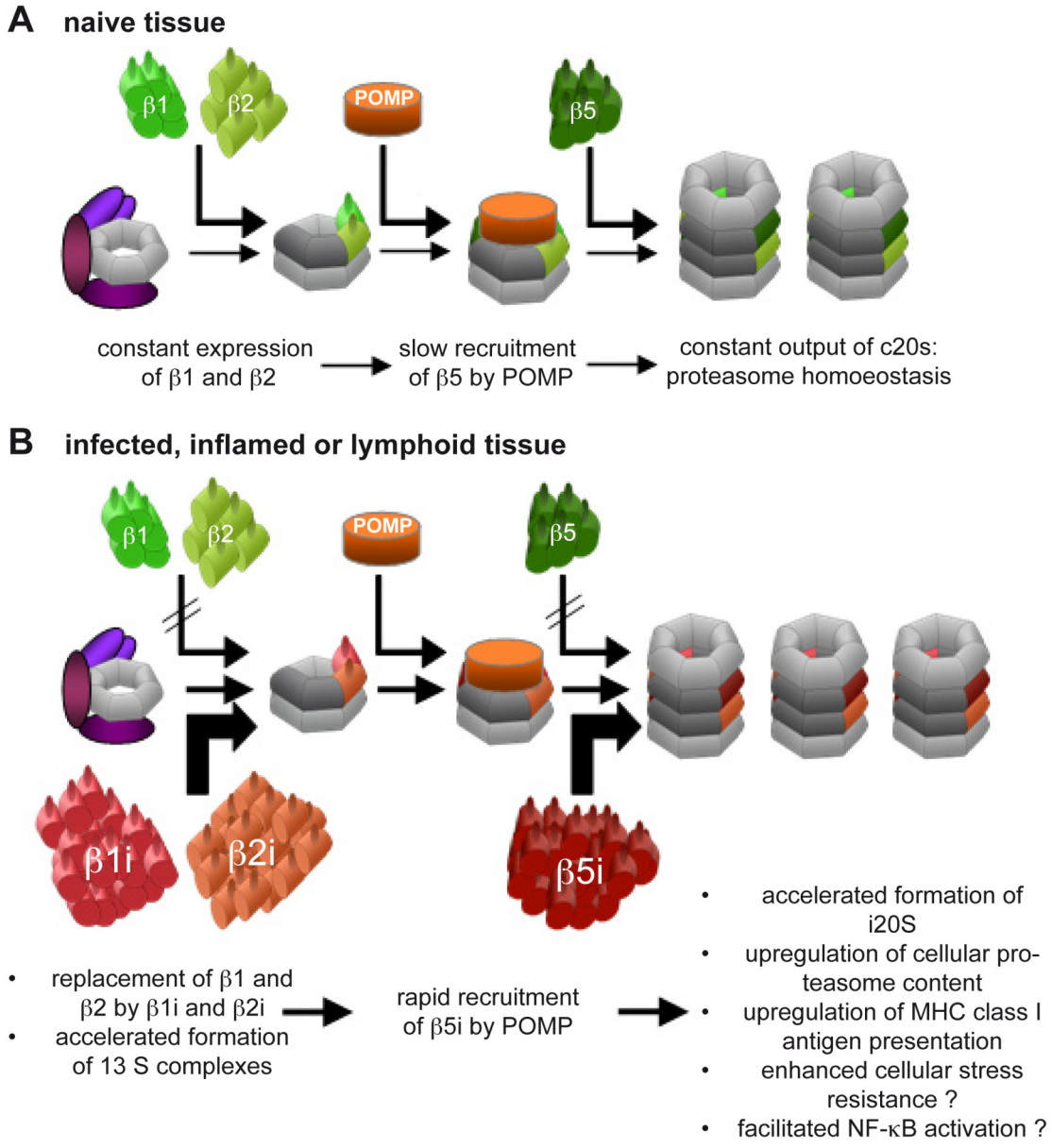

Figure III. The model of competitive integration of catalytic β-subunits during proteasome assembly
Shown are the events that lead to the formation of c20S (A) or i20S (B) according to the model of competitive integration of catalytic β-subunits.

Immunosubunits were shown to possess higher affinity to assembling proteasome complexes as compared to constitutive subunits, which is a function of their propeptides (De, et al., 2003; Kingsbury, et al., 2000; Nandi, et al., 1997). In our model of competitive integration, the high affinity of immunosubunits to assembling proteasome complexes means a substantial advantage for their integration and thus contributes to the replacement of c20S by i20S.

Recently, various forms of proteasome subtypes with mixtures of constitutive and immunosubunits have been identified (Klare, et al., 2007). Formation of mixed proteasomes

can be easily explained by competitive integration, because it is likely that these subtypes arise in a situation in which neither the expression of constitutive nor immunosubunits predominates.

Further, we suggest that the strong interaction of β5i and POMP does not only accelerate the assembly of 20S proteasomes to aid the rapid neogenesis of i20S (Heink, et al., 2005), but also promotes the transient upregulation of cellular proteasome content in infection. This increase in proteasome quantity during infection might be important for the defence against oxidative stress, activation of NF-κB and optimal MHC class I antigen presentation (Fig. IIIB).

In contrast, in *lmp7*$^{-/-}$ mice the slower proteasome assembly rate in the presence of β5 cannot cope with the strong neosynthesis of precursor proteasomes induced in infection. Accordingly, an accumulation of precursor proteasomes with impaired maturation of β1i and β2i and reduced cellular proteasome content is observed in these mice (Fig. IV).

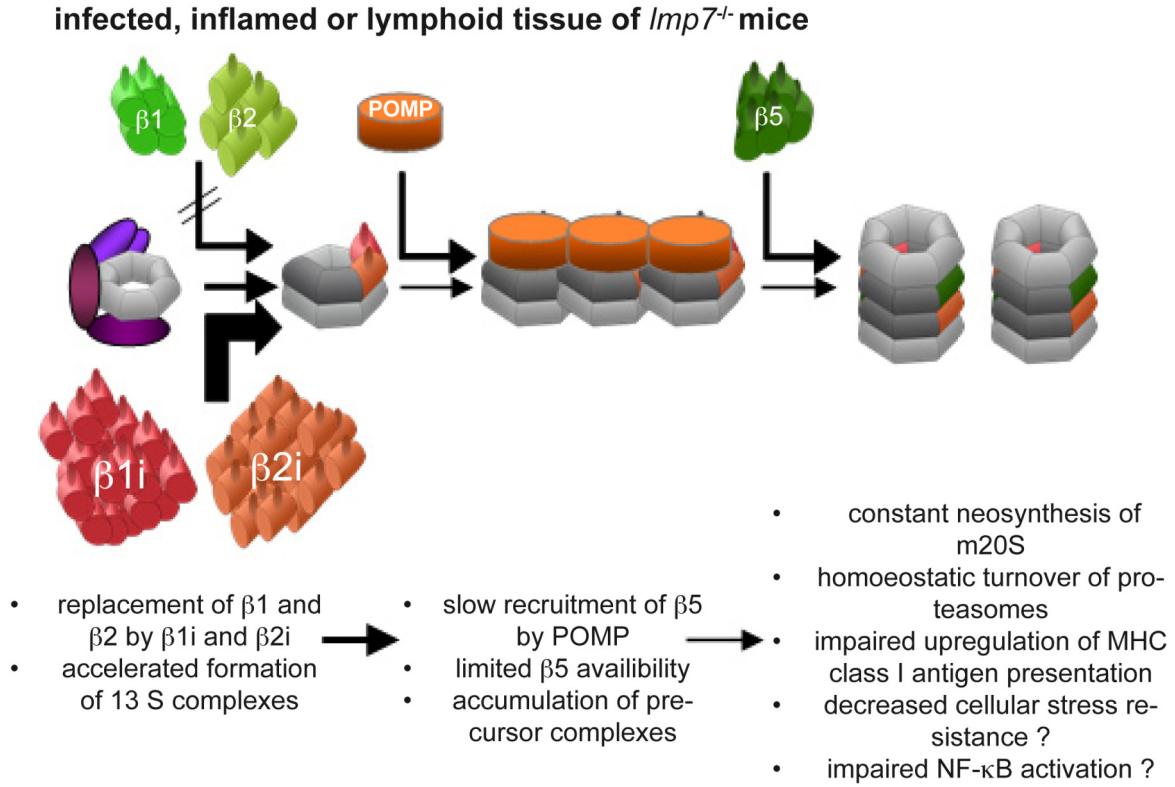

Figure IV. The model of competitive proteasome assembly applied to *lmp7*$^{-/-}$ mice
Shown are the events that lead to the accumulation of precursor proteasomes and the formation of m20S in *lmp7*$^{-/-}$ mice according to the model of competitive integration of catalytic β-subunits.

4.2 The effects of β5i-deficiency on the immune response against Listeria

A central question of this thesis is how β5i-deficiency impacts the immune response against *Listeria monocytognes*. The major phenotype of *lmp7*$^{-/-}$ mice is the reduced MHC class I surface expression caused by a lack of peptides produced by the proteasome system (Fehling, et al., 1994). In addition, we know that efficient generation of the listerial epitope $LLO_{296-304}$ depends on the activity of i20S (Strehl, et al., 2006). Thus, we wondered wether presentation of $LLO_{296-304}$ is impaired in Listeria-infected *lmp7*$^{-/-}$ mice. As antigen presentation can be limiting for priming and expansion of $CD8^+$ effector T cells (Wong and Pamer, 2003), we also studied if the $LLO_{296-304}$ specific $CD8^+$ T cell response is impaired in these mice. Further, we were interested in the impact of β5i-deficiency on bacterial control.

4.2.1 Reduced MHC class I antigen presentation in *lmp7*$^{-/-}$ mice is not limiting for $CD8^+$ T cell priming

Presentation of peptides on MHC class I molecules is a highly inefficient process, in which less than 0.01% of peptides generated by proteasomes are presented on the cell surface (Yewdell, et al., 2003). i20S are believed to facilitate antigen processing, because the generation of peptides with suitable anchor residues for MHC class I binding is increased (Groettrup, et al., 2001). This altered cleavage site specificity of i20S also results in improved generation of the correct C-terminus of the epitope $LLO_{296-304}$, while resulting in fewer cleavages, which destroy the epitope (Strehl and Kloetzel, unpublished results).
An increase in antigen presentation in the presence of i20S was described for a variety of epitopes (Kuckelkorn, et al., 1995; Kuckelkorn, et al., 2002; Sijts, et al., 2000; Sijts, et al., 2000). However, i20S do not generally improve epitope processing as others are inefficiently presented in their presence (Basler, et al., 2004; Chapiro, et al., 2006; Van den Eynde and Morel, 2001). Still, the reduced MHC class I surface expression of *lmp7*$^{-/-}$ mice suggests that the function of i20S is crucial for efficient presentation of the majority of antigens. Particularly, the restored MHC class I presentation by the exogenous adminstration of peptides demonstrates that the amount of epitopes is limited in *lmp7*$^{-/-}$ mice (Fehling, et al., 1994).

According to the concept of cooperative i20S assembly, the reduced MHC class I expression in *lmp7*$^{-/-}$ mice is caused by a general lack of immunosubunits (Griffin, et al., 1998). However, our results reveal considerable integration of β1i and β2i in m20S. Still, the MHC class I surface expression was reduced on professional APCs of infected *lmp7*$^{-/-}$ mice. Further, processing of the LLO-substrate was not restored by the induction of m20S, indicating that the specific activity of β5i is required for generation of the $LLO_{296-304}$ epitope. This is in contrast to the finding that presentation of some epitopes on β5i deficient cells was restored by overexpression of an inactive β5i subunit (Gileadi, et al., 1999; Sijts, et al., 2000). Further, m20S isolated from the spleen of *lmp7*$^{-/-}$ mice display a 3fold enhanced chymotryptic activity compared to i20S (Stohwasser, et al., 1996). In conclusion, these findings suggest that the catalytic activity of β5i itself is not critical for i20S function. Instead, the structural alterations that it introduces to the 20S complex seem to be critical for optimal i20S activity (Sijts, et al., 2000). Accordingly, Kisselev et al. have previously described an allosteric regulation between catalytic β-subunits, which is based on structural alterations in the cavity of the 20S complex (Kisselev, et al., 1999). Still, it is currently not clear whether the intrinsic catalytic activity of β5i or its structural impact is responsible for improved $LLO_{296-304}$ epitope generation by i20S.

We found an upregulation in the amount of proteaomes following infection of WT mice, which is abrogated in *lmp7*$^{-/-}$ mice. Interestingly, the reduction in MHC class I surface expression of 25-40% directly correlates with the 25-40% reduced proteasome content in lymphoid and infected tissue of *lmp7*$^{-/-}$ mice. This suggests that not only improved cleavage site specificity and enhanced substrate turnover by i20S facilitates MHC class I antigen presentation, but that also the amount of proteasomes substantially contributes to this process. Accordingly, inhibition of POMP expression by siRNA, which leads to a reduction in the cellular proteasome content, was shown to decrease the MHC class I surface expression (Heink, et al., 2005).

As previously discussed, we assume that the upregulation of the cellular proteasome content is achieved by accelerated recruitment of β5i by POMP. Considering these results, restored antigen presentation by expression of a catalytically inactive β5i subunit may also be explained by the upregulation of proteasomes induced by this subunit. This finding might explain why MHC class I surface expression is reduced in *lmp7*$^{-/-}$ but not *lmp2*$^{-/-}$ or *mecl1*$^{-/-}$ mice.

However, for the *in vitro* processing of the LLO-substrate same amounts of purified 20S proteasomes were used. Still, m20S isolated from *lmp7*$^{-/-}$ mice were inefficient in generating

the $LLO_{296-304}$ epitope. This demonstrates that presentation of the $LLO_{296-304}$ epitope in *lmp7*$^{-/-}$ mice is affected in two ways: By reduced proteasome quantity and the lack of specific i20S activity.

Previous reports analysed the impact of immunosubunit-deficiency on $CD8^+$ T cell responses in infection. It was shown that β1i-deficiency influences the immunodominance hierarchy and the repertoir of $CD8^+$ T cells responding to influenza virus infection (Chen, et al., 2001). Similar results were found in *mecl1*$^{-/-}$ mice, which also display an altered T cell repertoire and thus reveal decreased $CD8^+$ T cell frequencies in response to *Lymphocytic choriomeningitis virus* (LCMV) infection (Basler, et al., 2006). However, LCMV infection of *lmp2*$^{-/-}$ and *lmp7*$^{-/-}$ mice revealed only minor differences in $CD8^+$ T cell frequencies and immunodominance hierarchies compared to WT mice (Nussbaum, et al., 2005).

While these reports focused on viral infection models, we investigated the impact of β5i-deficiency on $CD8^+$ T cell responses in a bacterial infection. Due to the escape of Listeria into the host cell cytosol, clearance of the bacteria depends on the activation of pathogen specific $CD8^+$ T cells (Ladel, et al., 1994). In contrast to virus-infected cells, which are forced to produce high amounts of viral proteins (Buchmeier, et al., 1980), Listeria secrete only few proteins into the host cell cytosol. One of these proteins, LLO, is secreted for lysis of the phagosome and subsequently down-regulated as continuous secretion would be toxic for the host cell (Villanueva, et al., 1995). Due to the limited secretion of bacterial proteins, efficient processing of these antigens is critical compared to viral infection.

However, the magnitude of a $CD8^+$ T cell response is only minimally affected by the abundance of antigenic peptides on infected cells (Vijh, et al., 1998). When antigens are presented above a certain threshold within the first 48 h of infection, priming and expansion of $CD8^+$ T cells is largely independent of further antigen presentation (Badovinac, et al., 2002; Mercado, et al., 2000; Wong and Pamer, 2003).

Here, we detected reduced MHC class I surface expression on professional APCs of *lmp7*$^{-/-}$ mice within the first 48 h of infection and impaired processing of LLO. Thus, we anticipated that the threshold of antigen presentation necessary for priming of $LLO_{296-304}$ specific $CD8^+$ T cells is not overcome in *lmp7*$^{-/-}$ mice.

Suprisingly, we could not detect any differences in $LLO_{296-304}$ specific $CD8^+$ T cell frequencies between WT and *lmp7*$^{-/-}$ mice. This shows, that reduced proteasomal processing and presentation of $LLO_{296-304}$ in *lmp7*$^{-/-}$ mice is not limiting for priming of $LLO_{296-304}$ specific

$CD8^+$ T cells, which agrees with the results derived from LCMV infection (Nussbaum, et al., 2005).

In contrast, it was shown that expression of β5i is essential for efficient cross priming of $CD8^+$ T cells in a skin graft rejection model. In this report, Palmowski et al. demonstrated that WT male skin grafts were not rejected by female *lmp7*$^{-/-}$ mice due to impaired priming of $CD8^+$ T cells directed against the male, immunodominant HY epitope $Uty_{246-254}$. Generation of this epitope is dependent on the specific activity of i20S (Palmowski, et al., 2006).

Another study demonstrated impaired priming of $CD8^+$ T cells in *lmp7*$^{-/-}$ x *mecl1*$^{-/-}$ mice. Here, a recombinant Listeria strain secreting the two model antigens $E1B_{192-200}$ and $E1A_{234-243}$ was constructed. While processing of $E1B_{192-200}$ was shown to be i20S dependent, $E1A_{234-243}$ is processed i20S independent. Accordingly, only priming of $E1B_{192-200}$ but not $E1A_{234-243}$ specific $CD8^+$ T cells is abrogated in *lmp7*$^{-/-}$ x *mecl1*$^{-/-}$ mice. This deficit in priming of $E1B_{192-200}$ specific $CD8^+$ T cells was caused by delayed presentation of the corresponding epitope, as the treshold of antigen necessary for efficient priming was not achieved in the critical time frame (Deol, et al., 2007).

Further, in chimeric HLA-A2 x *lmp7*$^{-/-}$ mice, the $CD8^+$ T cell response directed against two immunodominant epitopes of hepatitis B virus was substantially decreased compared to HLA-A2 x *lmp7*$^{+/-}$ littermates, whereas $CD8^+$ T cell frequencies against a subdominat epitope were increased (Robek, et al., 2007).

In summary, these reports reveal, that i20S or specific immunosubunits are not generally dispensable for $CD8^+$ T cell priming. However, taken our results into account, we conclude that the influence of i20S or distinct catalytic β-subunits on epitope processing and $CD8^+$ T cell priming must be elucidated individually for each analysed epitope.

4.2.2 Impaired recognition of non-lymphoid target cells in *lmp7*$^{-/-}$ mice

Clearance of Listeria depends on the activity of $CD8^+$ T cells (Ladel, et al., 1994). The infection experiments demonstrated delayed clearance of the bacteria in *lmp7*$^{-/-}$ mice. Interestingly, the deficit during late bacterial control was detected in the liver but not the spleen, although the frequencies of $LLO_{296-304}$ specific $CD8^+$ T cells in both organs were similar to WT mice. However, normal clearance of Listeria in the spleen of *lmp7*$^{-/-}$ mice suggests that the intrinsic function of $CD8^+$ T cells is not affected in these mice.

While in the spleen, Listeria predominantly infect MΦ and DCs, hepatocytes are the main host cell in the liver (Gregory, et al., 1992). In contrast to DCs and MΦ, which are professional APCs and consequently display a high MHC class I surface expression, non-lymphoid cells like hepatocytes have to upregulate their MHC class I antigen presentation machinery in response to infection. Important mediators of MHC class I induction in infection are interferons. However, Chen et al. revealed that MHC class I surface expression is remarkably high on naive hepatocytes and comparable to splenocytes. Still, upregulation of the MHC class I presentation machinery including induction of β5i is observed following IFNγ stimulation of hepatocytes (Chen, et al., 2005).

As naïve hepatocytes were shown to be tolerogenic (Crispe, 2003), it is believed that IFNγ-stimulation enables $CD8^+$ T cell mediated cytolysis of hepatocytes (Chen, et al., 2005). Interestingly, recently primed $CD8^+$ T cells themselves induce MHC class I expression on hepatocytes by secretion of IFNγ (Dikopoulos, et al., 2004). Further, elimination of recombinant adenovirus infected hepatocytes by $CD8^+$ T cells was shown to depend on IFNγ secretion by T_{H1} $CD4^+$ T cells (Yang, et al., 1995). In accordance, infection of IFNγ receptor deficient mice demonstrated that induction of i20S in the liver is strictly IFNγ dependent (Strehl, et al., 2006).

As previously discussed, induction of i20S facilitates MHC class I surface expression by improved cleavage site specificity and enhanced cellular proteasome content. As these mechanisms are abrogated in *lmp7*$^{-/-}$ mice, we suggest that delayed clearance of Listeria in the liver of *lmp7*$^{-/-}$ mice is caused by impaired recognition and lysis of infected hepatocytes by $CD8^+$ T cells.

In agreement, it was shown in a model of autoimmune type I diabetes that lysis of parenchymal pancreatic islet cells by $CD8^+$ T cells depends on the induction of MHC class I surface expression mediated by LCMV infection and subsequent IFNα/β secretion (Lang, et al., 2005). However, the impact of i20S induction on MHC class I surface expression, which occurs in the liver following LCMV and Listeria infection (Khan, et al., 2001), was not analysed in this report.

In contrast to Listeria, clearance of LCMV infection is not affected in *lmp7*$^{-/-}$ mice (Nussbaum, et al., 2005). However, this might be explained by the strong expression of viral proteins by the host cell (Buchmeier, et al., 1980), which consequently results in high amounts of viral $CD8^+$ cell epitopes. Thus, antigen presentation on LCMV infected hepatocytes might not be limiting for recognition by $CD8^+$ T cells.

Further, LCMV elicits a strong $CD8^+$ T cell response against various epitopes in the $H2^b$ background, i.e. peak frequencies of 10-30% directed against the immunodominant epitopes GP33 and NP396. In addition, frequencies of 0.5-8% are specific for the subdominant epitopes GP276, GP92, GP34 and NP205 (Fuller, et al., 2004; Murali-Krishna, et al., 1998; van der Most, et al., 1998). For comparison, the $LLO_{296-304}$ specific $CD8^+$ T cell response with peak frequencies of about 0.5% is the strongest in Listeria infection (Geginat, et al., 2001). Therefore, the high frequencies of LCMV-specific $CD8^+$ effector T cells, which are not affected in *lmp7*$^{-/-}$ mice (Nussbaum, et al., 2005), might compensate for the reduced MHC class I antigen presentation on non-lymphoid cells by high effector-to-target ratios. Accordingly, Jiang et al. have shown that Listeria-infected hepatocytes are lysed by MHC class I restricted $CD8^+$ T cells independently of IFNγ stimualtion *in vitro* (Jiang, et al., 1997), which might also depend on high effector-to-target ratios and strong presentation of immunodominant T cell epitopes.

The clearance of Listeria in the liver of *lmp7*$^{-/-}$ mice was only two days delayed. However, it cannot be excluded that other immune defence mechanisms compensate for the impaired recognition of Listeria-infected cells by $CD8^+$ T cells. Accordingly, the function of MHC class Ib restricted $CD8^+$ T cells is most likely not affected by β5i-deficiency, as we found unaltered surface expression of H2-M3. These MHC class Ib restricted $CD8^+$ T cells were shown to provide protection against Listeria infection in mice deficient in the classical MHC class I molecules $H2K^b$ and $H2D^b$ (Seaman, et al., 2000).

Further, Listeria induce apoptosis of hepatocytes, which attracts neutrophils to eliminate extracellular bacteria (Rogers, et al., 1996) and allows cross presentation of bacterial antigens on professional APCs. However, cross presentation on APCs could compensate for insufficient MHC class I antigen presentation on hepatocytes.

In summary, we suggest that the induction of i20S in non-lymphoid tissue is crucial for efficient upregulation of MHC class I surface expression on infected cells, which then enables their recognition and lysis by effector $CD8^+$ T cells. In contrast, the MHC class I antigen presentation on lymphoid cells of *lmp7*$^{-/-}$ mice seems to be sufficient for recognition by $CD8^+$ T cells. Unfortunately, attempts to prove inefficient cytolysis of non-lymphoid target cells derived from *lmp7*$^{-/-}$ mice failed due to technical limitations.

4.2.3 Possible influences of β5i-deficiency on innate immune defence mechanisms in Listeria infection

Besides delayed clearance of Listeria in the liver, the early bacterial control was impaired in *lmp7*$^{-/-}$ mice. As this suggests a defect in innate immune defence, we will discuss how β5i-deficiency could affect innate immune defence mechanisms.

Following intravenous inoculation most bacteria are filtered from the bloodstream by Kupffer cells in the liver and are rapidly killed by immigrating neutrophils (Cousens and Wing, 2000; Gregory, et al., 1996). However, the surviving Listeria start to replicate within hepatocytes. The bacterial titers reach a plateau 3-4 days post infection, because their replication is controlled by various innate defence mechanisms (Gregory, et al., 1992; Mackaness, 1962).

NKT cells participate in the early immune response against Listeria (Ranson, et al., 2005), but an impact of β5i-deficiency on the CD1d restricted NKT cells can be largely excluded as they react to lipid antigens, which are not processed by the proteasome.

H2-M3 deficient mice were shown to exhibit a similar phenotype with increased listerial titers 3-4 days post infection in spleen and liver (Xu, et al., 2006). Since, we found unaltered H2-M3 surface expression in *lmp7*$^{-/-}$ compared to WT mice, the MHC class Ib restricted CD8^{+} T cell response is most likely not impaired. Thus, we speculate that other innate immune defence mechanisms are affected by β5i-deficiency.

An important early effector mechanism of innate immunity is the synthesis of proinflammatory cytokines, such as IL-1, IL-6, IL-12 and TNFα. These cytokines, e.g. recruit neutrophils and activate NK cells to release IFNγ (Cousens and Wing, 2000). In hepatocytes, IFNγ induces antibacterial mechanisms synergystically with IL-6 and TNFα and at the same time activates MΦ. Whereas hepatocytes exert their bactericidal effects primarily by secretion of reactive oxygene intermediates (ROI) (Gregory and Wing, 1993; Szalay, et al., 1995), MΦ attack Listeria by production of reactive nitrogen intermediates (RNI) (MacMicking, et al., 1995). In the spleen, a population of TNFα and iNOS producing DCs (TipDCs) was found to substantially contribute to control of listerial growth by RNI secretion (Serbina, et al., 2003). Thus, the oxidative burst is an important effector mechanism that restricts bacterial replication.

We detected reduced secretion of IL-6 and TNFα by Listeria infected *lmp7*$^{-/-}$ compared to WT BM-MΦ. As these cytokines are involved in the induction of the oxidative burst, we speculate that this defence mechanism may be impaired in *lmp7*$^{-/-}$ mice. Accodingly, mice that lack IL-6 or TNFα reveal impaired control of Listeria (Dalrymple, et al., 1995; van Furth, et al., 1994).

Another possibility is that the oxidative burst itself is involved in the increased susceptibility of *lmp7*$^{-/-}$ mice to Listeria infection, because removal of toxic, oxidated proteins is a function of the ubiquitin-proteasome pathway.
It was shown that in endothelial cells β1i and β5i are inducible by NO, presumably as an antioxidative defence mechanism (Kotamraju, et al., 2006). Indeed, *lmp2*$^{-/-}$ mice revealed an accumulation of oxidatively damaged proteins, suggesting that the increased chymotryptic activity of i20S facilitates the removal of such proteins (Ding, et al., 2006). Further, we demonstrated an increase in cellular proteasome content following induction of i20S and it was reported that the upregulation of proteasome content enhances the resistance to oxidative stress (Chondrogianni, et al., 2003; Chondrogianni, et al., 2005; Liu, et al., 2007). Thus, reduced chymotryptic activity and impaired upregulation of the proteasome system could result in an impaired antioxidative stress response in *lmp7*$^{-/-}$ mice, which could consequently result in increased tissue damage and enhanced bacterial titers.

The expression of IL-6 and TNFα is controlled by the NF-κB transcription factor family and proteasomes are involved in the activation of NF-κB. It has been shown that especially the chymotrypsin-like activity of proteasomes is essential for efficient processing of p105 and degradation of IκBα (Petrof, et al., 2004). Accordingly, splenocytes of *lmp2*$^{-/-}$ mice and the β1i and β5i deficient T2 cells revealed reduced NF-κB activation following TNFα stimulation (Hayashi and Faustman, 1999; Hayashi and Faustman, 2000). Although these results were controversially discussed in the literature (Runnels, et al., 2000), further evidence for a role of i20S in NF-κB activation comes from our own work. We could show increased turnover of IκB and improved processing of p105 by proteasomes isolated from patients with inflammatory bowel disease (IBD) *in vitro*. As these proteasomes predominantly contained i20S, we found a positive correlation between increased levels of i20S and enhanced NF-κB activation in IBD (Visekruna, et al., 2006).
In addition, a reduction in cellular proteasome content in aging cells was shown to affect the activation of NF-κB (Carrard, et al., 2002).
Thus, induction of i20S can influence NF-κB activation by increased chymotryptic activity and enhanced cellular proteasome content. As both processes are impaired in *lmp7*$^{-/-}$ mice, a reduced activation of NF-κB following Listeria infection is conceivable. However, the function of NF-κB is essential for the antilisterial immune defence (Edelson and Unanue, 2002; Sha, et al., 1995; Weih, et al., 1997). In conclusion, reduced NF-κB activation may be responsible for impaired innate immunity in *lmp7*$^{-/-}$ mice during Listeria infection.

References

Alvarez-Castelao, B. and Castano, J. G. (2005): Mechanism of direct degradation of IkappaBalpha by 20S proteasome, FEBS Lett. 579 [21], pp. 4797-4802.

Antoniou, A. N.; Powis, S. J. and Elliott, T. (2003): Assembly and export of MHC class I peptide ligands, Curr Opin Immunol 15 [1], pp. 75-81.

Arendt, C. S. and Hochstrasser, M. (1997): Identification of the yeast 20S proteasome catalytic centers and subunit interactions required for active-site formation, Proc Natl Acad Sci U S A 94 [14], pp. 7156-61.

Arendt, C. S. and Hochstrasser, M. (1999): Eukaryotic 20S proteasome catalytic subunit propeptides prevent active site inactivation by N-terminal acetylation and promote particle assembly, Embo J 18 [13], pp. 3575-85.

Badovinac, V. P.; Porter, B. B. and Harty, J. T. (2002): Programmed contraction of CD8(+) T cells after infection, Nat.Immunol. 3 [7], pp. 619-626.

Basler, M.; Moebius, J.; Elenich, L.; Groettrup, M. and Monaco, J. J. (2006): An altered T cell repertoire in MECL-1-deficient mice, J.Immunol. 176 [11], pp. 6665-6672.

Basler, M.; Youhnovski, N.; van den, Broek M.; Przybylski, M. and Groettrup, M. (2004): Immunoproteasomes down-regulate presentation of a subdominant T cell epitope from lymphocytic choriomeningitis virus, J.Immunol. 173 [6], pp. 3925-3934.

Baugh, J. M. and Pilipenko, E. V. (2004): 20S proteasome differentially alters translation of different mRNAs via the cleavage of eIF4F and eIF3, Mol.Cell 16 [4], pp. 575-586.

Baumeister, W.; Walz, J.; Zuhl, F. and Seemuller, E. (1998): The proteasome: paradigm of a self-compartmentalizing protease, Cell 92 [3], pp. 367-380.

Benham, A. M. and Neefjes, J. J. (1997): Proteasome activity limits the assembly of MHC class I molecules after IFN-gamma stimulation, J.Immunol. 159 [12], pp. 5896-5904.

Bonizzi, G. and Karin, M. (2004): The two NF-kappaB activation pathways and their role in innate and adaptive immunity, Trends Immunol. 25 [6], pp. 280-288.

Buchmeier, M. J.; Welsh, R. M.; Dutko, F. J. and Oldstone, M. B. (1980): The virology and immunobiology of lymphocytic choriomeningitis virus infection, Adv Immunol 30, pp. 275-331.

Burri, L.; Hockendorff, J.; Boehm, U.; Klamp, T.; Dohmen, R. J. and Levy, F. (2000): Identification and characterization of a mammalian protein interacting with 20S proteasome precursors, Proc Natl Acad Sci U S A 97 [19], pp. 10348-53.

Camacho-Carvajal, M. M.; Wollscheid, B.; Aebersold, R.; Steimle, V. and Schamel, W. W. (2004): Two-dimensional Blue native/SDS gel electrophoresis of multi-protein complexes from whole cellular lysates: a proteomics approach, Mol.Cell Proteomics. 3 [2], pp. 176-182.

Carrard, G.; Bulteau, A. L.; Petropoulos, I. and Friguet, B. (2002): Impairment of proteasome structure and function in aging, Int.J.Biochem.Cell Biol. 34 [11], pp. 1461-1474.

Cascio, P.; Hilton, C.; Kisselev, A. F.; Rock, K. L. and Goldberg, A. L. (2001): 26S proteasomes and immunoproteasomes produce mainly N-extended versions of an antigenic peptide, EMBO J. 20 [10], pp. 2357-2366.

Chang, Y. C.; Lee, Y. S.; Tejima, T.; Tanaka, K.; Omura, S.; Heintz, N. H.; Mitsui, Y. and Magae, J. (1998): mdm2 and bax, downstream mediators of the p53 response, are degraded by the ubiquitin-proteasome pathway, Cell Growth Differ. 9 [1], pp. 79-84.

Chapiro, J.; Claverol, S.; Piette, F.; Ma, W.; Stroobant, V.; Guillaume, B.; Gairin, J. E.; Morel, S.; Burlet-Schiltz, O.; Monsarrat, B.; Boon, T. and Van den Eynde, B. J. (2006): Destructive cleavage of antigenic peptides either by the immunoproteasome or by the standard proteasome results in differential antigen presentation, J.Immunol. 176 [2], pp. 1053-1061.

Chen, M.; Tabaczewski, P.; Truscott, S. M.; Van Kaer, L. and Stroynowski, I. (2005): Hepatocytes express abundant surface class I MHC and efficiently use transporter associated with antigen processing, tapasin, and low molecular weight polypeptide proteasome subunit components of antigen processing and presentation pathway, J.Immunol. 175 [2], pp. 1047-1055.

Chen, P. and Hochstrasser, M. (1996): Autocatalytic subunit processing couples active site formation in the 20S proteasome to completion of assembly, Cell 86 [6], pp. 961-972.

Chen, W.; Anton, L. C.; Bennink, J. R. and Yewdell, J. W. (2000): Dissecting the multifactorial causes of immunodominance in class I-restricted T cell responses to viruses, Immunity. 12 [1], pp. 83-93.

Chen, W.; Norbury, C. C.; Cho, Y.; Yewdell, J. W. and Bennink, J. R. (2001): Immunoproteasomes shape immunodominance hierarchies of antiviral CD8(+) T cells at the levels of T cell repertoire and presentation of viral antigens, J.Exp.Med. 193 [11], pp. 1319-1326.

Chondrogianni, N. and Gonos, E. S. (2007): Overexpression of hUMP1/POMP proteasome accessory protein enhances proteasome-mediated antioxidant defence, Exp Gerontol 42 [9], pp. 899-903.

Chondrogianni, N.; Stratford, F. L.; Trougakos, I. P.; Friguet, B.; Rivett, A. J. and Gonos, E. S. (2003): Central role of the proteasome in senescence and survival of human fibroblasts: induction of a senescence-like phenotype upon its inhibition and resistance to stress upon its activation, J.Biol.Chem. 278 [30], pp. 28026-28037.

Chondrogianni, N.; Tzavelas, C.; Pemberton, A. J.; Nezis, I. P.; Rivett, A. J. and Gonos, E. S. (2005): Overexpression of proteasome beta5 assembled subunit increases the amount of proteasome and confers ameliorated response to oxidative stress and higher survival rates, J.Biol.Chem. 280 [12], pp. 11840-11850.

Conlan, J. W. and North, R. J. (1994): Neutrophils are essential for early anti-Listeria defense in the liver, but not in the spleen or peritoneal cavity, as revealed by a granulocyte-depleting monoclonal antibody, J.Exp.Med. 179 [1], pp. 259-268.

Cousens, L. P. and Wing, E. J. (2000): Innate defenses in the liver during Listeria infection, Immunol.Rev. 174, pp. 150-159.

Coux, O.; Tanaka, K. and Goldberg, A. L. (1996): Structure and functions of the 20S and 26S proteasomes, Annu.Rev.Biochem. 65, pp. 801-847.

Crispe, I. N. (2003): Hepatic T cells and liver tolerance, Nat Rev Immunol 3 [1], pp. 51-62.

Dalrymple, S. A.; Lucian, L. A.; Slattery, R.; McNeil, T.; Aud, D. M.; Fuchino, S.; Lee, F. and Murray, R. (1995): Interleukin-6-deficient mice are highly susceptible to Listeria monocytogenes infection: correlation with inefficient neutrophilia, Infect Immun 63 [6], pp. 2262-8.

Das, R.; Ponnappan, S. and Ponnappan, U. (2007): Redox regulation of the proteasome in T lymphocytes during aging, Free Radic.Biol.Med. 42 [4], pp. 541-551.

De, M.; Jayarapu, K.; Elenich, L.; Monaco, J. J.; Colbert, R. A. and Griffin, T. A. (2003): Beta 2 subunit propeptides influence cooperative proteasome assembly, J.Biol.Chem. 278 [8], pp. 6153-6159.

Demartino, G. N. and Gillette, T. G. (2007): Proteasomes: machines for all reasons, Cell 129 [4], pp. 659-62.

Deol, P.; Zaiss, D. M.; Monaco, J. J. and Sijts, A. J. (2007): Rates of processing determine the immunogenicity of immunoproteasome-generated epitopes, J.Immunol. 178 [12], pp. 7557-7562.

Dick, L. R.; Cruikshank, A. A.; Destree, A. T.; Grenier, L.; McCormack, T. A.; Melandri, F. D.; Nunes, S. L.; Palombella, V. J.; Parent, L. A.; Plamondon, L. and Stein, R. L. (1997): Mechanistic studies on the inactivation of the proteasome by lactacystin in cultured cells, J Biol Chem 272 [1], pp. 182-8.

Dikopoulos, N.; Wegenka, U.; Kroger, A.; Hauser, H.; Schirmbeck, R. and Reimann, J. (2004): Recently primed CD8+ T cells entering the liver induce hepatocytes to interact with naive CD8+ T cells in the mouse, Hepatology 39 [5], pp. 1256-1266.

Ding, Q.; Martin, S.; Dimayuga, E.; Bruce-Keller, A. J. and Keller, J. N. (2006): LMP2 knock-out mice have reduced proteasome activities and increased levels of oxidatively damaged proteins, Antioxid.Redox.Signal. 8 [1-2], pp. 130-135.

Dohmen, R. J.; Willers, I. and Marques, A. J. (2007): Biting the hand that feeds: Rpn4-dependent feedback regulation of proteasome function, Biochim Biophys Acta.

Drews, O.; Wildgruber, R.; Zong, C.; Sukop, U.; Nissum, M.; Weber, G.; Gomes, A. V. and Ping, P. (2007): Mammalian proteasome subpopulations with distinct molecular compositions and proteolytic activities, Mol Cell Proteomics 6 [11], pp. 2021-31.

Dubiel, W.; Pratt, G.; Ferrell, K. and Rechsteiner, M. (1992): Purification of an 11 S regulator of the multicatalytic protease, J Biol Chem 267 [31], pp. 22369-77.

Edelson, B. T. and Unanue, E. R. (2002): MyD88-dependent but Toll-like receptor 2-independent innate immunity to Listeria: no role for either in macrophage listericidal activity, J.Immunol. 169 [7], pp. 3869-3875.

Elliott, T. (2006): The 'chop-and-change' of MHC class I assembly, Nat Immunol 7 [1], pp. 7-9.

Fehling, H. J.; Swat, W.; Laplace, C.; Kuhn, R.; Rajewsky, K.; Muller, U. and von Boehmer, H. (1994): MHC class I expression in mice lacking the proteasome subunit LMP-7, Science 265 [5176], pp. 1234-1237.

Fitzpatrick, L. R.; Khare, V.; Small, J. S. and Koltun, W. A. (2006): Dextran Sulfate Sodium-Induced Colitis Is Associated with Enhanced Low Molecular Mass Polypeptide 2 (LMP2) Expression and Is Attenuated in LMP2 Knockout Mice, Dig.Dis.Sci. 51 [7], pp. 1269-1276.

Frentzel, S.; Pesold-Hurt, B.; Seelig, A. and Kloetzel, P. M. (1994): 20 S proteasomes are assembled via distinct precursor complexes. Processing of LMP2 and LMP7 proproteins takes place in 13-16 S preproteasome complexes, J.Mol.Biol. 236 [4], pp. 975-981.

Fricke, B.; Heink, S.; Steffen, J.; Kloetzel, P. M. and Kruger, E. (2007): The proteasome maturation protein POMP facilitates major steps of 20S proteasome formation at the endoplasmic reticulum, EMBO Rep 8 [12], pp. 1170-5.

Fricke, B.; Heink, S.; Steffen, J.; Kloetzel, P. M. and Kruger, E. (2007): The proteasome maturation protein POMP facilitates major steps of 20S proteasome formation at the endoplasmic reticulum, EMBO Rep.

Fuller, M. J.; Khanolkar, A.; Tebo, A. E. and Zajac, A. J. (2004): Maintenance, loss, and resurgence of T cell responses during acute, protracted, and chronic viral infections, J.Immunol. 172 [7], pp. 4204-4214.

Gaczynska, M.; Goldberg, A. L.; Tanaka, K.; Hendil, K. B. and Rock, K. L. (1996): Proteasome subunits X and Y alter peptidase activities in opposite ways to the interferon-gamma-induced subunits LMP2 and LMP7, J.Biol.Chem. 271 [29], pp. 17275-17280.

Gaczynska, M.; Rock, K. L.; Spies, T. and Goldberg, A. L. (1994): Peptidase activities of proteasomes are differentially regulated by the major histocompatibility complex-encoded genes for LMP2 and LMP7, Proc.Natl.Acad.Sci.U.S.A 91 [20], pp. 9213-9217.

Geginat, G.; Schenk, S.; Skoberne, M.; Goebel, W. and Hof, H. (2001): A novel approach of direct ex vivo epitope mapping identifies dominant and subdominant CD4 and CD8 T cell epitopes from Listeria monocytogenes, J.Immunol. 166 [3], pp. 1877-1884.

Gerards, W. L.; de Jong, W. W.; Boelens, W. and Bloemendal, H. (1998): Structure and assembly of the 20S proteasome, Cell Mol.Life Sci. 54 [3], pp. 253-262.

Gileadi, U.; Moins-Teisserenc, H. T.; Correa, I.; Booth, B. L., Jr.; Dunbar, P. R.; Sewell, A. K.; Trowsdale, J.; Phillips, R. E. and Cerundolo, V. (1999): Generation of an immunodominant CTL epitope is affected by proteasome subunit composition and stability of the antigenic protein, J.Immunol. 163 [11], pp. 6045-6052.

Glynne, R.; Powis, S. H.; Beck, S.; Kelly, A.; Kerr, L. A. and Trowsdale, J. (1991): A proteasome-related gene between the two ABC transporter loci in the class II region of the human MHC, Nature 353 [6342], pp. 357-60.

Goldberg, A. L.; Cascio, P.; Saric, T. and Rock, K. L. (2002): The importance of the proteasome and subsequent proteolytic steps in the generation of antigenic peptides, Mol.Immunol. 39 [3-4], pp. 147-164.

Gregory, S. H.; Barczynski, L. K. and Wing, E. J. (1992): Effector function of hepatocytes and Kupffer cells in the resolution of systemic bacterial infections, J Leukoc Biol 51 [4], pp. 421-4.

Gregory, S. H.; Sagnimeni, A. J. and Wing, E. J. (1996): Bacteria in the bloodstream are trapped in the liver and killed by immigrating neutrophils, J.Immunol. 157 [6], pp. 2514-2520.

Gregory, S. H. and Wing, E. J. (1993): IFN-gamma inhibits the replication of Listeria monocytogenes in hepatocytes, J.Immunol. 151 [3], pp. 1401-1409.

Griffin, T. A.; Nandi, D.; Cruz, M.; Fehling, H. J.; Kaer, L. V.; Monaco, J. J. and Colbert, R. A. (1998): Immunoproteasome assembly: cooperative incorporation of interferon gamma (IFN-gamma)-inducible subunits, J.Exp.Med. 187 [1], pp. 97-104.

Griffin, T. A.; Slack, J. P.; McCluskey, T. S.; Monaco, J. J. and Colbert, R. A. (2000): Identification of proteassemblin, a mammalian homologue of the yeast protein, Ump1p, that is required for normal proteasome assembly, Mol Cell Biol Res Commun 3 [4], pp. 212-7.

Groettrup, M.; Khan, S.; Schwarz, K. and Schmidtke, G. (2001): Interferon-gamma inducible exchanges of 20S proteasome active site subunits: why?, Biochimie 83 [3-4], pp. 367-372.

Groettrup, M.; Kraft, R.; Kostka, S.; Standera, S.; Stohwasser, R. and Kloetzel, P. M. (1996): A third interferon-gamma-induced subunit exchange in the 20S proteasome, Eur.J.Immunol. 26 [4], pp. 863-869.

Groettrup, M.; Soza, A.; Eggers, M.; Kuehn, L.; Dick, T. P.; Schild, H.; Rammensee, H. G.; Koszinowski, U. H. and Kloetzel, P. M. (1996): A role for the proteasome regulator PA28alpha in antigen presentation, Nature 381 [6578], pp. 166-168.

Groettrup, M.; Standera, S.; Stohwasser, R. and Kloetzel, P. M. (1997): The subunits MECL-1 and LMP2 are mutually required for incorporation into the 20S proteasome, Proc.Natl.Acad.Sci.U.S.A 94 [17], pp. 8970-8975.

Groll, M.; Ditzel, L.; Lowe, J.; Stock, D.; Bochtler, M.; Bartunik, H. D. and Huber, R. (1997): Structure of 20S proteasome from yeast at 2.4 A resolution, Nature 386 [6624], pp. 463-471.

Hayashi, T. and Faustman, D. (1999): NOD mice are defective in proteasome production and activation of NF-kappaB, Mol.Cell Biol. 19 [12], pp. 8646-8659.

Hayashi, T. and Faustman, D. (2000): Essential role of human leukocyte antigen-encoded proteasome subunits in NF-kappaB activation and prevention of tumor necrosis factor-alpha-induced apoptosis, J.Biol.Chem. 275 [7], pp. 5238-5247.

Heemels, M. T. and Ploegh, H. (1995): Generation, translocation, and presentation of MHC class I-restricted peptides, Annu Rev Biochem 64, pp. 463-91.

Heink, S.; Fricke, B.; Ludwig, D.; Kloetzel, P. M. and Kruger, E. (2006): Tumor cell lines expressing the proteasome subunit isoform LMP7E1 exhibit immunoproteasome deficiency, Cancer Res. 66 [2], pp. 649-652.

Heink, S.; Ludwig, D.; Kloetzel, P. M. and Kruger, E. (2005): IFN-gamma-induced immune adaptation of the proteasome system is an accelerated and transient response, Proc.Natl.Acad.Sci.U.S.A 102 [26], pp. 9241-9246.

Hershko, A. and Ciechanover, A. (1998): The ubiquitin system, Annu Rev Biochem 67, pp. 425-79.

Hirano, Y.; Hayashi, H.; Iemura, S.; Hendil, K. B.; Niwa, S.; Kishimoto, T.; Kasahara, M.; Natsume, T.; Tanaka, K. and Murata, S. (2006): Cooperation of Multiple Chaperones Required for the Assembly of Mammalian 20S Proteasomes, Mol.Cell 24 [6], pp. 977-984.

Hirano, Y.; Hendil, K. B.; Yashiroda, H.; Iemura, S.; Nagane, R.; Hioki, Y.; Natsume, T.; Tanaka, K. and Murata, S. (2005): A heterodimeric complex that promotes the assembly of mammalian 20S proteasomes, Nature 437 [7063], pp. 1381-1385.

Hisamatsu, H.; Shimbara, N.; Saito, Y.; Kristensen, P.; Hendil, K. B.; Fujiwara, T.; Takahashi, E.; Tanahashi, N.; Tamura, T.; Ichihara, A. and Tanaka, K. (1996): Newly identified pair of proteasomal subunits regulated reciprocally by interferon gamma, J.Exp.Med. 183 [4], pp. 1807-1816.

Janeway, C. A.; Travers, P.; Walport, M. and Shlomchik, M. (2001): Immunobiology - The immune sytem in health and disease, 5th edition. ed., Gibbs, S., Ed, Garland Publishing, New York, USA, ISBN: 0-4430-7098-9.

Jayarapu, K. and Griffin, T. A. (2004): Protein-protein interactions among human 20S proteasome subunits and proteassemblin, Biochem Biophys Res Commun 314 [2], pp. 523-8.

Jiang, X.; Gregory, S. H. and Wing, E. J. (1997): Immune CD8+ T lymphocytes lyse Listeria monocytogenes-infected hepatocytes by a classical MHC class I-restricted mechanism, J.Immunol. 158 [1], pp. 287-293.

Kerksiek, K. M.; Busch, D. H.; Pilip, I. M.; Allen, S. E. and Pamer, E. G. (1999): H2-M3-restricted T cells in bacterial infection: rapid primary but diminished memory responses, J.Exp.Med. 190 [2], pp. 195-204.

Khan, S.; van den, Broek M.; Schwarz, K.; de Giuli, R.; Diener, P. A. and Groettrup, M. (2001): Immunoproteasomes largely replace constitutive proteasomes during an antiviral and antibacterial immune response in the liver, J.Immunol. 167 [12], pp. 6859-6868.

King, R. W.; Deshaies, R. J.; Peters, J. M. and Kirschner, M. W. (1996): How proteolysis drives the cell cycle, Science 274 [5293], pp. 1652-1659.

Kingsbury, D. J.; Griffin, T. A. and Colbert, R. A. (2000): Novel propeptide function in 20 S proteasome assembly influences beta subunit composition, J.Biol.Chem. 275 [31], pp. 24156-24162.

Kisselev, A. F.; Akopian, T. N.; Castillo, V. and Goldberg, A. L. (1999): Proteasome active sites allosterically regulate each other, suggesting a cyclical bite-chew mechanism for protein breakdown, Mol.Cell 4 [3], pp. 395-402.

Kisselev, A. F.; Akopian, T. N.; Woo, K. M. and Goldberg, A. L. (1999): The sizes of peptides generated from protein by mammalian 26 and 20 S proteasomes. Implications for understanding the degradative mechanism and antigen presentation, J Biol Chem 274 [6], pp. 3363-71.

Klare, N.; Seeger, M.; Janek, K.; Jungblut, P. R. and Dahlmann, B. (2007): Intermediate-type 20 S proteasomes in HeLa cells: "asymmetric" subunit composition, diversity and adaptation, J Mol Biol 373 [1], pp. 1-10.

Kloetzel, P. M. (2001): Antigen processing by the proteasome, Nat.Rev.Mol.Cell Biol. 2 [3], pp. 179-187.

Kloetzel, P. M. (2004): Generation of major histocompatibility complex class I antigens: functional interplay between proteasomes and TPPII, Nat.Immunol. 5 [7], pp. 661-669.

Kornitzer, D. and Ciechanover, A. (2000): Modes of regulation of ubiquitin-mediated protein degradation, J Cell Physiol 182 [1], pp. 1-11.

Kotamraju, S.; Matalon, S.; Matsunaga, T.; Shang, T.; Hickman-Davis, J. M. and Kalyanaraman, B. (2006): Upregulation of immunoproteasomes by nitric oxide: potential antioxidative mechanism in endothelial cells, Free Radic.Biol.Med. 40 [6], pp. 1034-1044.

Kuckelkorn, U.; Frentzel, S.; Kraft, R.; Kostka, S.; Groettrup, M. and Kloetzel, P. M. (1995): Incorporation of major histocompatibility complex--encoded subunits LMP2 and LMP7 changes the quality of the 20S proteasome polypeptide processing products independent of interferon-gamma, Eur.J.Immunol. 25 [9], pp. 2605-2611.

Kuckelkorn, U.; Ruppert, T.; Strehl, B.; Jungblut, P. R.; Zimny-Arndt, U.; Lamer, S.; Prinz, I.; Drung, I.; Kloetzel, P. M.; Kaufmann, S. H. and Steinhoff, U. (2002): Link between organ-specific antigen processing by 20S proteasomes and CD8(+) T cell-mediated autoimmunity, J.Exp.Med. 195 [8], pp. 983-990.

Kwak, M. K.; Itoh, K.; Yamamoto, M. and Kensler, T. W. (2002): Enhanced expression of the transcription factor Nrf2 by cancer chemopreventive agents: role of antioxidant response element-like sequences in the nrf2 promoter, Mol Cell Biol 22 [9], pp. 2883-92.

Kwak, M. K.; Wakabayashi, N.; Greenlaw, J. L.; Yamamoto, M. and Kensler, T. W. (2003): Antioxidants enhance mammalian proteasome expression through the Keap1-Nrf2 signaling pathway, Mol Cell Biol 23 [23], pp. 8786-94.

Ladel, C. H.; Flesch, I. E.; Arnoldi, J. and Kaufmann, S. H. (1994): Studies with MHC-deficient knock-out mice reveal impact of both MHC I- and MHC II-dependent T cell responses on Listeria monocytogenes infection, J Immunol 153 [7], pp. 3116-22.

Laemmli, U. K. (1970): Cleavage of structural proteins during the assembly of the head of bacteriophage T4, Nature 227 [5259], pp. 680-5.

Lang, K. S.; Recher, M.; Junt, T.; Navarini, A. A.; Harris, N. L.; Freigang, S.; Odermatt, B.; Conrad, C.; Ittner, L. M.; Bauer, S.; Luther, S. A.; Uematsu, S.; Akira, S.; Hengartner, H. and Zinkernagel, R. M. (2005): Toll-like receptor engagement converts T-cell autoreactivity into overt autoimmune disease, Nat.Med. 11 [2], pp. 138-145.

Le Tallec, B.; Barrault, M. B.; Courbeyrette, R.; Guerois, R.; Marsolier-Kergoat, M. C. and Peyroche, A. (2007): 20S proteasome assembly is orchestrated by two distinct pairs of chaperones in yeast and in mammals, Mol Cell 27 [4], pp. 660-74.

Li, J.; Schuler-Thurner, B.; Schuler, G.; Huber, C. and Seliger, B. (2001): Bipartite regulation of different components of the MHC class I antigen-processing machinery during dendritic cell maturation, Int.Immunol. 13 [12], pp. 1515-1523.

Li, X.; Kusmierczyk, A. R.; Wong, P.; Emili, A. and Hochstrasser, M. (2007): beta-Subunit appendages promote 20S proteasome assembly by overcoming an Ump1-dependent checkpoint, EMBO J.

Liu, Y.; Liu, X.; Zhang, T.; Luna, C.; Liton, P. B. and Gonzalez, P. (2007): Cytoprotective effects of proteasome beta5 subunit overexpression in lens epithelial cells, Mol.Vis. 13, pp. 31-38.

Macagno, A.; Gilliet, M.; Sallusto, F.; Lanzavecchia, A.; Nestle, F. O. and Groettrup, M. (1999): Dendritic cells up-regulate immunoproteasomes and the proteasome regulator PA28 during maturation, Eur.J.Immunol. 29 [12], pp. 4037-4042.

Macagno, A.; Kuehn, L.; de Giuli, R. and Groettrup, M. (2001): Pronounced up-regulation of the PA28alpha/beta proteasome regulator but little increase in the steady-state content of immunoproteasome during dendritic cell maturation, Eur.J.Immunol. 31 [11], pp. 3271-3280.

Mackaness, G. B. (1962): Cellular resistance to infection, J Exp Med 116, pp. 381-406.

MacMicking, J. D.; Nathan, C.; Hom, G.; Chartrain, N.; Fletcher, D. S.; Trumbauer, M.; Stevens, K.; Xie, Q. W.; Sokol, K. and Hutchinson, N. (1995): Altered responses to bacterial infection and endotoxic shock in mice lacking inducible nitric oxide synthase, Cell 81 [4], pp. 641-650.

Meiners, S.; Heyken, D.; Weller, A.; Ludwig, A.; Stangl, K.; Kloetzel, P. M. and Kruger, E. (2003): Inhibition of proteasome activity induces concerted expression of proteasome genes and de novo formation of Mammalian proteasomes, J.Biol.Chem. 278 [24], pp. 21517-21525.

Mercado, R.; Vijh, S.; Allen, S. E.; Kerksiek, K.; Pilip, I. M. and Pamer, E. G. (2000): Early programming of T cell populations responding to bacterial infection, J.Immunol. 165 [12], pp. 6833-6839.

Moorthy, A. K.; Savinova, O. V.; Ho, J. Q.; Wang, V. Y.; Vu, D. and Ghosh, G. (2006): The 20S proteasome processes NF-kappaB1 p105 into p50 in a translation-independent manner, EMBO J. 25 [9], pp. 1945-1956.

Morel, S.; Levy, F.; Burlet-Schiltz, O.; Brasseur, F.; Probst-Kepper, M.; Peitrequin, A. L.; Monsarrat, B.; Van Velthoven, R.; Cerottini, J. C.; Boon, T.; Gairin, J. E. and Van den Eynde, B. J. (2000): Processing of some antigens by the standard proteasome but not by the immunoproteasome results in poor presentation by dendritic cells, Immunity. 12 [1], pp. 107-117.

Murali-Krishna, K.; Altman, J. D.; Suresh, M.; Sourdive, D. J.; Zajac, A. J.; Miller, J. D.; Slansky, J. and Ahmed, R. (1998): Counting antigen-specific CD8 T cells: a reevaluation of bystander activation during viral infection, Immunity. 8 [2], pp. 177-187.

Murata, S.; Sasaki, K.; Kishimoto, T.; Niwa, S.; Hayashi, H.; Takahama, Y. and Tanaka, K. (2007): Regulation of CD8+ T cell development by thymus-specific proteasomes, Science 316 [5829], pp. 1349-1353.

Nandi, D.; Jiang, H. and Monaco, J. J. (1996): Identification of MECL-1 (LMP-10) as the third IFN-gamma-inducible proteasome subunit, J.Immunol. 156 [7], pp. 2361-2364.

Nandi, D.; Woodward, E.; Ginsburg, D. B. and Monaco, J. J. (1997): Intermediates in the formation of mouse 20S proteasomes: implications for the assembly of precursor beta subunits, EMBO J. 16 [17], pp. 5363-5375.

Nil, A.; Firat, E.; Sobek, V.; Eichmann, K. and Niedermann, G. (2004): Expression of housekeeping and immunoproteasome subunit genes is differentially regulated in positively and negatively selecting thymic stroma subsets, Eur.J.Immunol. 34 [10], p. 2681.

Norbury, C. C.; Basta, S.; Donohue, K. B.; Tscharke, D. C.; Princiotta, M. F.; Berglund, P.; Gibbs, J.; Bennink, J. R. and Yewdell, J. W. (2004): CD8+ T cell cross-priming via transfer of proteasome substrates, Science 304 [5675], pp. 1318-1321.

Nussbaum, A. K.; Rodriguez-Carreno, M. P.; Benning, N.; Botten, J. and Whitton, J. L. (2005): Immunoproteasome-Deficient Mice Mount Largely Normal CD8+ T Cell Responses to Lymphocytic Choriomeningitis Virus Infection and DNA Vaccination, J.Immunol. 175 [2], pp. 1153-1160.

Osterloh, P.; Linkemann, K.; Tenzer, S.; Rammensee, H. G.; Radsak, M. P.; Busch, D. H. and Schild, H. (2006): Proteasomes shape the repertoire of T cells participating in antigen-specific immune responses, Proc.Natl.Acad.Sci.U.S.A.

Palmowski, M. J.; Gileadi, U.; Salio, M.; Gallimore, A.; Millrain, M.; James, E.; Addey, C.; Scott, D.; Dyson, J.; Simpson, E. and Cerundolo, V. (2006): Role of Immunoproteasomes in Cross-Presentation, J.Immunol. 177 [2], pp. 983-990.

Pamer, E. G. (2004): Immune responses to Listeria monocytogenes, Nat.Rev.Immunol. 4 [10], pp. 812-823.

Petrof, E. O.; Kojima, K.; Ropeleski, M. J.; Musch, M. W.; Tao, Y.; De Simone, C. and Chang, E. B. (2004): Probiotics inhibit nuclear factor-kappaB and induce heat shock proteins in colonic epithelial cells through proteasome inhibition, Gastroenterology 127 [5], pp. 1474-1487.

Ploegh, H. L. (2004): Immunology. Nothing 'gainst time's scythe can make defense, Science 304 [5675], pp. 1262-1263.

Rammensee, H. G.; Falk, K. and Rotzschke, O. (1993): Peptides naturally presented by MHC class I molecules, Annu.Rev.Immunol. 11, pp. 213-244.

Ramos, P. C.; Hockendorff, J.; Johnson, E. S.; Varshavsky, A. and Dohmen, R. J. (1998): Ump1p is required for proper maturation of the 20S proteasome and becomes its substrate upon completion of the assembly, Cell 92 [4], pp. 489-99.

Ranson, T.; Bregenholt, S.; Lehuen, A.; Gaillot, O.; Leite-de-Moraes, M. C.; Herbelin, A.; Berche, P. and Di Santo, J. P. (2005): Invariant V alpha 14+ NKT cells participate in the early response to enteric Listeria monocytogenes infection, J.Immunol. 175 [2], pp. 1137-1144.

Realini, C.; Dubiel, W.; Pratt, G.; Ferrell, K. and Rechsteiner, M. (1994): Molecular cloning and expression of a gamma-interferon-inducible activator of the multicatalytic protease, J Biol Chem 269 [32], pp. 20727-32.

Reits, E.; Neijssen, J.; Herberts, C.; Benckhuijsen, W.; Janssen, L.; Drijfhout, J. W. and Neefjes, J. (2004): A major role for TPPII in trimming proteasomal degradation products for MHC class I antigen presentation, Immunity. 20 [4], pp. 495-506.

Robek, M. D.; Garcia, M. L.; Boyd, B. S. and Chisari, F. V. (2007): Role of immunoproteasome catalytic subunits in the immune response to hepatitis B virus, J.Virol. 81 [2], pp. 483-491.

Rock, K. L. and Goldberg, A. L. (1999): Degradation of cell proteins and the generation of MHC class I-presented peptides, Annu.Rev.Immunol. 17, pp. 739-779.

Rock, K. L.; Gramm, C.; Rothstein, L.; Clark, K.; Stein, R.; Dick, L.; Hwang, D. and Goldberg, A. L. (1994): Inhibitors of the proteasome block the degradation of most cell proteins and the generation of peptides presented on MHC class I molecules, Cell 78 [5], pp. 761-71.

Rock, K. L.; York, I. A. and Goldberg, A. L. (2004): Post-proteasomal antigen processing for major histocompatibility complex class I presentation, Nat.Immunol. 5 [7], pp. 670-677.

Rogers, H. W.; Callery, M. P.; Deck, B. and Unanue, E. R. (1996): Listeria monocytogenes induces apoptosis of infected hepatocytes, J.Immunol. 156 [2], pp. 679-684.

Runnels, H. A.; Watkins, W. A. and Monaco, J. J. (2000): LMP2 expression and proteasome activity in NOD mice, Nat.Med. 6 [10], pp. 1064-1065.

Salzmann, U.; Kral, S.; Braun, B.; Standera, S.; Schmidt, M.; Kloetzel, P. M. and Sijts, A. (1999): Mutational analysis of subunit i beta2 (MECL-1) demonstrates conservation of cleavage specificity between yeast and mammalian proteasomes, FEBS Lett. 454 [1-2], pp. 11-15.

Schmidt, M.; Schmidtke, G. and Kloetzel, P. M. (1997): Structure and structure formation of the 20S proteasome, Mol Biol Rep 24 [1-2], pp. 103-12.

Schmidt, M.; Zantopf, D.; Kraft, R.; Kostka, S.; Preissner, R. and Kloetzel, P. M. (1999): Sequence information within proteasomal prosequences mediates efficient integration of beta-subunits into the 20 S proteasome complex, J.Mol.Biol. 288 [1], pp. 117-128.

Schmidtke, G.; Kraft, R.; Kostka, S.; Henklein, P.; Frommel, C.; Lowe, J.; Huber, R.; Kloetzel, P. M. and Schmidt, M. (1996): Analysis of mammalian 20S proteasome biogenesis: the maturation of beta-subunits is an ordered two-step mechanism involving autocatalysis, EMBO J. 15 [24], pp. 6887-6898.

Schwarz, K.; Eggers, M.; Soza, A.; Koszinowski, U. H.; Kloetzel, P. M. and Groettrup, M. (2000): The proteasome regulator PA28alpha/beta can enhance antigen presentation without affecting 20S proteasome subunit composition, Eur.J.Immunol. 30 [12], pp. 3672-3679.

Seaman, M. S.; Wang, C. R. and Forman, J. (2000): MHC class Ib-restricted CTL provide protection against primary and secondary Listeria monocytogenes infection, J.Immunol. 165 [9], pp. 5192-5201.

Seifert, U.; Maranon, C.; Shmueli, A.; Desoutter, J. F.; Wesoloski, L.; Janek, K.; Henklein, P.; Diescher, S.; Andrieu, M.; de la Salle, H.; Weinschenk, T.; Schild, H.; Laderach, D.; Galy, A.; Haas, G.; Kloetzel, P. M.; Reiss, Y. and Hosmalin, A. (2003): An essential role for tripeptidyl peptidase in the generation of an MHC class I epitope, Nat Immunol 4 [4], pp. 375-9.

Seki, S.; Habu, Y.; Kawamura, T.; Takeda, K.; Dobashi, H.; Ohkawa, T. and Hiraide, H. (2000): The liver as a crucial organ in the first line of host defense: the roles of Kupffer cells, natural killer (NK) cells and NK1.1 Ag+ T cells in T helper 1 immune responses, Immunol.Rev. 174, pp. 35-46.

Serbina, N. V.; Salazar-Mather, T. P.; Biron, C. A.; Kuziel, W. A. and Pamer, E. G. (2003): TNF/iNOS-producing dendritic cells mediate innate immune defense against bacterial infection, Immunity 19 [1], pp. 59-70.

Sha, W. C.; Liou, H. C.; Tuomanen, E. I. and Baltimore, D. (1995): Targeted disruption of the p50 subunit of NF-kappa B leads to multifocal defects in immune responses, Cell 80 [2], pp. 321-330.

Shedlock, D. J.; Whitmire, J. K.; Tan, J.; MacDonald, A. S.; Ahmed, R. and Shen, H. (2003): Role of CD4 T cell help and costimulation in CD8 T cell responses during Listeria monocytogenes infection, J.Immunol. 170 [4], pp. 2053-2063.

Sijts, A. J.; Ruppert, T.; Rehermann, B.; Schmidt, M.; Koszinowski, U. and Kloetzel, P. M. (2000): Efficient generation of a hepatitis B virus cytotoxic T lymphocyte epitope requires the structural features of immunoproteasomes, J.Exp.Med. 191 [3], pp. 503-514.

Sijts, A. J.; Standera, S.; Toes, R. E.; Ruppert, T.; Beekman, N. J.; van Veelen, P. A.; Ossendorp, F. A.; Melief, C. J. and Kloetzel, P. M. (2000): MHC class I antigen processing of an adenovirus CTL epitope is linked to the levels of immunoproteasomes in infected cells, J.Immunol. 164 [9], pp. 4500-4506.

Stohwasser, R.; Kuckelkorn, U.; Kraft, R.; Kostka, S. and Kloetzel, P. M. (1996): 20S proteasome from LMP7 knock out mice reveals altered proteolytic activities and cleavage site preferences, FEBS Lett. 383 [1-2], pp. 109-113.

Stohwasser, R.; Salzmann, U.; Giesebrecht, J.; Kloetzel, P. M. and Holzhutter, H. G. (2000): Kinetic evidences for facilitation of peptide channelling by the proteasome activator PA28, Eur J Biochem 267 [20], pp. 6221-30.

Strehl, B.; Joeris, T.; Rieger, M.; Visekruna, A.; Textoris-Taube, K.; Kaufmann, S. H.; Kloetzel, P. M.; Kuckelkorn, U. and Steinhoff, U. (2006): Immunoproteasomes Are Essential for Clearance of Listeria monocytogenes in Nonlymphoid Tissues but Not for Induction of Bacteria-Specific CD8+ T Cells, J.Immunol. 177 [9], pp. 6238-6244.

Strehl, B.; Textoris-Taube, K.; Jakel, S.; Voigt, A.; Henklein, P.; Steinhoff, U.; Kloetzel, P. M. and Kuckelkorn, U. (2008): Antitopes define preferential proteasomal cleavage site usage, J Biol Chem.

Szalay, G.; Hess, J. and Kaufmann, S. H. (1995): Restricted replication of Listeria monocytogenes in a gamma interferon-activated murine hepatocyte line, Infect.Immun. 63 [8], pp. 3187-3195.

Tanahashi, N.; Murakami, Y.; Minami, Y.; Shimbara, N.; Hendil, K. B. and Tanaka, K. (2000): Hybrid proteasomes. Induction by interferon-gamma and contribution to ATP-dependent proteolysis, J Biol Chem 275 [19], pp. 14336-45.

Toes, R. E.; Nussbaum, A. K.; Degermann, S.; Schirle, M.; Emmerich, N. P.; Kraft, M.; Laplace, C.; Zwinderman, A.; Dick, T. P.; Muller, J.; Schonfisch, B.; Schmid, C.; Fehling, H. J.; Stevanovic, S.; Rammensee, H. G. and Schild, H. (2001): Discrete cleavage motifs of constitutive and immunoproteasomes revealed by quantitative analysis of cleavage products, J.Exp.Med. 194 [1], pp. 1-12.

Van den Eynde, B. J. and Morel, S. (2001): Differential processing of class-I-restricted epitopes by the standard proteasome and the immunoproteasome, Curr.Opin.Immunol. 13 [2], pp. 147-153.

van der Most, R. G.; Murali-Krishna, K.; Whitton, J. L.; Oseroff, C.; Alexander, J.; Southwood, S.; Sidney, J.; Chesnut, R. W.; Sette, A. and Ahmed, R. (1998): Identification of Db- and Kb-restricted subdominant cytotoxic T-cell responses in lymphocytic choriomeningitis virus-infected mice, Virology 240 [1], pp. 158-167.

van Furth, R.; van Zwet, T. L.; Buisman, A. M. and van Dissel, J. T. (1994): Anti-tumor necrosis factor antibodies inhibit the influx of granulocytes and monocytes into an inflammatory exudate and enhance the growth of Listeria monocytogenes in various organs, J Infect Dis 170 [1], pp. 234-7.

van Hall, T.; Sijts, A.; Camps, M.; Offringa, R.; Melief, C.; Kloetzel, P. M. and Ossendorp, F. (2000): Differential influence on cytotoxic T lymphocyte epitope presentation by controlled expression of either proteasome immunosubunits or PA28, J.Exp.Med. 192 [4], pp. 483-494.

Vijh, S.; Pilip, I. M. and Pamer, E. G. (1998): Effect of antigen-processing efficiency on in vivo T cell response magnitudes, J.Immunol. 160 [8], pp. 3971-3977.

Villanueva, M. S.; Sijts, A. J. and Pamer, E. G. (1995): Listeriolysin is processed efficiently into an MHC class I-associated epitope in Listeria monocytogenes-infected cells, J Immunol 155 [11], pp. 5227-33.

Visekruna, A.; Joeris, T.; Seidel, D.; Kroesen, A.; Loddenkemper, C.; Zeitz, M.; Kaufmann, S. H.; Schmidt-Ullrich, R. and Steinhoff, U. (2006): Proteasome-mediated degradation of IkappaBalpha and processing of p105 in Crohn disease and ulcerative colitis, J.Clin.Invest 116 [12], pp. 3195-3203.

von Boehmer, H.; Aifantis, I.; Gounari, F.; Azogui, O.; Haughn, L.; Apostolou, I.; Jaeckel, E.; Grassi, F. and Klein, L. (2003): Thymic selection revisited: how essential is it?, Immunol Rev 191, pp. 62-78.

Weih, F.; Warr, G.; Yang, H. and Bravo, R. (1997): Multifocal defects in immune responses in RelB-deficient mice, J.Immunol. 158 [11], pp. 5211-5218.

Weninger, W.; Manjunath, N. and von Andrian, U. H. (2002): Migration and differentiation of CD8+ T cells, Immunol Rev 186, pp. 221-33.

Whitmire, J. K. and Ahmed, R. (2000): Costimulation in antiviral immunity: differential requirements for CD4(+) and CD8(+) T cell responses, Curr Opin Immunol 12 [4], pp. 448-55.

Williams, M. A. and Bevan, M. J. (2004): Shortening the infectious period does not alter expansion of CD8 T cells but diminishes their capacity to differentiate into memory cells, J.Immunol. 173 [11], pp. 6694-6702.

Witt, E.; Zantopf, D.; Schmidt, M.; Kraft, R.; Kloetzel, P. M. and Kruger, E. (2000): Characterisation of the newly identified human Ump1 homologue POMP and analysis of LMP7(beta 5i) incorporation into 20 S proteasomes, J.Mol.Biol. 301 [1], pp. 1-9.

Wong, P. and Pamer, E. G. (2004): Disparate in vitro and in vivo requirements for IL-2 during antigen-independent CD8 T cell expansion, J Immunol 172 [4], pp. 2171-6.

Wong, P. and Pamer, E. G. (2001): Cutting edge: antigen-independent CD8 T cell proliferation, J.Immunol. 166 [10], pp. 5864-5868.

Wong, P. and Pamer, E. G. (2003): Feedback regulation of pathogen-specific T cell priming, Immunity. 18 [4], pp. 499-511.

Xu, H.; Chun, T.; Choi, H. J.; Wang, B. and Wang, C. R. (2006): Impaired response to Listeria in H2-M3-deficient mice reveals a nonredundant role of MHC class Ib-specific T cells in host defense, J.Exp.Med. 203 [2], pp. 449-459.

Yang, Y.; Xiang, Z.; Ertl, H. C. and Wilson, J. M. (1995): Upregulation of class I major histocompatibility complex antigens by interferon gamma is necessary for T-cell-mediated elimination of recombinant adenovirus-infected hepatocytes in vivo, Proc Natl Acad Sci U S A 92 [16], pp. 7257-61.

Yewdell, J. W. and Bennink, J. R. (1999): Immunodominance in major histocompatibility complex class I-restricted T lymphocyte responses, Annu.Rev.Immunol. 17, pp. 51-88.

Yewdell, J. W.; Reits, E. and Neefjes, J. (2003): Making sense of mass destruction: quantitating MHC class I antigen presentation, Nat.Rev.Immunol. 3 [12], pp. 952-961.

Yewdell, J. W.; Schubert, U. and Bennink, J. R. (2001): At the crossroads of cell biology and immunology: DRiPs and other sources of peptide ligands for MHC class I molecules, J.Cell Sci. 114 [Pt 5], pp. 845-851.

York, I. A.; Chang, S. C.; Saric, T.; Keys, J. A.; Favreau, J. M.; Goldberg, A. L. and Rock, K. L. (2002): The ER aminopeptidase ERAP1 enhances or limits antigen presentation by trimming epitopes to 8-9 residues, Nat.Immunol. 3 [12], pp. 1177-1184.

Abbreviations

µg	microgramm
µl	microlitre
µM	micromolar
µm	micrometre
2D	two dimensional
AMC	7-Amido-4-Methylcoumarin
APC	antigen presenting cell
ATP	adenosine-tri-phosphate
BM-Mϕ	bone marrow macrophages
c20S	constitutive proteasome
CD	cluster of differentiation
cDNA	copy desoxyribonucleic acid
cfu	colony forming unit
cm	centimetre
CO_2	carbondioxide
C-terminal	carboxy-terminal
DC	dendritic cell
DDM	N-dodecyl D-maltoside
DEAE	diethylaminoethyl
DMEM	Dubelccos Modified Eagle Medium
DNA	desoxyribonucleic acid
DRiPs	defective ribosomal products
DTT	dithiothreitol
EDTA	ethylendiamin tetra acetate
e.g.	for example
ER	endoplasmatic reticulum
FACS	fluorescence activated cell sorting
FCS	fetal calf serum
Fig.	figure
g	acceleration of gravity
GAPDH	Glyceraldehyde 3-phosphate dehydrogenase
h	hours
i.e.	that means
i.v.	intraveniously
i20S	immunoproteasome
ICS	intracellular cytokine staining
IFN	Interferon
IgG	immunoglobulin G
IκB	inhibitor of kappa B
IL	interleukin
kDa	kilo-Dalton
LC-ESI-MS	liquid chromatography-electrospray ionization-ion trap mass spectrometry
LCMV	*Lymphocytic choriomeningitis virus*
Listeria	*Listeria monocytogenes*
LLO	Listeriolysin O
lmp-	low molecular mass peptide
LTR	long terminal repeat
Lys	lysine
m20S	mixed proteasomes

mA	milli-Ampere
mecl-	multicatalytic endopeptidase complex-like-
MEFs	murine embryonic fibroblasts
Mϕ	macrophages
MHC	major histocompatibility complex
min	minute
ml	millilitre
mM	millimolar
MPIIB	Max Planck Institute for Infection Biology
mRNA	messenger ribonucleic acid
MSCV	*Murine Stem Cell Virus*
NaCl	Sodium Chloride
NADPH	Nicotinamide adenine dinucleotide phosphate
NaN_3	sodium azide
NF-κB	Nuclear Factor kappa B
NH_4Cl	ammonium chloride
NK cell	natural killer cell
nm	nanometre
NO	nitric oxide
N-terminal	amino-terminal
p.i.	post infection
PAC	proteasome assembling chaperone
PAGE	polyacrylamide gel electrophoresis
PBS	phosphate buffered saline
PCR	polymerase chain reaction
pmol	picomol
PMSF	phenylmethylsulfonylfluoride
POMP	proteasome maturation protein
pre-	precursor-
PVDF	polyvinylidenfluoride
RNA	ribonucleic acid
RNI	reactive nitrogen intermediates
ROI	reactive oxygen intermediates
rpm	rotations per minute
RPS9	ribosomal protein subunit 9
RT	reverse transcriptase
SDS	sodiumdodecylsulfate
sec	seconds
SPF	special pathogen free
t20S	thymic proteasomes
TAP	transporter associated with antigen presentation
TBS	Tris buffered saline
TCR	T cell receptor
TNF	tumor necrosis factor
TPPII	tripeptidylpeptidase II
U	units
UBA	ubiquitin associated
UBL	ubiquitin-like
V	Volt
v/v	volume per volume
w/v	weight per volume
WT	wild type

Publications

Paper:

1. Hahnen, S., **Joeris, T.**, F. Kreuzaler, and C. Peterhansel. 2003. Quantification of photosynthetic gene expression in maize C(3) and C(4) tissues by real-time PCR. *Photosynth.Res.* 75:183-192.

2. Strehl, B.[*], **Joeris, T.[*],** M. Rieger, A. Visekruna, S. H. E. Kaufmann, P. M. Kloetzel, U. Kuckelkorn, and U. Steinhoff. 2006. Immunoproteasomes Are Essential for Clearance of *Listeria monocytogenes* in Nonlymphoid Tissues but Not for Induction of Bacteria-Specific $CD8^+$ T Cells. *J.Immunol.* 177: 6238-6244. [*]**authors contributed equally to this work**

3. Visekruna, A., **Joeris, T.**, D. Seidel, A. Kroesen, D. Loddenkemper, M. Zeitz, S. H. E. Kaufmann, R. Schmidt-Ullrich, and U. Steinhoff. 2006. Proteasome-mediated degradation of IkBa and processing of p105 in Crohn´s disease and ulcerative colitis. *J.Clin.Invest* 116: 3195-3203.

Poster / Abstracts:

1. **Joeris, T.,** Krienke, P., Behnck-Knoblau, S., Kuckelkorn, U., Kaufmann, S. H. E., and Steinhoff, U. Immune responses in the absence of Immunoproteasome subunit β5i. Immunobiology 210(6-8), 554-555. DGFI Herbsttagung, Kiel, 2005.

2. **Joeris, T.,** Krienke, P., Behnck-Knoblau, S., Kuckelkorn, U., Kaufmann, S. H. E., and Steinhoff, U. Immune responses to *Listeria monocytogenes* in the absence of Immunoproteasome subunit β5i. EIMID meeting, Stockholm, Oct2005

3. **Joeris, T.,** Krienke, P., Kuckelkorn, U., Kaufmann, S. H. E., and Steinhoff, U. Formation of hybridproteasomes containing constitutive and immuno subunits *in vivo*. 16th European Congress of Immunology, Paris, Sepember 2006(PB2494)

4. **Joeris, T.,** Krienke, P., Visekruna, A., Schmidt, N., Kuckelkorn, U., Kaufmann, S. H. E., and Steinhoff, U. Proteasome assembly: Competetive integration constitutive and IFNγ-inducible catalytic β-subunits. DGFI Herbsttagung, Heidelberg, 2007.

Berlin, den

Danksagung

Diese Arbeit wurde über einen Zeitraum von drei Jahren von der Deutschen Forschungsgesellschaft im Rahmen des Projekts KU1261 gefördert. Desweiteren möchte ich mich bei der Charité Berlin und der Sonnenfeld-Stiftung bedanken, die mir über die Förderung der DFG hinaus durch Promotiosstipendien ermöglicht haben, diese Arbeit zu einem sinnvollen und erfolgreichen Abschluß zu bringen.

Ich danke meinen Kollegen im Institut für Biochemie der Charité für die gute Zusammenarbeit, insbesondere Dr. Katrin Textoris-Taube für die Durchführung der Massenspektrometrischen Analysen und Ilse Drung für die Einarbeitung in die Proteasom-Aufreinigung.
Desweiteren danke ich Dr. Britta Strehl für die hervorragenden Vorarbeiten und die gute Zusammenarbeit bei der gemeinsamen Publikation unserer Daten.
Ganz besonders möchte ich Dr. Ulrike Kuckelkorn für die vielen Proteasom-Insider-Tips, die goße Hilfsbereitschaft und die stets freundliche Zusammenarbeit danken.

Meinen Kollegen am Max Planck Institut für Infektionsbiologie danke ich für die große Unterstützung in den letzten Jahren und die gute Arbeitsatmosphäre, speziell im Büro 3.59 ;-).
Im einzelnen möchte ich Dr. Uwe Klemm und seinem Team von Tierpflegern für ihre gute Arbeit, David Ermert für die Bereitstellung seines großartigen retroviralen Vektors und der Unterstützung bei der Klonierung sowie Robert Hurwitz für die Hilfe an der FPLC danken.
Besonderer Dank gilt Christiane Desel, Sabine Seibert, Maik Stein, Andrea Gutschmidt und Martin Beisiegel. Ohne Euch hätte die Zeit am MPI nur halb so viel Spaß gemacht.
Prof. Stefan H.E. Kaufmann danke ich für die Möglichkeit, die Arbeiten in seiner hervorragend ausgerüsteten Abteilung am Max Planck Institut für Infektionsbiologie durchführen zu können.

Bei meiner Arbeitsgruppe, den „Steinis“, möchte ich mich für die gute Zusammenarbeit und viel Spaß im Labor danken, besonders Silke Behnck und Dagmar Oberbeck-Müller für die praktische Unterstützung sowie meinen Doktoranden-Kollegen Alexander Visekruna und Nicole Schmidt für den guten Zusammenhalt und interessante Diskussionen.
Tausend Dank an Petra Krienke für die tatkräftige Unterstützung im Labor und die sehr angenehme Zusammenarbeit.
Bei meinem Betreuer, Ulrich Steinhoff, möchte ich mich für die Möglichkeit bedanken, eigene Ideen einzubringen und zu verwirklichen, vor allem aber für die große Unterstützung, den fast unzerstörbaren Enthusiasmus und das mir entgegengebrachte Vertrauen.

Zu guter Letzt danke ich meinen Freunden und meiner Familie für die Unterstützung auf meinem Weg.
Besonders aber möchte ich Andrea, für die langjährige und liebevolle Unterstützung in Höhen und Tiefen, das Ertragen von Nicht-Enden-Wollendem Job-Talk und das Verständnis für die wenige Freizeit danken.

Erklärung

Hiermit erkläre ich, die Dissertation selbständig und ohne unerlaubte Hilfe angefertigt zu haben.

Berlin, den